PROPAGATION OF MULTIWAVELENGTH LASER RADIATION THROUGH ATMOSPHERIC TURBULENCE

J. Richard Kerr, et al

Oregon Graduate Center

Prepared for:

Rome Air Development Center

31 May 1974

Unclassified

SECURITY CLASSIFICATION OF THIS PAGE (When Date Entered)

REPORT DOCUMENTATION PAGE		READ INSTRUCTIONS BEFORE COMPLETING FORM
1. REPORT NUMBER RADC-TR- 74-183	2. GOVT ACCESSION NO.	3. RECIPIENT'S CATALOG NUMBER AD 783 277
4. TITLE (and Subtitle) PROPAGATION OF MULTIWAVELENGTH LASER RADIATION THROUGH ATMOSPHERIC TURBULENCE		5. TYPE OF REPORT & PERIOD COVERED Interim Technical Report (1 Dec. 73 - 30 Apr. 74) 6. PERFORMING ORG. REPORT NUMBER 1103-1
7. AUTHOR(s) J. Richard Kerr James R. Dunphy		8. CONTRACT OR GRANT NUMBER(s) F30602-74-C-0082
9. PERFORMING ORGANIZATION NAME AND ADDRESS Oregon Graduate Center 19600 N. W. Walker Road Beaverton, Oregon 97005		10. PROGRAM ELEMENT, PROJECT, TASK AREA & WORK UNIT NUMBERS 62301E 12790212
11. CONTROLLING OFFICE NAME AND ADDRESS Defense Advanced Research Projects Agency 1400 Wilson Boulevard Arlington, Virginia 22209		12. REPORT DATE May 31, 1974 13. NUMBER OF PAGES 80
14. MONITORING AGENCY NAME & ADDRESS(if different from Controlling Office) Rome Air Development Center (OCSE) ATTN: Capt Darryl P. Greenwood Griffiss Air Force Base, New York 13441		15. SECURITY CLASS. (of this report) Unclassified 15a. DECLASSIFICATION/DOWNGRADING SCHEDULE

16. DISTRIBUTION STATEMENT (of this Report)

Approved for public release; distribution unlimited.

17. DISTRIBUTION STATEMENT (of the abstract entered in Block 20, if different from Report)

Approved for public release; distribution unlimited.

18. SUPPLEMENTARY NOTES

None

19. KEY WORDS (Continue on reverse side if necessary and identify by block number)

Propagation
Turbulence
Atmospheric optics
Scintillation

20. ABSTRACT (Continue on reverse side if necessary and identify by block number)

The effects of atmospheric turbulence on target irradiance using a near-field, wander-tracking laser transmitter have been investigated in detail. A unified analytical and phenomenological treatment of the mean irradiance and its fluctuations is presented, with supporting experimental data. The advantages to be gained through the use of wander cancellation are seen to be substantial, and in many cases larger than predicted by the basic theory.

(Continued - Reverse side)

DD FORM 1 JAN 73 1473 EDITION OF 1 NOV 65 IS OBSOLETE

Unclassified

SECURITY CLASSIFICATION OF THIS PAGE (When Date Entered)

20. Abstract (Continued)

A brief description is also given of recent progress in the investigation of the short-term statistics of turbulence and scintillations. Theoretical and experimental results have been obtained for the prediction of confidence intervals or data spread in such measurements, and the effects of averaging times. In addition, a computer simulation technique has been formulated for the generation of an ensemble of instantaneous, short propagation paths through turbulence.

PROPAGATION OF MULTIWAVELENGTH LASER RADIATION THROUGH ATMOSPHERIC TURBULENCE

J. Richard Kerr
James R. Dunphy

Contractor: Oregon Graduate Center
Contract Number: F30602-74-C-0082
Effective Date of Contract: 1 December 1973
Contract Expiration Date: 1 September 1974
Amount of Contract: $64,715.00
Program Code Number: 4E20

Principal Investigator: Dr. J. Richard Kerr
Phone: 503 645-1121

Project Engineer: Capt Darryl P. Greenwood
Phone: 315 330-3145

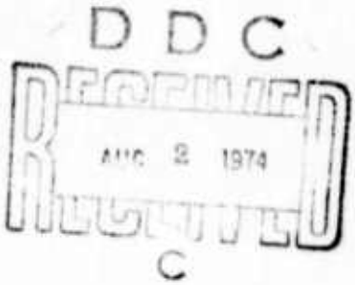

This research was supported by the Defense Advanced Research Projects Agency of the Department of Defense and was monitored by Capt Darryl P. Greenwood RADC (OCSE), GAFB, NY 13441 under Contract F30602-74-C-0082, Job Order No. 12790212.

ib

This report has been reviewed by the RADC Information Office (OI) and is releasable to the National Technical Information Service (NTIS).

This technical report has been reviewed and is approved.

Daryl P. Hammond
RADC Project Engineer

Summary

Current work on this program involves two projects. In the first of these, the effects of atmospheric turbulence on target irradiance using a near-field, wander-tracking laser transmitter have been investigated in detail. A unified analytical and phenomenological treatment of the mean irradiance and its fluctuations is presented, with supporting experimental data. The advantages to be gained through the use of wander cancellation are seen to be substantial, and in many cases larger than predicted by the basic theory. The discussion includes the observability of transmitter-aperture-smoothing effects on scintillation, and the implications of empirical probability distributions and power spectra for irradiance-fading and wander-tracking signals. Ongoing analytical and multiwavelength, multipathlength experimental efforts are expected to result in a complete understanding of these phenomena.

Regarding the second topic, a brief description is also given of recent progress in the investigation of the short-term statistics of turbulence and scintillations. Theoretical and experimental results have been obtained for the prediction of confidence intervals or data spread in such measurements, and the effects of averaging times. In addition, a computer simulation technique has been formulated for the generation of an ensemble of instantaneous, short propagation paths through turbulence. The results of these efforts will enable the prediction of limits on short-term scintillation effects, and the probabilistic description of such parameters as target irradiance given apriori optical/infrared information on the instantaneous propagation path.

TABLE OF CONTENTS

I. INTRODUCTION

This report describes progress on two projects. In the first (Section II), a detailed analytical and experimental discussion is given on target irradiance effects caused by the action of atmospheric turbulence on an extended, wander-tracking laser beam. Ongoing and future activities are also described. In the second (Section III), a brief review is given of recent progress on the problem of short-term propagation statistics. The latter topic will be covered in detail in the next technical report on this program.

II. TURBULENCE EFFECTS ON TARGET IRRADIANCE FOR A WANDER-TRACKING, FINITE-APERTURE LASER TRANSMITTER

Finite-Aperture Laser Transmitter

Since the preceding report[1] was written, substantial progress has been made in completing the theoretical problem of finite-transmitter effects, including both the phenomenological and complete analytical descriptions, and their interrelation. In addition, experimental data have been obtained which support these treatments. In this section, the theoretical treatment will be described in detail, and the experimental results given.

A. Theoretical Considerations

As described in our previous reports on this work,[1,2] we have taken a dual theoretical approach to the problem of finite transmitter effects (with wander tracking) on target irradiance. First, we have approximated the effects with a unified phenomenological or physical description, and second, we have expanded and clarified the complete analytical treatment based on the successful Huygens-Fresnel approach[3,4] and reciprocity.[5] Although there remain unsolved details, the overall topic is now considered to be well understood, as described below.

1. Mean Irradiance

The general expression for the mean irradiance is given by[3,4,6]

$$\bar{I}(\bar{\rho}) = \left(\frac{k}{2\pi z}\right)^2 \int d^2\bar{\rho}\, M(\bar{\rho})\, e^{-\frac{ik}{z}\bar{p}\cdot\bar{\rho}} \times \int d^2\bar{R}\, U\left(\bar{R}+\frac{\bar{\rho}}{2}\right) U^*\left(\bar{R}-\frac{\bar{\rho}}{2}\right) e^{\frac{ik}{z}\bar{\rho}\cdot\bar{R}}, \qquad (1)$$

---

1. J. R. Kerr, "Propagation of Multiwavelength Laser Radiation Through Atmospheric Turbulence", RADC-TR-73-322, August, 1973.
2. J. R. Kerr, "Propagation of Multiwavelength Laser Radiation Through Atmospheric Turbulence", RADC-TR-73-54, January 1973.
3. R. F. Lutomirski and H. T. Yura, Appl. Opt. 10, 1652 (1971).
4. H. T. Yura, Appl. Opt. 10, 2771 (1971).
5. D. L. Fried and H. T. Yura, J. Opt. Soc. Am. 62, 600 (1972).
6. H. T. Yura, J. Opt. Soc. Am. 63, 567 (1973).

where

$\bar{\rho}$ = transverse position vector for target point under consideration
k = optical wavenumber
z = path length
$\bar{R},\bar{\rho}$ = sum and difference coordinates in the transmitter aperture, respectively
M = atmospheric modulation transfer function
and U = complex transmitter amplitude distribution.

We immediately specialize the transmitter to the case of a gaussian beam with nominal radius (a) and output focal length or radius-of-curvature f:

$$U(\bar{r}) = U_o e^{-\frac{1}{2} r^2 \left(\frac{1}{a^2} + \frac{ik}{f} \right)} \tag{2}$$

The second integral in Eq. (1) then becomes

$$I' = e^{-\frac{\rho^2}{4a^2}} |U_o|^2 \int d^2\bar{R}\, e^{-\frac{R^2}{a^2}} e^{ik\,\bar{R}\cdot\bar{\rho}\left(\frac{1}{z} - \frac{1}{f}\right)}$$

$$= \pi a^2 e^{-\frac{\rho^2}{4a^2}} |U_o|^2 e^{-\frac{k^2 a^2 \rho^2}{4}\left(\frac{1}{z} - \frac{1}{f}\right)^2} . \tag{3}$$

We note immediately that the $(\bar{R}\cdot\bar{\rho})$ exponential term vanishes in the case of a focused beam (f=z), including focus on infinity (collimation). Thus the expression may be immediately compared with that for the reciprocal case of a heterodyne receiver, in which a plane wave (or infinite focus) has generally been assumed.[7]

We now use Eq. (3) with (1) to write

---

7. D. L. Fried, Proc. IEEE. 55, 57-67, January 1967.

$$\bar{I}(\bar{p}) = \left(\frac{k}{2\pi z}\right)^2 \pi a^2 |U_o|^2 \int d^2\bar{\rho}\, M(\bar{\rho})\, e^{-\frac{ik}{z}\bar{p}\cdot\bar{\rho}}$$

$$\text{Xe}^{-\rho^2/4\left[\frac{1}{a^2} + k^2a^2\left(\frac{1}{z} - \frac{1}{f}\right)^2\right]} \quad . \tag{4}$$

We let $d^2\bar{\rho} = \rho d\rho\, d\phi$ and integrate over ϕ to obtain a single integral equation:

$$\bar{I}(\bar{p}) = \frac{k^2a^2}{2z^2} |U_o|^2 \int_o^\infty d\rho\, \rho\, M(\rho)\, J_o\left(\frac{k}{z} p\rho\right)$$

$$\text{Xe}^{-\frac{\rho^2}{4}\left[\frac{1}{a^2} + k^2a^2\left(\frac{1}{z} - \frac{1}{f}\right)^2\right]} \quad . \tag{5}$$

This constitutes a generalization of Eq. (A3) in Ref. 6.

We now consider the special case of interest here, in which the target point is on-axis ($\bar{p}=0$) and the transmitter is focused on the target ($f=z$):

$$\bar{I} = \frac{k^2a^2}{2z^2} |U_o|^2 \int_o^\infty d\rho\, \rho\, M(\rho)\, e^{-\rho^2/4a^2} \quad . \tag{6}$$

It may be pointed out that the dependence on the Fresnel number $(ka^2/z)^{1/2} \equiv \beta$ has disappeared from the integral: the pertinent independent variable will simply be (a/ρ_o), where ρ_o is the coherence scale owing to turbulence. This means that basic conclusions drawn from earlier analyses[7] of the reciprocal, heterodyne receiver case will be valid for a focused or collimated transmitter with $f=z$, over an arbitrary (nonuniform) path; it is only necessary to know $M(\rho)$ for the path. If we define the transmitter diameter $D=2a$, and also define $x \equiv \rho/D$, we can write Eq. (6) in the notation of Ref. 6:

$$\bar{I} = 2\beta^2 |U_o|^2 \int_o^\infty dx \; x \; M(Dx) \; e^{-x^2} \quad . \tag{7}$$

For the collimated case with $z < \infty$, the exponent in the integrand is multiplied by $(1 + \beta^2)$. Finally, for the vacuum or turbulence-free case, we let M=1 and find

$$\bar{I}_o = 2\beta^2 |U_o|^2 \int_o^\infty x \; e^{-x^2} \; dx$$

$$= \beta^2 |U_o|^2$$

$$= \frac{k^2 D^4}{16 z^2} |U_o|^2 \quad . \tag{8}$$

If wander-tracking is not employed, we have the so-called "long-term case", for which the atmospheric modulation transfer function is[3,4,6]

$$M(\rho) = e^{-\left(\frac{\rho}{\rho_o}\right)^{5/3}}$$

$$M(Dx) = e^{-\left(\frac{Dx}{\rho_o}\right)^{5/3}} \tag{9}$$

where ρ_o is the turbulence-induced coherence scale. The complete expression for the irradiance is thus

$$\bar{I}_{LT} = 2 \bar{I}_o \int_o^\infty dx \; x \; e^{-x^2} e^{-\left(\frac{Dx}{\rho_o}\right)^{5/3}} \tag{10}$$

(Eq. A8 of Ref. 6).

For the wander-tracking case, the "short-term modulation transfer function (M_{ST})" is required, which is dependent on the optical configuration, and which is related to the reciprocal problem of wavefront-tilt-tracking in a heterodyne receiver[8] or short-exposure resolution in an imaging system.[9] Unfortunately, this problem has not been adequately solved. In Ref. 6, a result for M_{ST} is used which was derived by Fried[8,9] for a uniformly-weighted, truncated aperture:

$$M_{ST} = e^{\left(-\frac{Dx}{\rho_o}\right)^{5/3}\left[1 - 0.62 \times {}^{1/3}\right]} \quad . \tag{11}$$

If this is substituted in Eq. (7), it is seen that, for D much greater than ρ_o, the integral diverges; i.e., the equivalent structure function in the exponent becomes negative.

The basic problem here is that, in the derivation of Eq. (11), a certain assumption was made regarding the independence of the wavefront tilt and higher-order phase distortions over the aperture. If this assumption is dropped, higher-order terms appear in the exponent of (11), which prevent the exponent from becoming positive and hence diverging the integral.[10] Although the correction may be small for the case of a truncated, uniform aperture, it is mathematically and physically crucial for the infinite-gaussian beam. A complete expression for the latter aperture-distribution is under investigation by R. Lutomirski.[11]

Unfortunately, the results of Ref. 6 for the wander-tracked problem must be entirely discounted. We summarize the reasons as follows:

(1) The concept of a "short-term coherence scale" is not justified, since the 1/e radius of M_{ST} is not meaningfully related to a "short-term beam spread". [1]

---

8. D. L. Fried, "Effects of Atmospheric Turbulence on Static and Tracking Optical Heterodyne Receivers/Average Antenna Gain and Antenna Gain Variation", Technical Report No. TR-027, Optical Science Consultants, Aug.1971.
9. D. L. Fried, J. Opt. Soc. Am. 56, 1372 (1966).
10. R. Lutomirski, "The Tilt-Corrected MTF", Preliminary Report, Pacific-Sierra Research Corp., Santa Monica, California, March 1974.
11. D. L. Fried and R. Lutomirski, private communications.

(2) The function M_{ST} used was inappropriate for the gaussian case considered.

(3) A simple MacClaurin expansion will show that Eq. (12) of Ref. 6 represents a good approximation to Eq. (11) only over a very limited and uninteresting range of ρ_o/D, even though the figures in the paper imply a much wider range of validity. Specifically, ρ_o/D must be smaller than 0.03 if the second-order term is to be less than 10% of the first-order term used in Eq. (12) of that paper.

Although we do not yet have a correct M_{ST}, we point out that the gaussian-beam case will not be significantly different from that for a uniformly-weighted aperture, and that Fried's corresponding result is expected to be a good approximation. This is further supported in the discussions below of the phenomenological model and the experimental data.

We now distinguish two cases. Although Eq. (10) may be plotted universally as a function of (D/ρ_o), the normalization by $\bar{I}_o$, the turbulence-free or $D/\rho_o \to 0$ value, implies that $\beta^2 = k^2D^4/16z^2$ remains constant (note that $\bar{I}_o = |U_o|^2 D^2 \frac{k^2D^2}{16z^2} \sim$ Transmitter Power $\times \frac{k^2D^2}{z^2}$). Hence, the implied independent variable is ρ_o, i.e., the turbulence strength. As an alternative normalizer, let us consider the limit in the case $D/\rho_o \to \infty$. We define $\alpha = D/\rho_o$, and consider the limit of the integral in Eq. (10):

$$\lim_{\alpha\to\infty} \int_o^\infty dx\, x\, e^{-x^2}\, e^{-(\alpha x)^{5/3}}$$

$$= \lim_{\alpha\to\infty} \int_o^\infty dx\, x\, e^{-(\alpha x)^{5/3}} \left(1 - x^2 + \frac{x^4}{2!} - \frac{x^6}{3!} + \ldots\ldots\right) \quad . \qquad (12)$$

We then let $y=x^{5/3}$, and write this as

$$\lim_{\alpha\to\infty} \frac{3}{5} \int_0^\infty dy\, e^{-\alpha^{5/3} y} \left(y^{\frac{1}{5}} - y^{\frac{7}{5}} + \frac{y^{\frac{13}{5}}}{2!} \quad \cdots\cdots \right)$$

$$= \lim_{\alpha\to\infty} \frac{3}{5} \left\{ \frac{\Gamma\left(\frac{6}{5}\right)}{\alpha^2} - \frac{\Gamma\left(\frac{12}{5}\right)}{\alpha^4} \quad \cdots\cdots \right\}$$

$$\equiv \frac{3}{5\alpha^2} \Gamma\left(\frac{6}{5}\right)$$

$$= \frac{0.551}{\alpha^2} \qquad . \qquad (13)$$

Hence we may write

$$\lim_{D/\rho_o \to \infty} \bar{I}_{LT} \equiv \bar{I}_\infty = 2\, \bar{I}_o \times 0.551\, \frac{\rho_o^2}{D^2}$$

$$= 2 \times 0.551\, |U_o|^2\, \frac{k^2 D^4}{16 z^2}\, \frac{\rho_o^2}{D^2}$$

$$= 0.0689\, |U_o|^2\, \frac{k^2 \rho_o^2 D^2}{z^2}$$

$$\sim \text{Transmitter Power X } \frac{k^2 \rho_o^2}{z^2} \qquad . \qquad (14)$$

In particular, this justifies the viewpoint of a diffraction spread from a scale length (ρ_o), i.e., proportional to $(1/k\rho_o)^2$, and it furthermore provides a definite numerical constant for the asymptote in Fig. 1a of Ref. 1. This will be further discussed below. The expression corresponding to Eq. (10) is

$$\bar{I}_{LT} = \bar{I}_{\infty}\left(\frac{D^2}{0.551\,\rho_o^{\,2}}\right) \int_0^{\infty} dx\; x\, e^{-x^2}\, e^{-\left(\frac{Dx}{\rho_o}\right)^{5/3}} \qquad (15)$$

and the implied independent variable is D, such that the normalizer $\bar{I}_{\infty}$ is constant with constant transmitter power.

It is instructive to compare the results (8) and (14) with corresponding results for the reciprocal cases in the literature--noting that the latter are for a uniform, truncated aperture. Anticipating a simple result, let us identify the effective diameter D' of an equivalent uniform truncated aperture with our gaussian D as follows:

$$D' = 2D = 4a \qquad (16)$$

We also note that parameter r_o as utilized in Refs. 7-9 is related to ρ_o by

$$r_o = 2.0986\,\rho_o \qquad (17)$$

We then state the results for three cases:

(1) Gaussian transmitter (Eqs. 8, 14):

$$\frac{\bar{I}_o}{D^2|U_o|^2} = 0.0625\,\frac{k^2D^2}{z^2}$$

$$\frac{\bar{I}_{\infty}}{D^2|U_o|^2} = 0.0689\,\frac{k^2\rho_o^{\,2}}{z^2}$$

$$\frac{\bar{I}_\infty}{\bar{I}_o} = 1.1 \frac{\rho_o^2}{D^2} \tag{18a}$$

(2) Uniform, truncated image system: [9]

$$\text{Resolution } R_o = 0.020 \frac{k^2 D'^2}{z^2} = 0.080 \frac{k^2 D^2}{z^2}$$

$$R = 0.088 \frac{k^2 \rho_o^2}{z^2}$$

$$\frac{R_\infty}{R_o} = 1.1 \frac{\rho_o^2}{D^2} \tag{18b}$$

(3) Uniform, truncated heterodyne receiver: [7]

$$(SNR)_o \sim 0.39 D'^2 = 1.56 D^2$$

$$(SNR)_\infty \sim 1.73 \rho_o^2$$

$$\frac{(SNR)_\infty}{(SNR)_o} = 1.1 \frac{\rho_o^2}{D^2} \tag{18c}$$

The uniformity of the large-to-small aperture ratios in all three cases constitutes the basis for Eq. (16), and we note that $\frac{1.1 \rho_o^2}{D^2} = \frac{r_o^2}{D'^2}$.

Due to compatible dimensionality, Eqs. (18a) and (18b) provide a meaningful numerical comparison of the gaussian and uniform, truncated cases respectively.

The numberical evaluation of Eqs. (10) and (15) is shown in Fig. 1. Also shown is the corresponding result for the uniform-aperture imaging system;[9] Eqs. (16,17) have again been utilized, the former representing a shift to the left by one octave.

An analysis of the long-term and wander-tracked cases has appeared in the Russian literature.[12] In this derivation, Kon treats a focused, gaussian beam, and utilizes an expression for mean irradiance which is essentially identical to that of the Huygens-Fresnel formulation. For his wander-tracked results, he defines the beam centroid in a straightforward manner and calculates $\bar{I}$ following this centroid. His results are given in terms of $\bar{I}/I_o$ vs. the phase structure function D_ϕ (2a) in degrees; the relationship to our abscissa is

$$\frac{D}{\rho_o} = \left(\frac{D_\phi(D) \quad \text{(degrees)}}{307.1} \right)^{3/5} \tag{19}$$

Unfortunately, his long-term results disagree substantially with those of Eq. (15) and Ref. 9, and his tracking results are similarly in doubt. In particular, his results show $\tilde{\sim}$90% fall-off in $\bar{I}_{LT}$ for $\frac{D}{\rho_o} = 0.25$ (cf. Fig. 1).

As will be seen below, experimental wander-tracked results to date agree sufficiently with the predictions of Ref. 8 to indicate that the gaussian and uniform-truncated cases are not substantially different.

We return now to the phenomenological model discussed in Refs. 1,2. If we represent the total solid-angular beamspread as consisting of terms owing to diffraction $\left[\sim 1/k^2a^2\right]$, wander $\left[\sim D_\phi(2a)/k^2a^2 \sim \left(a^{1/3}\rho_o^{5/3}k^2\right)^{-1}\right]$, and beam breakup $\left(\sim 1/k^2\rho_o^2\right)$, we can write the mean irradiance as

$$\bar{I}_{LT} = |U_o|^2 \frac{a^2}{z^2} \frac{1}{\frac{C_1}{k^2a^2} + \left[C_2\left(\frac{a}{\rho_o}\right)^{-\frac{1}{3}} + C_3\right]\frac{1}{k^2\rho_o^2}} \tag{20}$$

---

12. A. I. Kon, Izv. VUZ Radiofizika 13, 61 (1970).

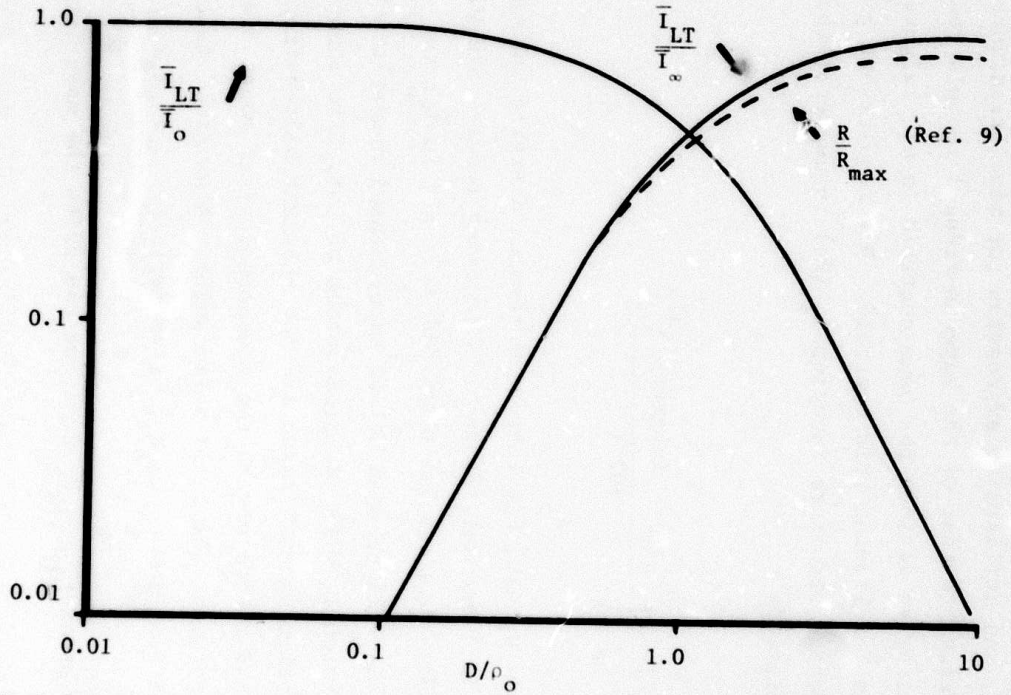

Figure 1. Theoretical long-term or non-tracking mean irradiance from Eqs. (10,15) and image resolution from Ref. 9.

where the coefficients C_{1-3} remain to be determined. We are implicitly defining our angular sizes in terms of their effect on $\bar{I}$, which removes the complication of alternative angular-beamwidth definitions. We note that for our gaussian beam (see Eq. 2),

$$I(r)_{\text{Transmitter}} = |U_o|^2 e^{-r^2/a^2}$$

$$\text{where } |U_o|^2 = \frac{\text{Transmitted Power}}{\pi a^2} \tag{21}$$

Diffraction-Limited Case $(a/\rho_o \to 0)$

From basic optics, we have at the target (focal point):

$$I = |U_o|^2 \frac{k^2 a^4}{z^2} = |U_o|^2 \frac{a^2}{w^2}$$

$$\text{where } w = \frac{z^2}{k^2 a^2} = \text{new gaussian-beam radius} \tag{22}$$

from which we conclude that

$$C_1 = 1 \tag{23}$$

for a gaussian beam.

Beam-Breakup Case $(a/\rho_o \to \infty)$

From Eq. (14), letting $a = D/2$, we immediately have

$$C_3 = 3.63 \tag{24}$$

(As an aside, we note that, since the transverse irradiance distribution is probably gaussian for this case, the gaussian-beam radius corresponding to Eq. (24) is

$$w' = \left[3.63z^2/k^2\rho_o{}^2\right]^{1/2} \quad .)$$

We now note that the asymptotic intersection of the two above cases occurs at

$$a = 0.525\rho_o = r_o/4$$

$$D = 1.05\rho_o = \frac{r_o}{2} \tag{25}$$

For the uniform, truncated aperture case, this breakpoint occurs at the fundamental point $D = r_o$, which again justifies our taking 2D as the equivalent uniform aperture diameter (Eq. 18).

Wander Case

The determination of the constant C_2 is less straightforward. It can be derived from approximate physical arguments, as discussed below, or from fitting Eq. (20) to the numerical results from Eq. (10). To facilitate this comparison, we rewrite (20) as

$$\frac{\bar{I}_{LT}}{\bar{I}_c} = \frac{1}{1 + \left[C_2\left(\frac{D}{2\rho_o}\right)^{-\frac{1}{3}} + 3.63\right]\frac{D^2}{4\rho_o{}^2}} \tag{26a}$$

$$\frac{\bar{I}_{LT}}{\bar{I}_\infty} = \frac{1}{\frac{1.10\ \rho_o{}^2}{D^2} + \left[\frac{C_2}{3.63}\left(\frac{D_o}{2\rho_o}\right)^{-\frac{1}{3}} + 1\right]} \tag{26b}$$

which correspond to Eqs. (10) and (15) respectively. The best fit occurs if C_2 is obtained from the breakpoint described above, and results in the value ($C_2 = 0.423$). The resulting curves are essentially indistinguishable from

those of Fig. 1. An approximate physical analysis from Titterton,[13] using Kon's[12] mean-square wander angle ($0.76C_n^2 za^{-1/3}$), results in $C_2 = 1.39$ and a less satisfactory fit to the curve.

It should be pointed out, however, that the values obtained from Eqs. (26a,b) are insensitive to C_2. In fact, a good approximation is to let $C_2 = 0$ (see Fig. 2); this suggests that most of the wander effect is contained in the $1/k^2\rho_o^2$ term of Eq. (20).

Since we wish to use this phenomenological description for the wander-tracked case, and most of the wander is contained in this ρ_o^{-2} term, we postulate that the proper coefficient C_2 for the tracked case is negative. Although we do not yet have a reliable Huygens-Fresnel result for the gaussian-beam case, as indicated above we believe that the truncated, uniform aperture results will be substantially similar. In Fig. 3, we plot Eq. (26a,b) with $C_2 = -3.44$, and the similar curves deduced from Ref. 8. This value was chosen so that the maximum from Eq. (26b) would agree with that from Ref. 8, which predicts a gain of 3.4 (5.3 dB) in target irradiance or 10.6 dB in receiver photocurrent over that for a very large transmitter. The peak of the latter curve occurs at $D/\rho_o = 4$ or $D/r_o = 1.9$; this is consistent with the antenna gain realized, and indicates that half the "effective" aperture of 2D is used coherently at this peak.* As will be seen below, the tracking improvement in irradiance fading is also optimized for $3 \lesssim D/\rho_o \lesssim 5$. We point out that the curves of Fig. 3 are generally consistent with those of Figs. 1a, 1b in Ref.1.

Finally, we plot the ratio of the mean irradiance with tracking ($\bar{I}_T$) to that without tracking ($\bar{I}_{NT}$) in Fig. 4, again using the uniform-aperture results of Ref. 8. In lieu of a result for the gaussian beam case, this curve will be used for comparison with experimental results below. The maximum value is predicted to be 6.2 dB. It may be pointed out that the peak in this curve suggests a possibility for instrumenting a "ρ_o-meter", utilizing a point source and an image-tracking, variable aperture test receiver at the target and transmitter respectively.

---

*In the remainder of this report, we identify the wander-tracked mean-irradiance and variance with the subscript T, and the corresponding non-tracking values with the subscript NT, where the latter is identical to the "long-term" case. Also, in plotting the results from Ref. 8, we have interpreted the diameter in that reference as being twice our D, as explained above, and have corrected for the use of ρ_o in the place of r_o.

---

13. P. J. Titterton, Appl. Opt. 12, 423 (1973).

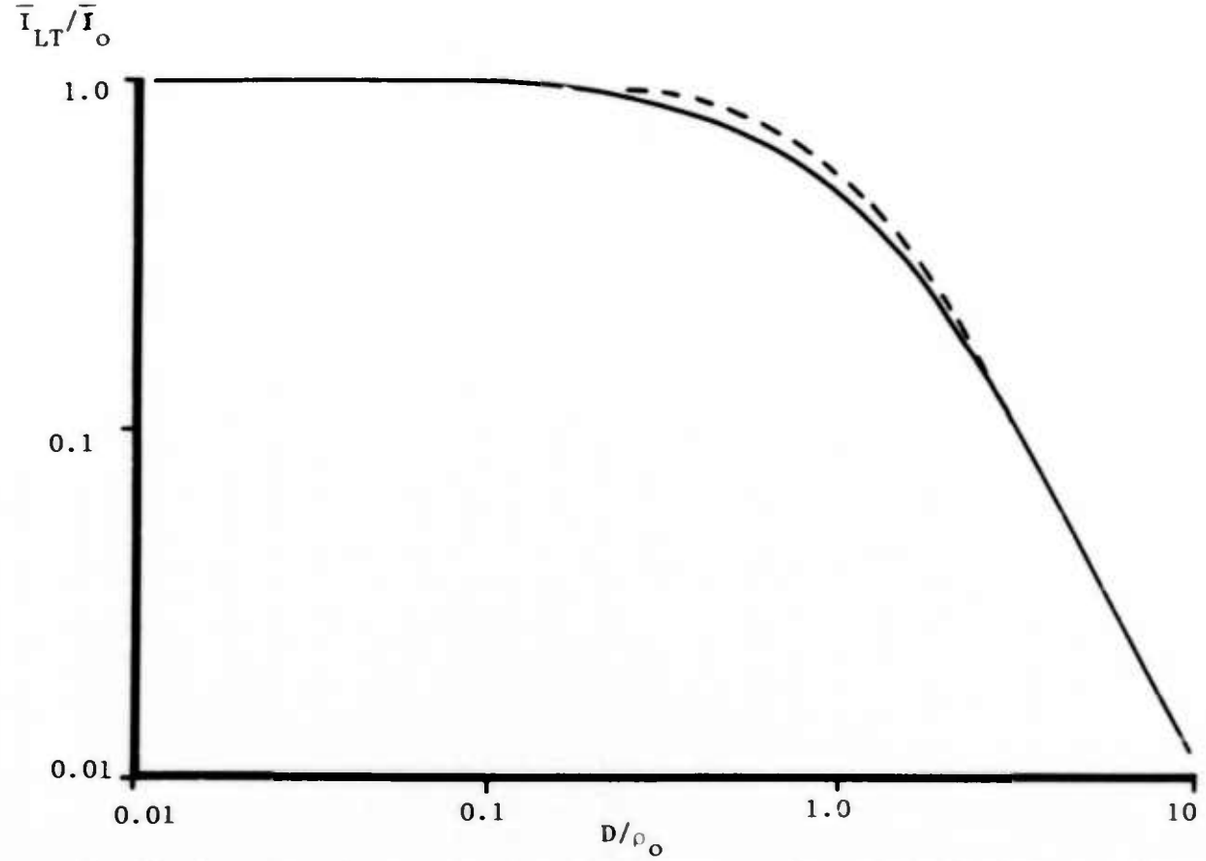

Figure 2. Theoretical $\bar{I}_{LT}/\bar{I}_o$ from Eq. (19) (———) and points from Eq. (26a) with $C_2 = 0$ (-----).

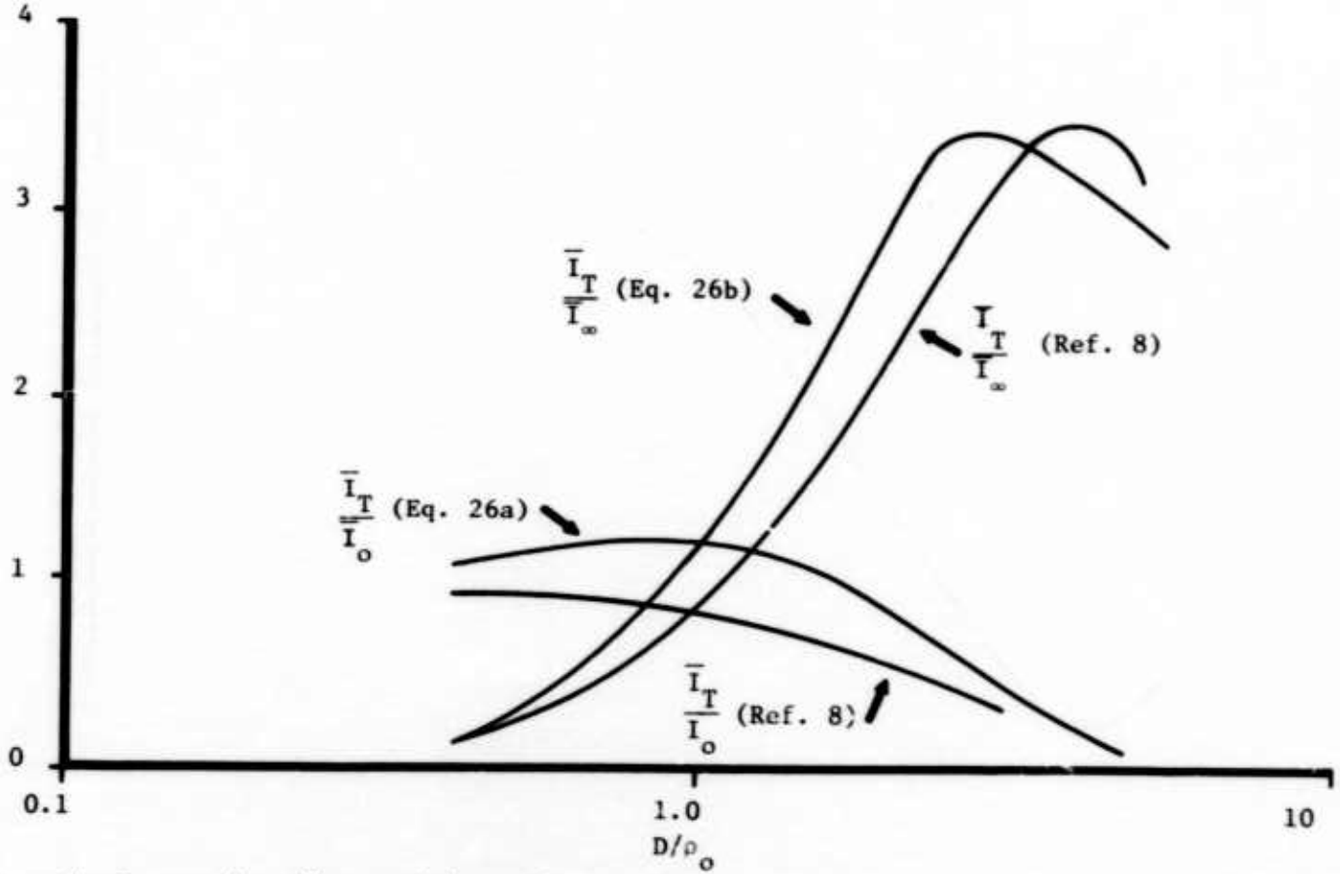

Figure 3. Theoretical mean irradiance with wander-tracking.

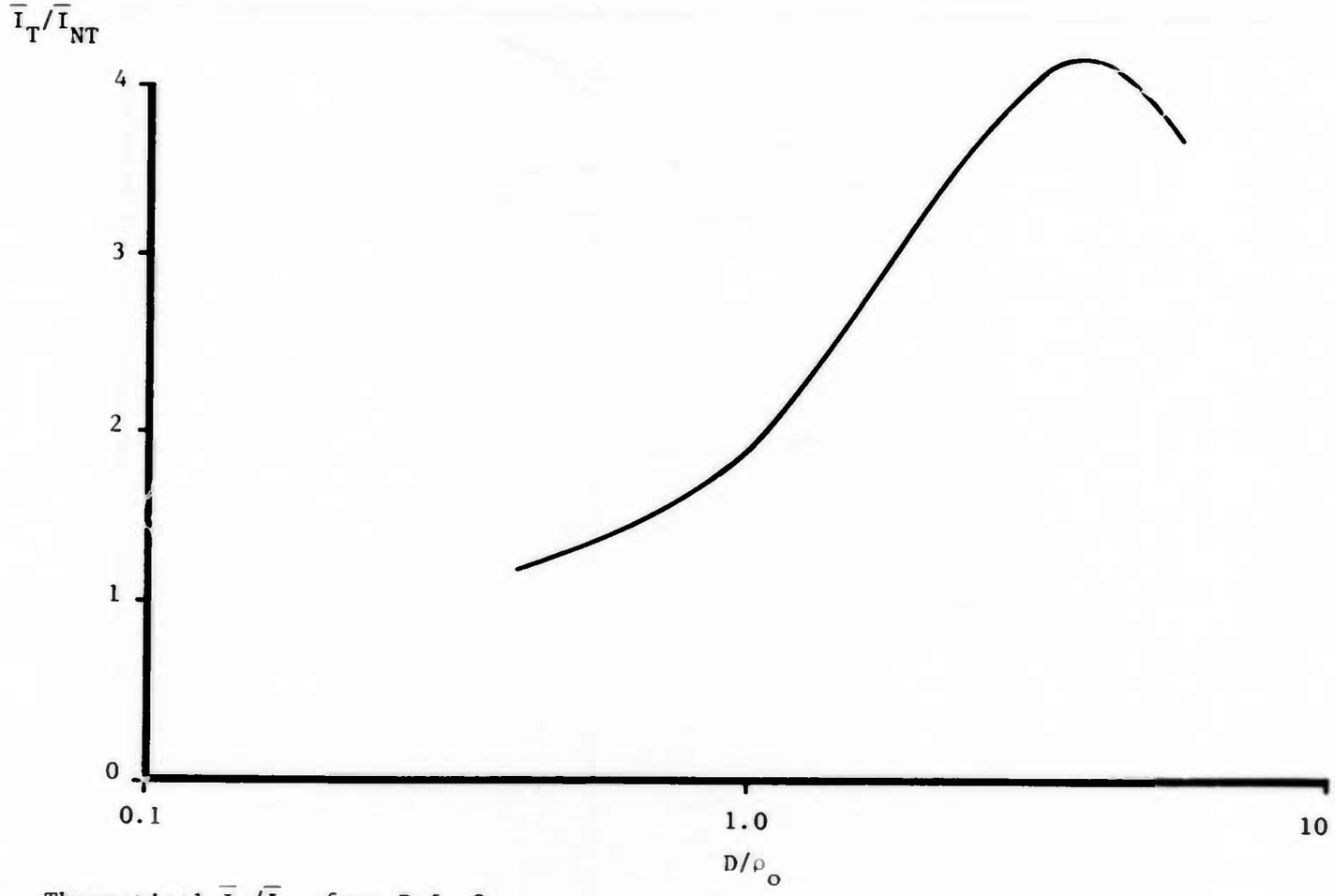

Figure 4. Theoretical $\bar{I}_T/\bar{I}_{NT}$ from Ref. 8.

2. Fluctuations in Irradiance (Fading)

The problem of fading due to beam wander and scintillation is considerably more difficult. In the Huygens-Fresnel formulation, this second moment of irradiance (fourth moment of amplitude) involves an eight-fold integral. The basic expression is given as Eq. (42) in Ref. 14, or equivalently, as Eq. (2.15) in Ref. 15. Until recently, the only attempt to evaluate this expression was in Fried's analysis of "atmospheric modulation noise" (coherent fading) in a heterodyne receiver;[8,15] however, the approximations used in these treatments lead to erroneous results.

Interesting work on this problem was recently reported by Russian investigators.[16] Using the assumptions that the atmospheric perturbation of the propagation Green's function is essentially a phase effect, and that the phase distribution is gaussian, they reduced the problem to a six-fold integral which they then evaluated using Monte Carlo techniques. The result will be seen below to agree in many respects with our phenomenological description. In particular, it predicts a value of unity for the normalized irradiance variance (σ_I^2) at large values of D/ρ_o, which agrees with our predictions.[1] This indicates that the Huygens-Fresnel formulation is valid under conditions of large phase-distortions.

The theoretical results of Ref. 16 can be converted to our parameters by squaring the ordinate and relating the abscissa as follows:

$$\frac{D}{\rho_o} = \left(\frac{\text{(Abscissa, Ref. 16)}}{\sqrt{2}} \right)^{6/5} \quad . \qquad (27)$$

The results are shown in Fig. 5. A major point is that, for a focused beam, the treatment of Ref. 16 results in a curve which is a universal function of the spherical-wave phase structure function or D/ρ_o. We believe that this is not entirely correct, and that the transmitter size or Fresnel number is explicitly involved, as explained in the phenomenological description below. This means that different curves should be derived depending upon which parameter (D or ρ_o) is varied; the results of Ref. 16 are apparently best related to the fixed-D, variable-ρ_o case.

---

14. H. T. Yura, Applied Optics 11, 1399-1406, June 1972.
15. D. L. Fried, J. Quantum Electr. QE-3, 213 (1967).
16. V. A. Banakh, et al, J. Opt. Soc. Am. 64, 516-518, April 1974.

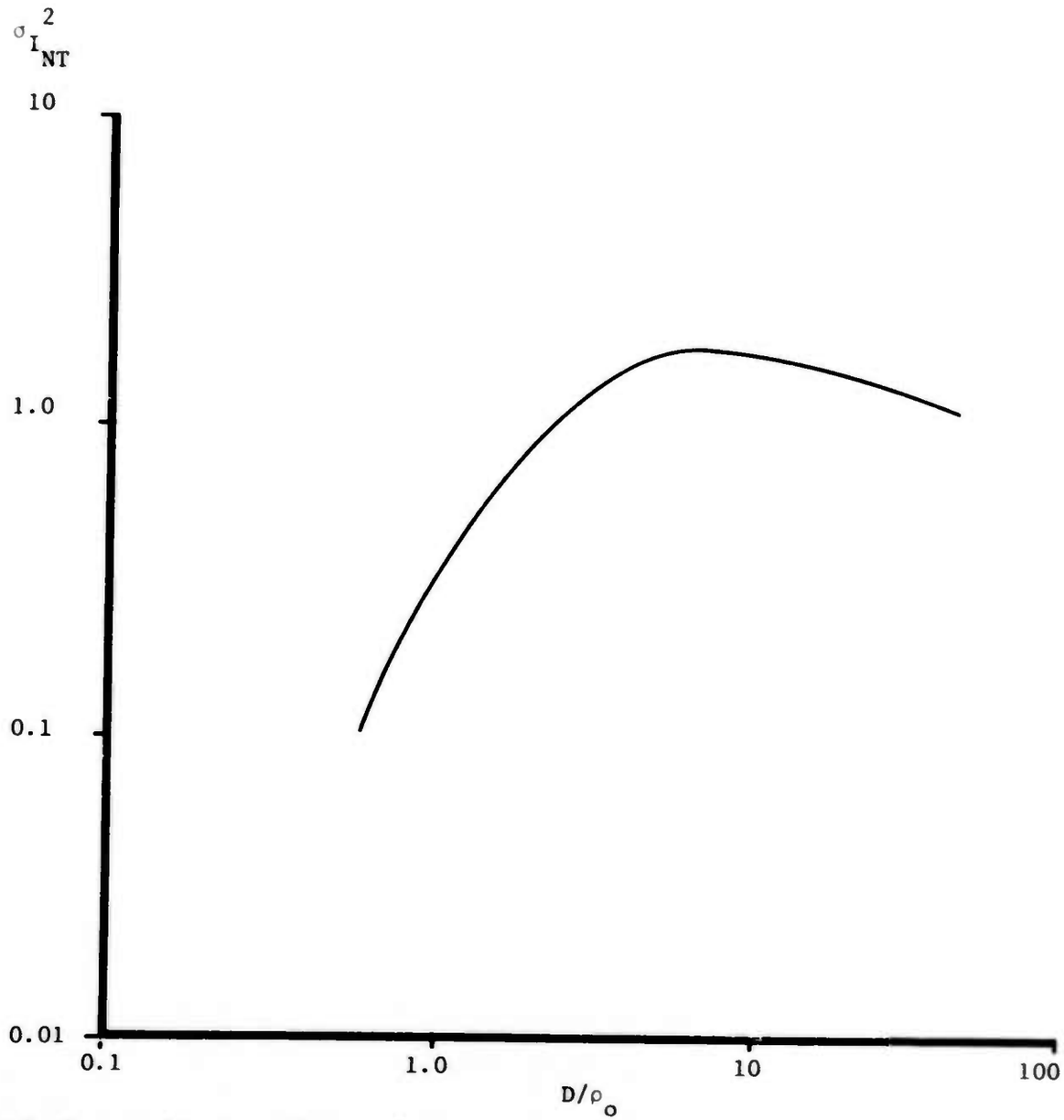

Figure 5. Theoretical normalized variance of irradiance without wander-tracking, from Ref. 16.

The fact that the assumptions used in Ref. 16 lead to inexact results is clearly seen through inspection of Eq. (17) of that reference for the mean irradiance: it is identical to the exact expression (Eq. 5 of the present report, with $\bar{p} = 0$) only for the focused case. The inexactness is probably related to the dropping of the amplitude term in the perturbation function.

We intend to pursue the implications of this interesting approach further, and to attempt to obtain a numerical solution for the full eight-fold expression. It will also be of great interest to incorporate the wander-tracking results when they are available. In the latter case, for a focused beam, the primary point of interest is whether or not the "transmitter smoothing of scintillations" is predicted by the Huygens-Fresnel formulation, in agreement with first-order theory.[17-19] This point will be discussed further below.

We now review the phenomenological description of the fading, with some added considerations over those reported in Refs. 1,2. We discuss three independent fading mechanisms: wander-fading, first-order scintillation, and coherent fading (beam-breakup scintillation).

Wander Fading

Using Titterton's development in Ref. 13, we write the normalized irradiance variance due to wander as

$$\sigma_{I\ \text{Wander}}^2 = \frac{4\gamma^2}{4\gamma + 1} \quad , \tag{28}$$

where γ is defined as the ratio of the mean-square wander angle to the short-term beamspread angle. Using Eq. (20), we write this as

$$\gamma = \frac{|C_2| \left(\frac{D}{2\rho_o}\right)^{-\frac{1}{3}} \frac{1}{k^2 \rho_o^{\,2}}}{\frac{4}{k^2 D^2} + \left[- |C_2| \left(\frac{D}{2\rho_o}\right)^{-\frac{1}{3}} + 3.63 \right] \frac{1}{k^2 \rho_o^{\,2}}}$$

---

17. A. Ishimaru, Radio Science 4, 295 (1969).
18. D. L. Fried and R. A. Schmeltzer, Applied Optics 6, 1729-1737, Oct. 1967.
19. J. R. Kerr and R. Eiss, J. Opt. Soc. Am. 62, 682 (1972).

$$= \frac{0.315\,|C_2|\,\left(\frac{D}{\rho_o}\right)^{5/3}}{1+\left[-|C_2|\times 0.315\left(\frac{D}{\rho_o}\right)^{-\frac{1}{3}}+0.91\right]\frac{D^2}{\rho_o{}^2}} \qquad (29)$$

where we interpret C_2 as the negative number relating to the wander-tracking results discussed above; this coefficient is taken as the best measure of the effective wander. We then combine Eqs. (28, 29) to write

$$\sigma_{I_{Wander}}^2 = \frac{0.397\,|C_2|^2\left(\frac{D}{\rho_o}\right)^{\frac{10}{3}}}{\left\{1+\left[-0.315\,|C_2|\left(\frac{D}{\rho_o}\right)^{-1/3}+0.91\right]\frac{D^2}{\rho_o{}^2}\right\}\left\{1.26\,|C_2|\left(\frac{D}{\rho_o}\right)^{5/3}+1+\left[-0.315\,|C_2|\left(\frac{D}{\rho_o}\right)^{-1/3}+0.91\right]\frac{D^2}{\rho_o{}^2}\right\}} \qquad (30)$$

For the particular choice of C_2 discussed above (-3.44), this becomes

$$\sigma_{I_{Wander}}^2 = \frac{4.70\left(\frac{D}{\rho_o}\right)^{\frac{10}{3}}}{\left\{1+\left[-1.08\left(\frac{D}{\rho_o}\right)^{-\frac{1}{3}}+0.91\right]\frac{D^2}{\rho_o{}^2}\right\}\left\{4.33\left(\frac{D}{\rho_o}\right)^{\frac{5}{3}}+1+\left[-1.08\left(\frac{D}{\rho_o}\right)^{-\frac{1}{3}}+0.91\right]\frac{D^2}{\rho_o{}^2}\right\}} \qquad (30a)$$

We note that the wander-fading term is a universal function of D/ρ_o.

The general behavior of Eq. (30) can be seen by approximating the function in terms of four log-linear realms (cf. Fig. 21, Ref. 2). This is shown in Fig. 6. The breakpoints occur at values of D/ρ_o on the order of 1/2, 1, and 100, with a maximum value of $\sigma_{I_{wander}}^2$ on the order of (in excess of) unity.

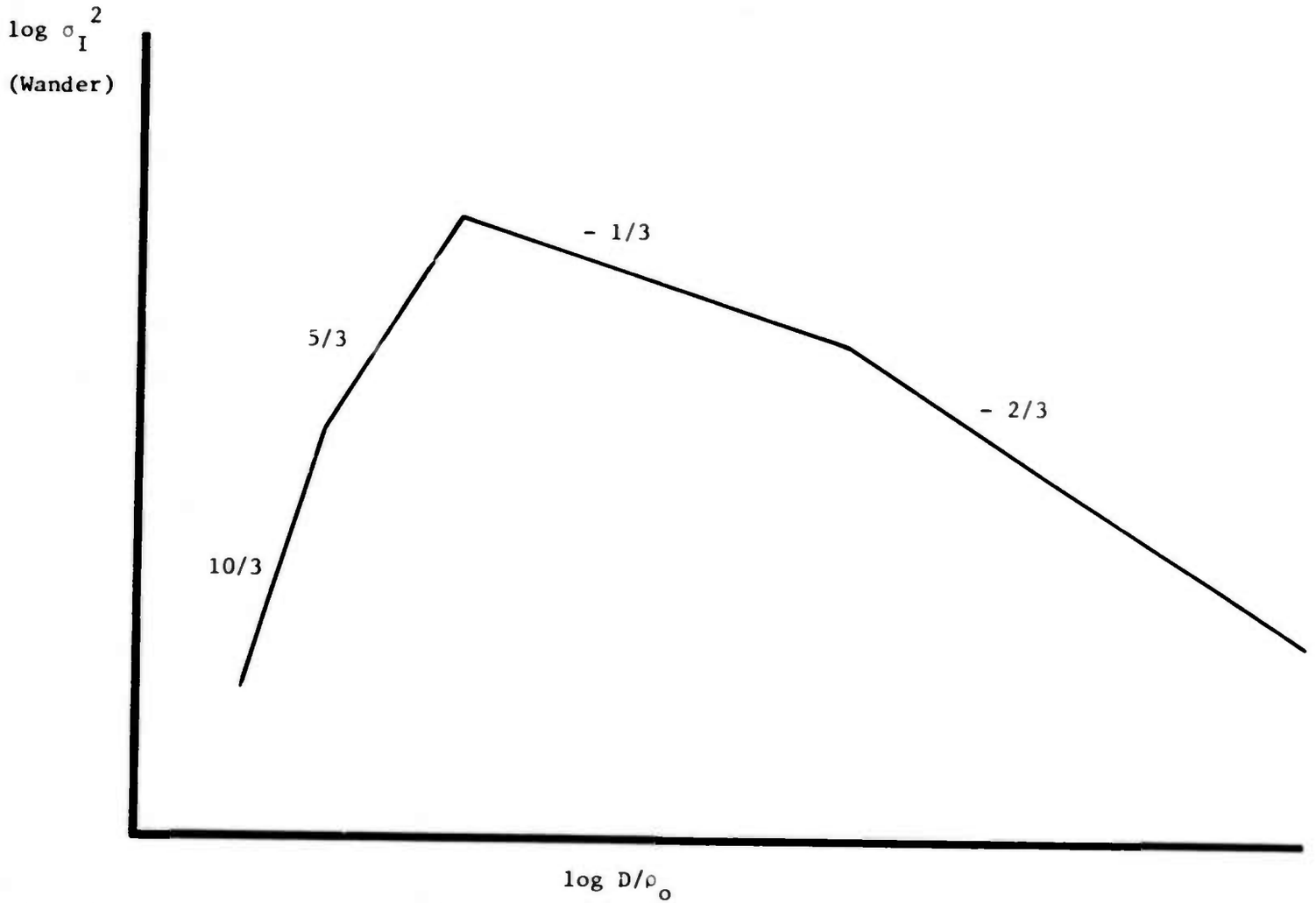

Figure 6. General behavior of Eq. (30) for fading due to beam wander.

First-Order Scintillation

By first-order scintillation, we mean that which would be predicted for a focused transmitter by the Rytov approach (Refs. 17-19). This includes the "transmitter smoothing of scintillations". It is now clear[1,2,20] that in order for this effect to exist, it is necessary that $\rho_o > D >> (z/k)^{1/2}$; the requirement that ρ_o be greater than $(z/k)^{1/2}$ is dimensionally equivalent (Eq. 32 below) to requiring that the scintillations from a point source be weak (unsaturated). As explained below in conjunction with the experimental data, it also appears that the inequality requirement ($\rho_o/D>1$) may in fact be ($\rho_o/D>>1$): a small amount of atmospheric phase distortion over the aperture may destroy the smoothing effect.

The customary way to write this fading term is[1,8,15]

$$\sigma^2_{I_{Scintillation}} = e^{4\beta'\sigma_\chi^2} - 1 \tag{31}$$

where σ_χ^2 is the log amplitude variance for a point source, and β' is the smoothing factor. In writing this it is assumed that the fluctuations are log normal. β' is a function of $D/(z/k)^{1/2}$ or the Fresnel number, and for large Fresnel numbers[19] is proportional to $D^{-7/3}$. Noting that

$$\sigma_\chi^2 = 0.228 \left[\frac{\sqrt{z/k}}{\rho_o}\right]^{5/3} \tag{32}$$

and assuming that $\beta'\sigma_\chi^2 << 1$, we may write (31) as

$$\sigma^2_{I_{Scintillation}} \approx 0.912\ \beta' \left[\frac{\sqrt{z/k}}{\rho_o}\right]^{5/3}$$

$$= 0.912\ f\left(\frac{D}{\sqrt{z/k}}\right) \cdot \left[\frac{\sqrt{z/k}}{\rho_o}\right]^{5/3} \tag{33}$$

This is obviously not a universal function of D/ρ_o.

---

20. K. S. Gochelashvily, "Focused Irradiance Fluctuations in a Turbulent Medium", Optica Acta 20, 193 (1973).

Coherent Fading

Coherent fading or beam-breakup scintillation corresponds in a reciprocal heterodyne receiver to "atmospheric modulation noise".[8,15] It becomes predominant when $D \geq$ some fraction of ρ_o. The correct form for this fading term is not known, but from the results of Ref. 16 and physical reasoning we expect it to be an increasing and perhaps nearly universal function of D/ρ_o. However, contrary to Refs. (8, 15), we do not expect it to increase without limit. For large values of D/ρ_o, we invoke an analysis of Brown's[21] involving $N = D^2/\rho_o^2$ oscillators having identical frequencies but independent mutual phases; the result is

$$\sigma_{I_{\text{Coherent Fading}}}^2 \approx 1 - \frac{1 - \left(e^{4\sigma_\chi^2} - 1 \right)}{D^2/\rho_o^2} \qquad (34)$$

$$\frac{D}{\rho_o} >> 1$$

which approaches unity for large (D/ρ_o). The expression is again not a universal function of (D/ρ_o), since it involves σ_χ^2 as given in Eq. (32). For $\sigma_\chi^2 << 1$ it is given by

$$\sigma_{I_{\text{Coherent Fading}}}^2 \left(\frac{D}{\rho_o} >> 1,\ \sigma_\chi^2 << 1 \right) \approx 1 - \frac{1 + 4\sigma_\chi^2}{\frac{D^2}{\rho_o^2}}$$

$$\approx 1 - \frac{\rho_o^2}{D^2} \qquad (34a)$$

For values of σ_χ^2 exceeding 0.17, the expression (34) indicates that $\sigma_{I_{\text{coherent fading}}}^2$ exceeds unity for sufficiently large D/ρ_o. The general behavior of the coherent fading term is shown in Fig. 7, where the hump is seen to be significant as σ_χ^2 approaches the saturation value of 0.6.

---

21. W. P. Brown, Jr., "Research in Interaction of Coherent Light with Solids and with Turbulent Atmospheres", Research Report, Hughes Research Laboratories, Malibu, Calif., May 1972.

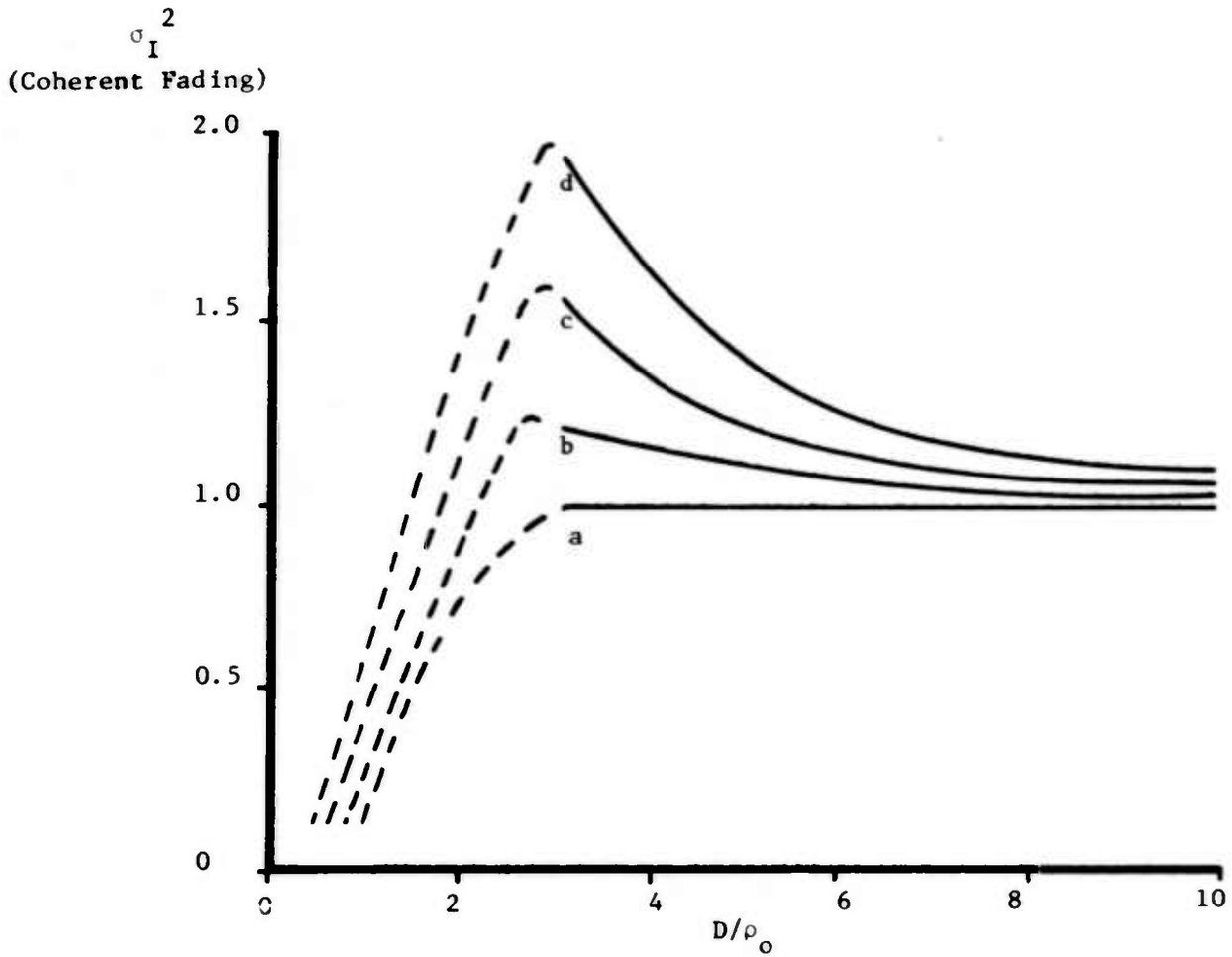

Figure 7. Normalized irradiance variance due to coherent fading for

curve	σ_χ^2
a	0.17
b	0.33
c	0.49
d	0.60

Combined Fading

In order to consider combined fading, we add Eqs. (30), (31 or 33), and the curve of Fig. 7. Since the latter two components are not universal functions of D/ρ_o, we must distinguish whether the aperture size or the coherence scale are being varied. In the former case, we must specify σ_χ^2 or $\rho_o/(z/k)^{1/2}$; we then obtain curves such as that shown in Fig. 8. In the latter case, we must specify the Fresnel number, and we obtain curves such as that shown in Fig. 9; this result with wander effects is in general agreement with that of Fig. 5.

With the exception of the exact behavior of coherent fading, and the knowledge of the best value for C_2, sufficient information is given here to construct a physically-based prediction of $\sigma_{I_{total}}^2$ vs.D (given σ_χ^2) or vs. ρ_o (given Fresnel number). Furthermore, the predicted behavior with wander tracking is readily determined by dropping the contribution from that mechanism. In particular, the curve of Fig. 9 will be shown later to agree well with both the tracking and non-tracking experimental data on fading. Also, the curve of Fig. 8 suggests an alternative "ρ_o-meter" to that mentioned above; a non-image-tracking receiver would be utilized to determine the aperture size D for maximum fluctuations in the photocurrent.

Finally, we emphasize that, in the presence of wander tracking, there is definitely an optimum aperture size from the standpoint of fading as well as mean irradiance, and too large an aperture can have significantly deleterious effects on fading performance.

3. Other Aspects

Generalized Focus Conditions; Nonuniform Turbulence (Vertical Propagation)

For the case of a general turbulence profile over the path, the atmospheric effect on the mean irradiance is still represented by Eq. (9), where

$$\rho_o = \left[1.45\, k^2 \int_o^z C_n^2\,(s) \left(\frac{s}{L}\right)^{5/3} ds \right]^{-3/5} , \qquad (35)$$

and the integration is from the target to the transmitter. The degrading effect of a given level of turbulence on transmitter coherence $\left(\rho_o^{-5/3}\right)$ is most heavily weighted towards the transmitter end. Hence, an uplink beam

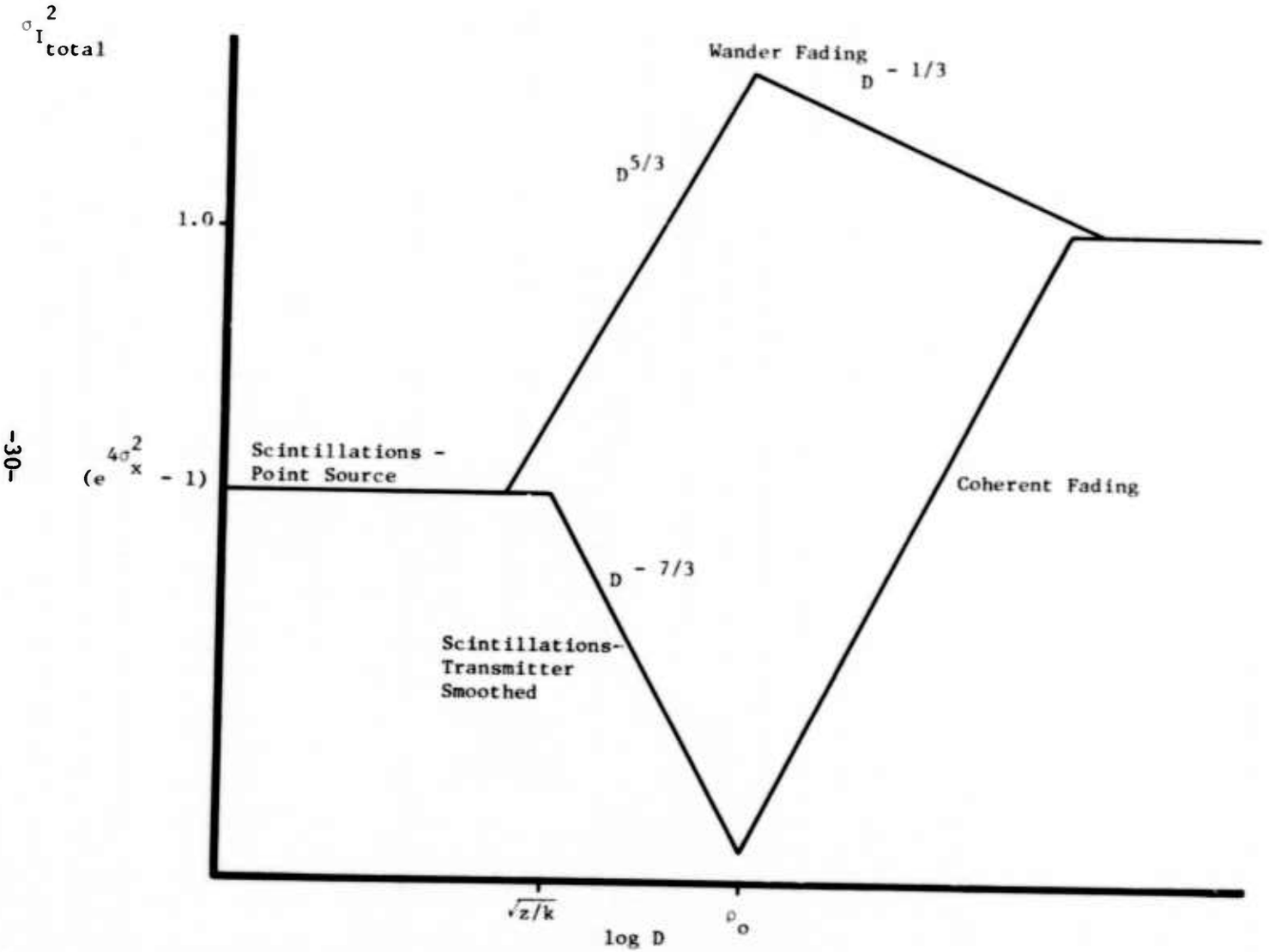

Figure 8. Normalized variance of irradiance vs. transmitter diameter, with and without wander-cancellation.

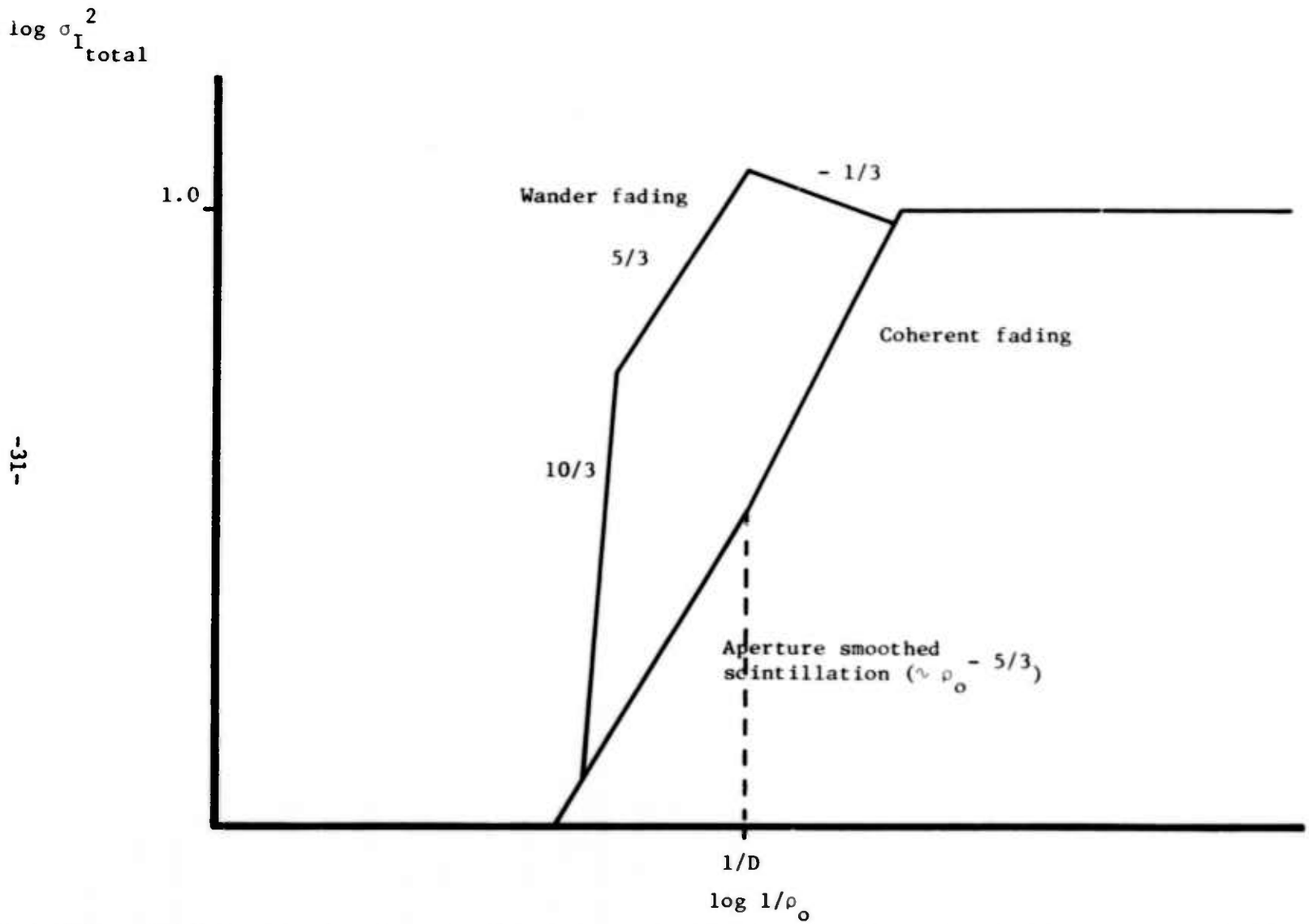

Figure 9. Normalized variance of irradiance vs. coherence scale, with and without wander cancellation.

tends to be incoherent or broken up, while a downlink beam remains intact. In any event, the nonuniform distribution of turbulence over the path is entirely accounted for in the parameter ρ_o.

Let us now consider the effect of an arbitrary beam focus. We write the on-axis mean irradiance from Eq. (5) as

$$\bar{I}_{LT} \sim \int_0^\infty d\rho\ \rho\ e^{-\left(\rho/\rho_o\right)^{5/3}}\ e^{-\rho^2/4\left[\frac{1}{a^2} + k^2a^2\left(\frac{1}{z} - \frac{1}{f}\right)^2\right]}$$

$$= \int_0^\infty d\rho\ \rho\ e^{-\left(\rho/\rho_o\right)^{5/3}}\ e^{-\rho^2/4a'^2} \quad , \tag{36}$$

where

$$a' \equiv \left[\frac{1}{a^2} + \left(\frac{1}{z} - \frac{1}{f}\right)^2 k^2a^2\right]^{-\frac{1}{2}} \tag{37}$$

is the generalized beam parameter. The defocusing term will reduce and wholly determine a' unless a precise focus adjustment (z = f) is used. In any event, if $\rho_o >> a'$, the beam term predominates in Eq. (36); this will apply to a downlink in particular. If $\rho_o << a'$, the atmospheric term predominates regardless of (reasonable) beam adjustment; this applies to a large-aperture uplink. In any far-field case, the actual focus adjustment is not important as long as k^2a^2/f^2 is smaller than $1/a^2$ (Eq. 37).

An important point is that, once a' is determined from Eq. (37) and ρ_o is known, the mean irradiance is determined from the same curve as in the horizontal, focused case. Hence this formulation greatly simplifies the treatment of the nonuniform, general-focus case.

For the wander-tracked case, there will appear an optical-system-dependent correction to the atmospheric term in Eq. (36). This will be significant only for a' on the order of ρ_o, which can be achieved with an uplink beam having a limited aperture size.

Similar reasonings can be applied to the fading. It appears that the results will again indicate that the turbulence profile is entirely contained in ρ_o. However, for a general, defocused beam, the parametric dependencies are complicated. From the first-order theory,[22] which implies wander-tracking, we expect significant transmitter smoothing of scintillations if the aperture is smaller than ρ_o and the turbulent region is confined to the near field of the transmitter. This has not yet been demonstrated from the Huygens-Fresnel equations.

Outer Scale Effects

We have so far in this discussion neglected effects relating to the limitation on the extent of the inertial subrange of turbulence. Lutomirski and Yura have considered the effects of the outer scale,[23,24] and in particular they derived first-order corrections to such quantities as turbulence-induced beamspread and coherence scale ρ_o, where "corrections" refer to the use of the modified von Karmann in place of the (nontruncated) Kolmogorov spectrum.[23]

The critical parameter in their development is the ratio (z/z_c), where z_c is a critical pathlength dependent on the outer scale (L_o), and the ratio is given by

$$\frac{z}{z_c} = 15.3\left(\frac{L_o}{\rho_o}\right)^{5/3} \tag{38}$$

In this expression, ρ_o is the uncorrected or Kolmogorov value. Hence, the outer scale effects are implied to be dependent only on L_o and ρ_o, and not explicitly related to z, C_n^2, k, or D.

The percentage correction of ρ_o is shown as approximately 18%, 25%, and 50% for z/z_c = 100, 10, and 2 respectively. The corrections are such as to increase ρ_o, since the von Karmann spectrum has less energy at small wavenumbers than does the Kolmogorov.

---

22. J. R. Kerr and J. R. Dunphy, J. Opt. Soc. Am. 63, 1 (1973).
23. R. F. Lutomirski and H. T. Yura, J. Opt. Soc. Am. 61, 482-487, April 1971.
24. H. T. Yura, J. Opt. Soc. Am. 63, 107-109, January 1973.

To avoid outer scale effects in experiments, it is apparently necessary to maximize z/z_c. For a given outer scale, this indicates small values of ρ_o. However, it may be desirable to work in the realm $\rho_o > D$ while maintaining a large Fresnel number $\left[\beta = D\,(k/z)^{1/2}\right]$. We therefore write Eq. (38) as

$$\frac{z}{z_c} = \frac{15.3\, L_o^{5/3}}{\left(\frac{\rho_o}{D}\right)^{5/3} \beta^{5/3} \left(\frac{z}{k}\right)^{5/6}} \tag{39}$$

which as expected shows that small wavelengths and pathlengths reduce outer-scale effects. Conversely, in order to perform experiments on outer scale effects, large wavelengths and/or pathlengths are required.

For the 1.6 km pathlength and 6328 Å wavelength utilized in the experiments to be described below, and with L_o = 1m, we have $z/z_c > 100$ in all cases. At 10.6 μ, with $\rho_o/D = 5$, $\beta = 5$, and L_o = 1m, we have $z/z_c = 100$ at a pathlength of z = 100 m. In any event, it should be noted that this treatment predicts a surprisingly large outer scale effect, even for $z >> z_c$.

In recent work,[25] Greenwood and co-workers have empirically determined a small-wavenumber turbulence spectrum which is intermediate between the Kolmogorov and von Karmann.* It would be useful to recompute structure functions and ρ_o based on this spectrum. In particular, the expected effect on beam wander should be computed.

As discussed below, our data (and those of others) clearly indicate a larger component of wander than predicted by our expressions, especially at large values of D/ρ_o, and this is thought to be related to large-scale bending of the (broken-up) beam. This suggests that there is more energy in certain (anisotropic) turbulence scales than any of the spectral models predict.

---

*The small-wavenumber dependence of the modified von Karmann is $\left(\kappa^2 + 1/\mathfrak{b}_o^2\right)^{-11/6}$, while that of Ref. 25 is $\kappa^{-11/6}\left(\kappa + 1/\mathfrak{b}_o\right)^{-11/6}$. In these expressions, $\mathfrak{b} \equiv L_o/2\pi$.

---

25. D. P. Greenwood and D. O. Tarazano,"A Proposed Form for the Atmospheric Microtemperature Spatial Spectrum in the Input Range",RADC-TR-74-19, February 1974.

There is clearly a need for further analytical work and experimentation on the problem of outer-scale effects, which will be important for infrared systems operating over reasonable pathlengths.

Inner Scale Effects

Inner-scale (ℓ_o) effects are governed in the Lutomirski-Yura formulation[3,4] by an expression similar to that for the outer scale. A new critical length z_i is defined, and the inner scale effects are determined by

$$\frac{z}{z_i} = 15.3 \left(\frac{\ell_o}{\rho_o}\right)^{5/3} \tag{40}$$

which is identical in form to Eq. (38). In order to avoid the effects, we require $z/z_i < 1$, which at visible wavelengths and our pathlength of 1.6 km may not always be true. Hence, depending upon the size of the inner scale, some of the data presented below may have been affected. However, as ρ_o is reduced due to stronger and more highly-developed turbulence, ℓ_o will tend to decrease also.

Retro-Reflector Effects

It has been reported[26] that image dancing or "angular scintillation" from a laser-illuminated retro-reflector are substantially greater than is observed from a nearby beacon. For that reason, the wander-tracking results presented below were obtained with a point-beacon which is coincident with the target point-receiver.

We intend to perform quantitative experiments on the retro case, and we point out here that R. Lutomirski[27] has preliminarily analyzed the effect for the near-field case. It appears that this is an important phenomenon for retro-tracking systems.

---

26. J. P. Hansen and S. Madhu, Applied Optics 11, 233-238, February 1972.
27. R. Lutomirski, private communication.

B. Experimental Results

In this section, we discuss experimental results for mean irradiance and fading, with and without tracking, obtained with a 15 cm transmitter over a 1.6 km path at 6328 Å. The range of the independent parameter (D/ρ_o) is $1 \lesssim (D/\rho_o) \lesssim 100$, where the actual variable is ρ_o or strength of turbulence. As discussed below, results for smaller values of this parameter require a shorter range, which has been established and is currently being utilized. We also discuss certain aspects of the wander signal per se.

As a matter of practical necessity, our actual transmitter consists of a truncated-gaussian with an aperture diameter of 15 cm. The experimental results reported here are in preliminary form, in that we have not yet determined the quantitative effect of this truncation. An effective diameter can certainly be found for the first moment of irradiance; a different diameter will apply to the second moment.

For the sake of initial simplicity, the diameter D utilized in plotting the data vs. D/ρ_o was taken as the total aperture diameter of 15 cm. It is apparent that the effective diameter will be less than this value, so that such data points will need to be moved to the left. This will be seen to improve the theoretical-experimental comparison in some cases.

1. Real-Time Irradiance Signals

The smoothed on-axis irradiance vs. time, with and without wander-tracking, is shown for the weak turbulence case $\left(\frac{D}{\rho_o} = 0.97\right)$ in Fig. 10. In the non-tracked case, the beam is initially centered in terms of its wander excursions, and it gradually drifts off due primarily to slow atmospheric refractive effects. The unsmoothed irradiance is shown in Fig. 11a, and the corresponding (ac-coupled) logarithmic signals in Fig. 11b. The low-frequency nature of the wander component of the signal fluctuations is evident.

Similarly, smoothed signals for the strong-turbulence case $(D/\rho_o = 63)$ are shown in Fig. 12. The unsmoothed linear and logarithmic signals are shown in Figs. 13a and 13b respectively. It is apparent that, in the high-turbulence case (beam break-up), the advantage of tracking is primarily limited to the longer-term refractive wander.

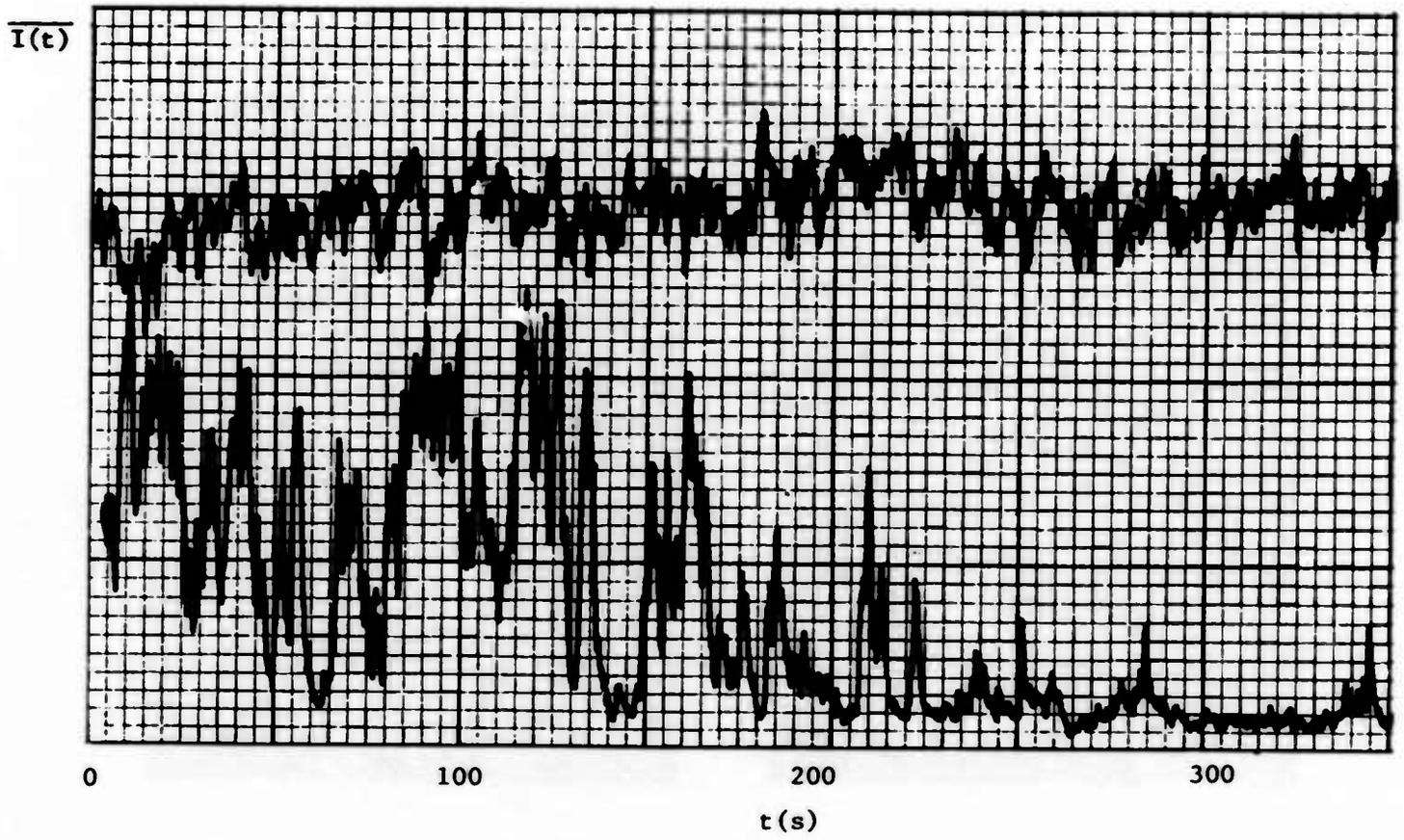

Figure 10. On-axis irradiance vs. time, with (upper trace) and without wander tracking (lower trace), for weak turbulence. The irradiance is smoothed with a 1-sec time constant.

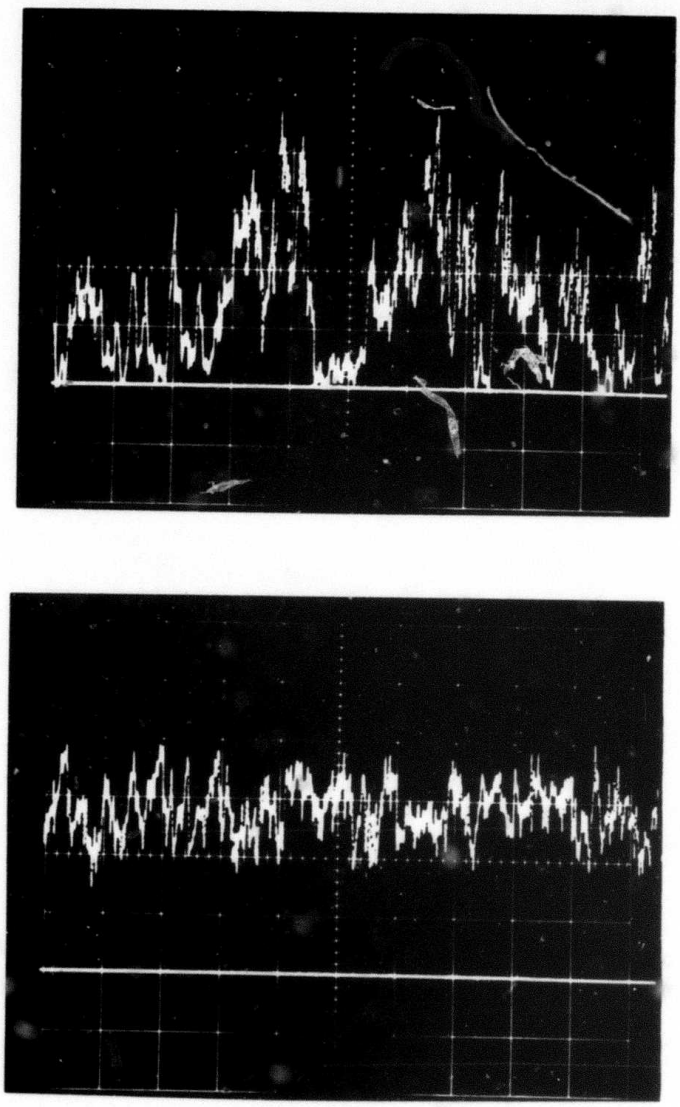

Figure 11a. Unsmoothed irradiance vs. time, for the case of Fig. 10 (lower trace is tracked). The abscissa is 0.5 sec/div.

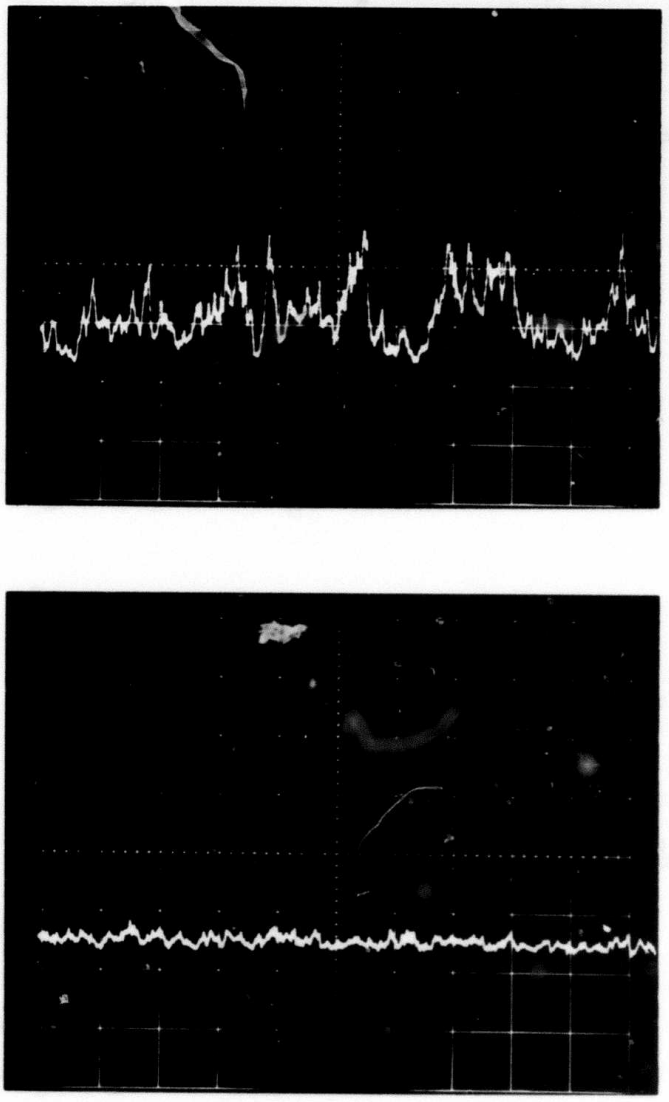

Fig. 11b. Log irradiance vs. time, for the case of Fig. 10 (lower trace is tracked).

Ordinate: One decade/div.
Abscissa: 0.5 sec/div.

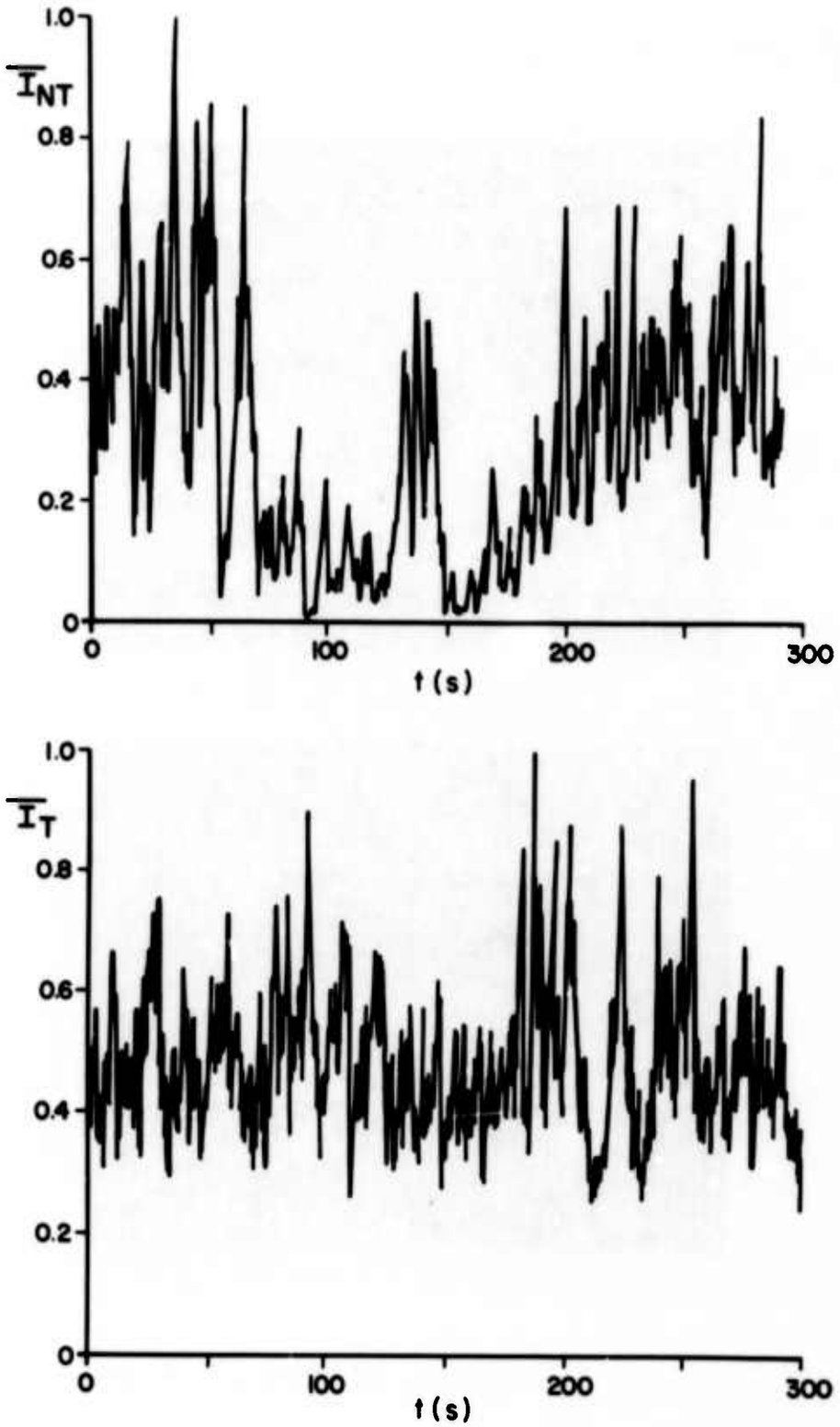

Figure 12. Smoothed (1-sec) irradiance vs. time, with (lower trace) and without wander tracking (upper trace), for strong turbulence.

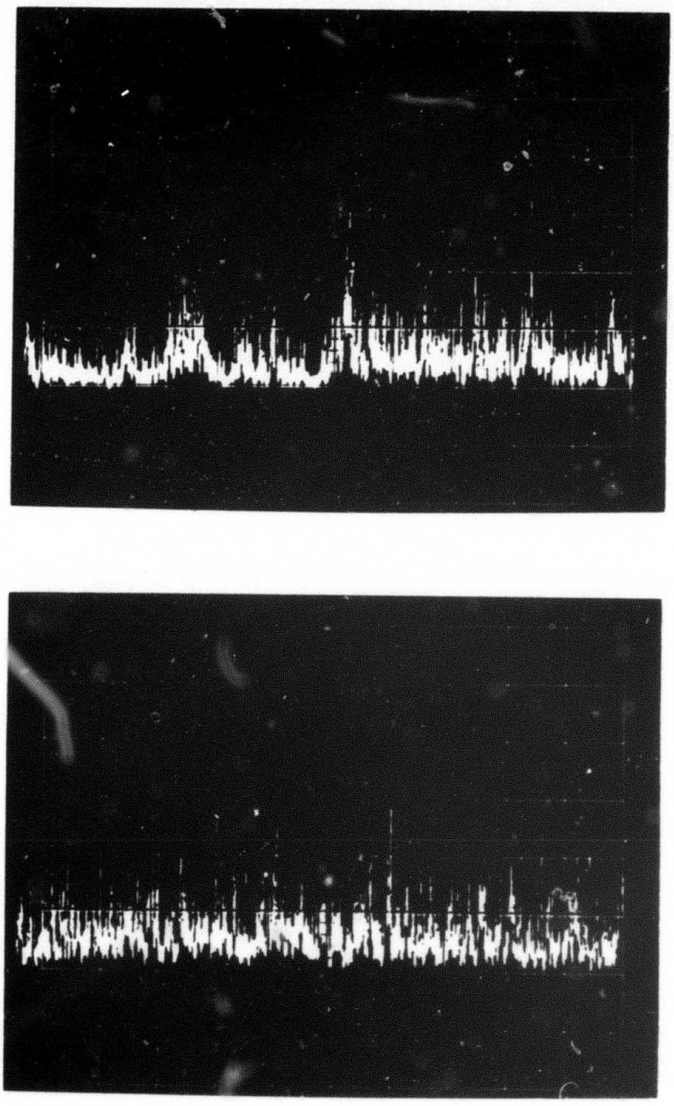

Figure 13a. Unsmoothed irradiance vs. time, for the case of Fig. 12 (lower trace is tracked). The abscissa is 0.5 sec/div.

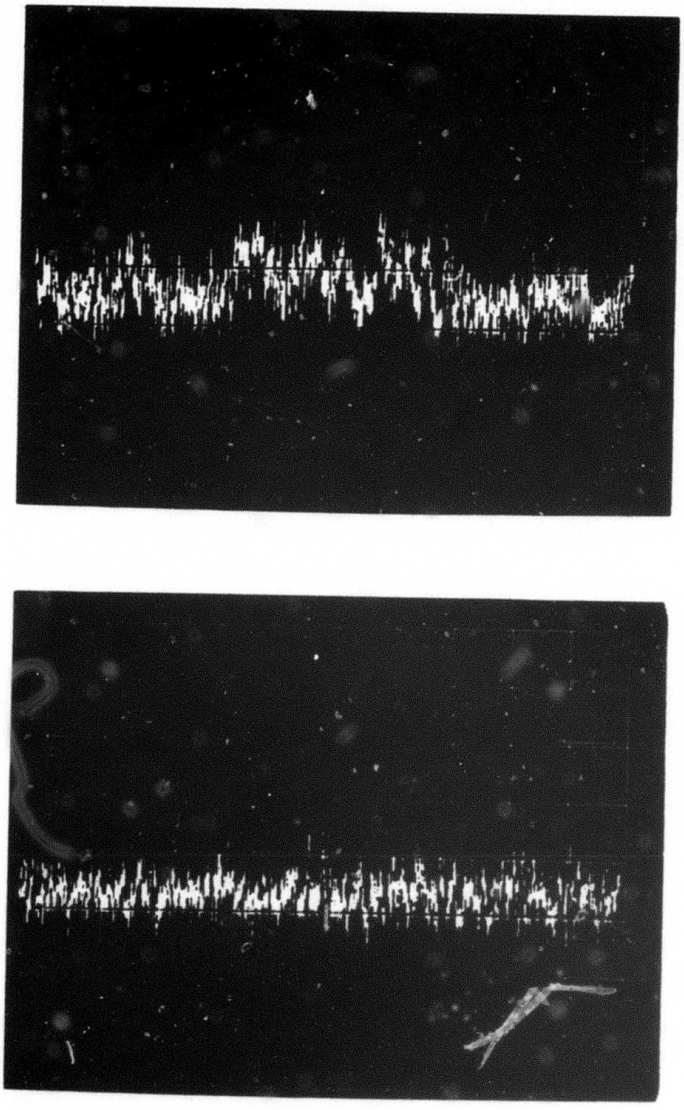

Figure 13b. Log irradiance vs. time, for the case of Fig. 12 (lower trace is tracked).

Ordinate: one decade/div.
Abscissa: 0.5 sec/div.

2. Mean Irradiance

The mean on-axis irradiance for the non-tracked and tracked cases is shown in Fig. 14 as a function of (D/ρ_o). These values were corrected for transmitter output-power variations from run-to-run. Since the aperture D was fixed, the appropriate theoretical curves for comparison are those of $\bar{I}_{NT,T}$ normalized by $\bar{I}_0$ (Figs. 1 and 3). As discussed below, small values of D/ρ_o could not be achieved over this path with reasonable turbulence, and hence $\bar{I}_0$ is not accurately known. However, from Fig. 3, we may expect that the largest $\bar{I}_T$ at small (D/ρ_o) is approximately equal to $\bar{I}_0$, and this normalization is used for fitting the ordinate to the data. The previously-mentioned bias in the abscissa is evident. It is noted that wander-tracking has more of an advantage than predicted at high D/ρ_o, as is generally observed in these experiments. This also agrees with the observations of Gilmartin and Holtz.[28] Also, a portion of the $\frac{\bar{I}_{NT}}{\bar{I}_0}$ data points may be depressed somewhat owing to longer-term refractive effects, i.e., which may show up in the 2 minute averages used. This is discussed further below.

The ρ_o^{-2} dependence of $\bar{I}$ for increasing (D/ρ_o) is generally borne out. For lower strengths of turbulence, the dependence of instantaneous beam spread $\left(\sim \bar{I}_T^{-1}\right)$ has been empirically stated[29] to be $\sim \gamma \equiv C_n^{0.85} z^{0.62} k^{0.65}$; we find a correlation coefficient of 0.89 for $\gamma < 10$, thus corroborating that observation. For $\gamma > 10$, the correlation coefficient is 6.8×10^{-4}, but we expect an approach to a (ρ_o^2) dependence in that regime. The correlation coefficient for $\left(I_{NT} \sim \rho_o^{-2}\right)$ is 0.59 for $\frac{D}{\rho_o} > 10$.

In Fig. 15, we show the ratio $\left(\bar{I}_T/\bar{I}_{NT}\right)$ vs. (D/ρ_o). For comparison, the theoretical curve of Fig. 4 is also shown. The tracking advantage is generally higher than expected; more data are being taken.

3. Fluctuations in Irradiance

The normalized variance of irradiance, with and without tracking, is shown vs. (D/ρ_o) in Fig. 16a. These results compare nicely with the curves of Fig. 9, which are shown again. For comparison with the non-tracked case, we also show the curve from Fig. 5 (Ref. 16).

---

28. T. J. Gilmartin and J. Z. Holtz, "Focused Beam and Atmospheric Coherence Measurements at 10.6μ and 0.63μ", preprint, Lincoln Laboratories, October 1973.
29. J. A. Dowling and P. M. Livingston, J. Opt. Soc. Am. 63, 846 (1973).

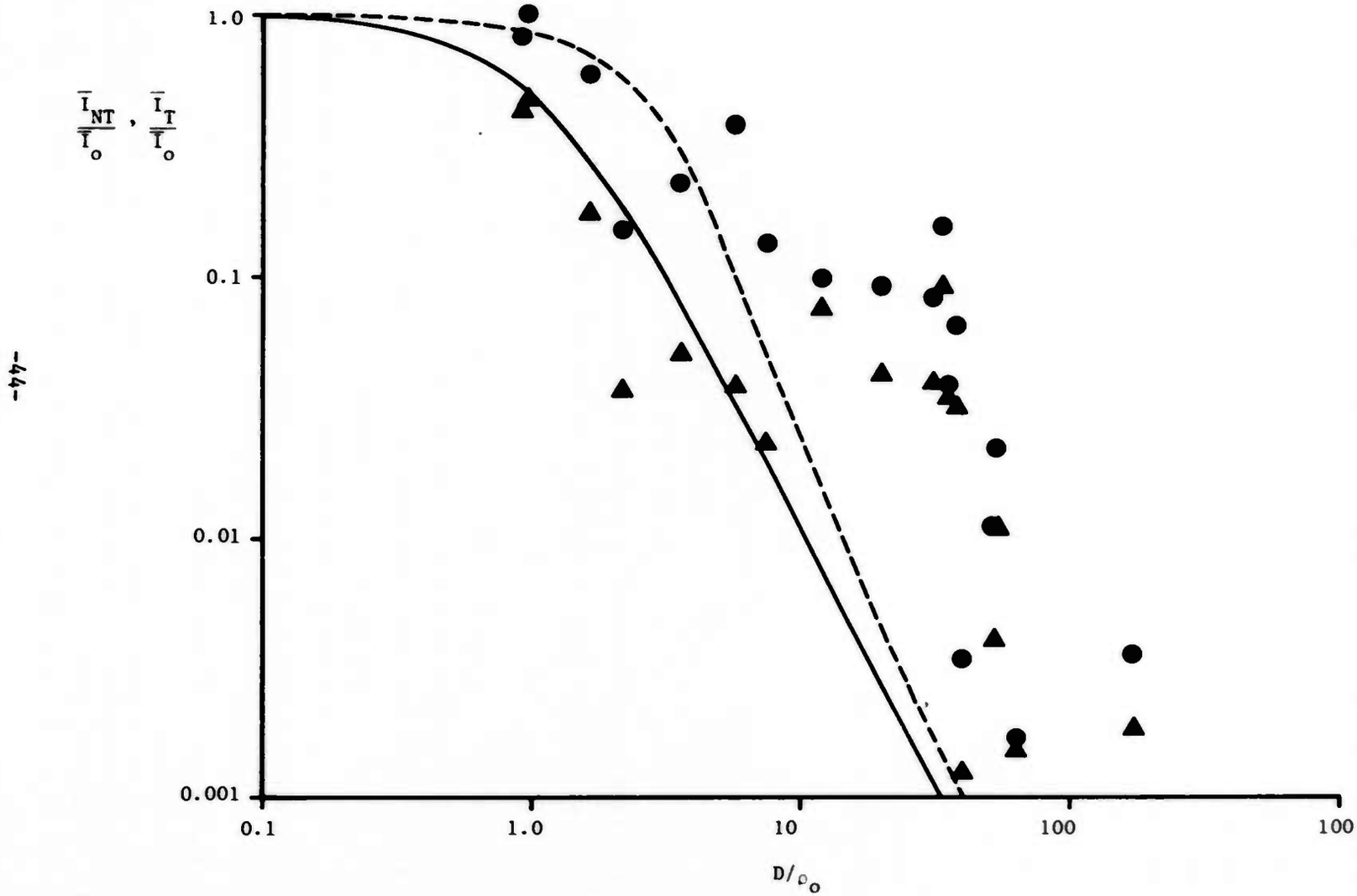

Figure 14. Experimental values of I_{NT}/I_0 (▲) and I_T/I_0 (●) vs. D/ρ_o. The theoretical curves are from Fig. 1 (———) and Fig. 3 (Ref. 8) (- - - -) respectively.

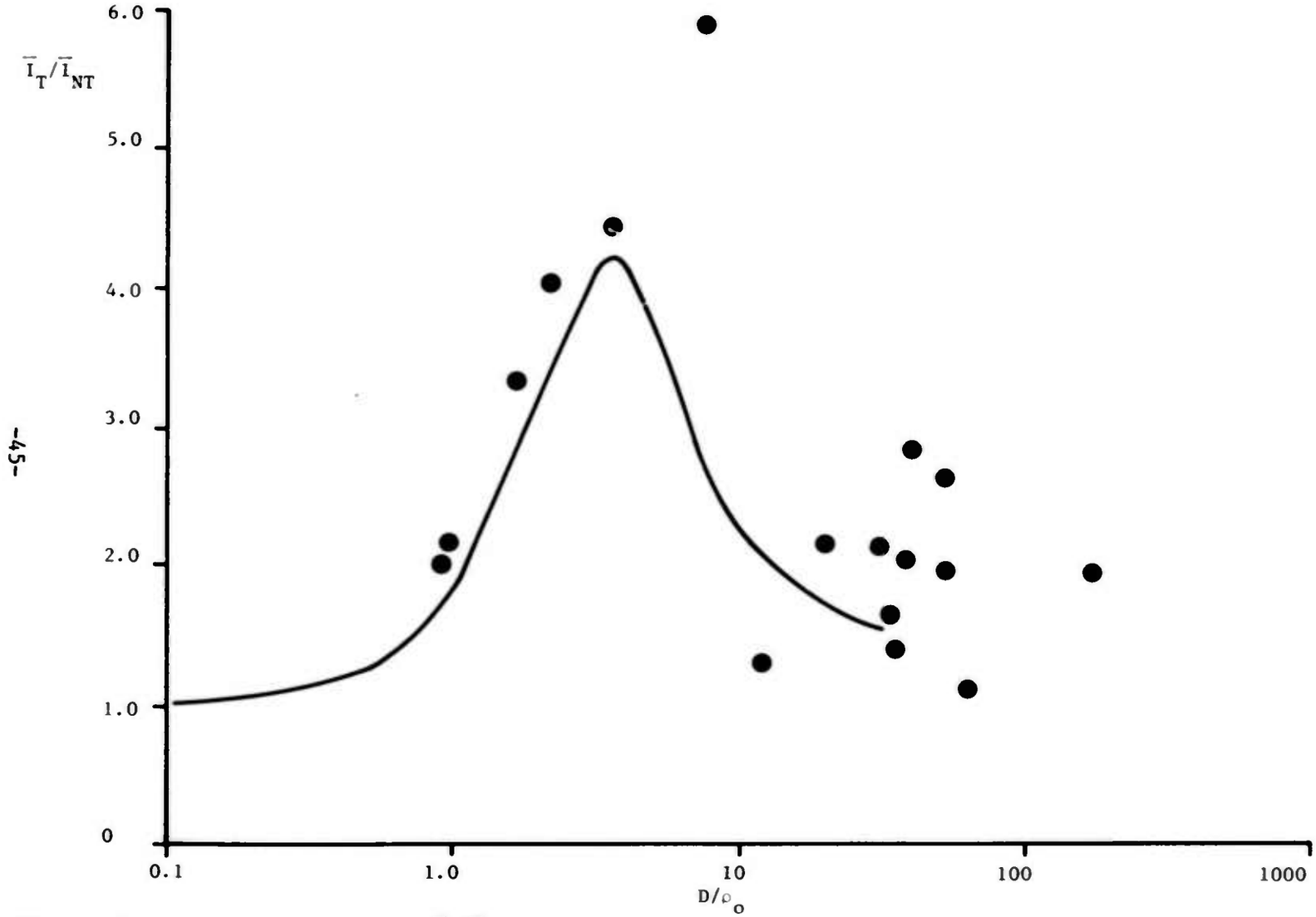

Figure 15. Experimental values of $\bar{I}_T/\bar{I}_{NT}$ vs. D/ρ_o. The theoretical curve is from Eq. 4 (Ref. 8).

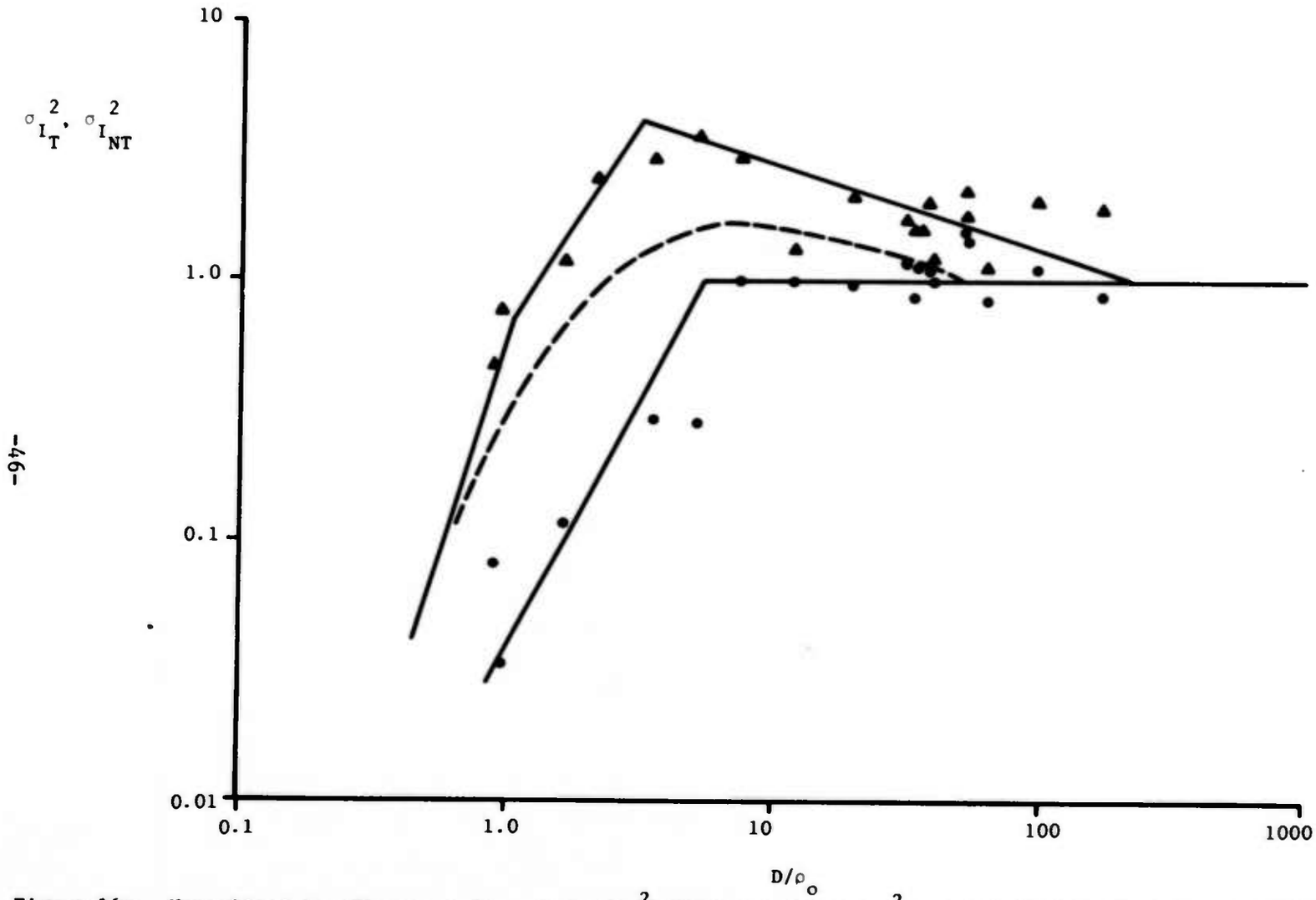

Figure 16a. Normalized irradiance variance with ($\sigma_{I_T}^2$)(●) and without ($\sigma_{I_{NT}}^2$) (▲) tracking, vs. D/ρ_o. The theoretical curves from Figs. 5 (-----) and 9 (———) are also shown.

The ratios of the corresponding tracked and non-tracked variances of Fig. 16a are shown in Fig. 16b. The advantage remains substantial for $\frac{D}{\rho_o} >> 1$, which again suggests large-scale wander effects greater than are included in the theory. For the tracked case, the asymptote is seen to be unity as expected; this would also be true for the non-tracked case at sufficiently large (D/ρ_o). More data are being taken.

It may be pointed out that the reduction in variance for the tracking case is much more substantial if the target signal is low-pass filtered,[1] or alternatively, if a finite (but small) target-receiver aperture is used.

If we process the fading signal directly for the log amplitude, rather than the linear irradiance, and then replot the abscissa in terms of the Rytov log-amplitude variance (σ_{χ}^2) for a point source, we obtain the curve of Fig. 17. In this graph, $D/\rho_o = 1$ corresponds to $\sigma_{\chi_T}^2 = 3.7 \times 10^{-3}$, and for values substantially larger than this we expect log normality and a simple relationship between the ordinates of Figs. 16a and 17 (i.e., Eq. 31 with $\beta^2 = 1$). In particular, the asymptote $\sigma_I^2 = 1$ corresponds to $\sigma_{\chi}^2 = 0.17$, and 2 corresponds to 0.27. It is interesting to note that, for the non-tracked case, which is not log-normal at small values of the abscissa in Fig. 17, the value of the log amplitude variance is more or less constant regardless of the turbulence level. In such a case, we expect the same to be true for the dynamic range of the fading.

The probability distributions for log irradiance are shown in Fig. 18 for the tracking and non-tracking cases in weak turbulence ($D/\rho_o = 0.97$). The residual non-log-normality in the tracking case is related to the details of fading for an approximately-diffraction-limited focal spot. The curve for the non-tracking case remains to be interpreted in terms of the statistics of wander-fading.[13] For strong turbulence ($D/\rho_o = 173$), nearly-log-normal distributions are observed, especially with wander-tracking (Fig. 19).

The spectra of the log fading signal for weak turbulence ($D/\rho_o = 0.97$) are shown in Fig. 20, for the tracking and non-tracking cases.* The significant spectral components are below e.g., 10 Hz, and are sharply reduced by tracking, indicating that wander is predominant. It is also interesting to

---

*In the spectra of Figs. 20-22, the transverse wind speed was not sufficiently large to measure meaningfully, while in Fig. 23, it was 1.4 m/sec. The general conclusions drawn here are not dependent on wind-speed normalization.

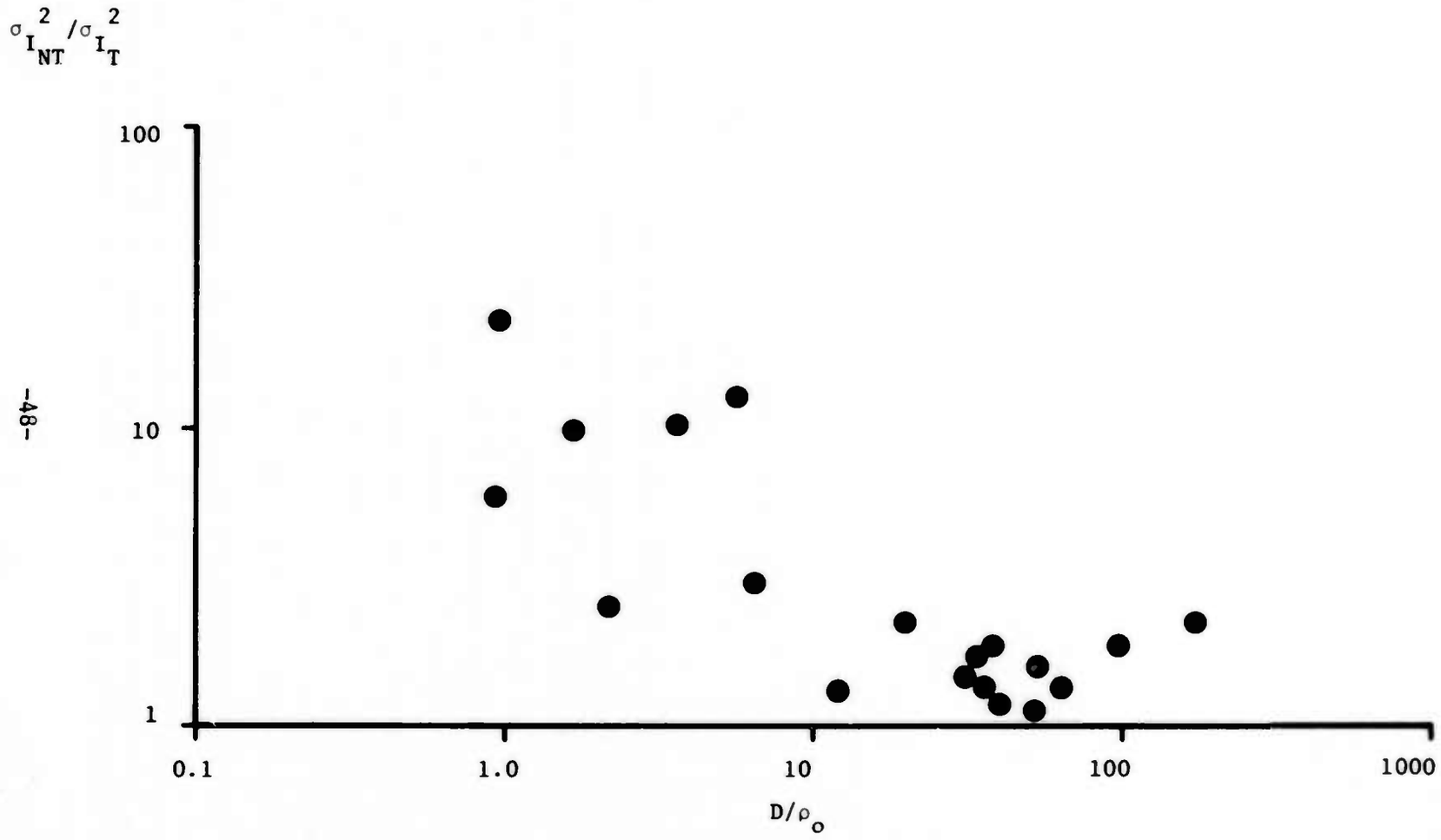

Figure 16b. Values of $\sigma_{I_{NT}}^2/\sigma_{I_T}^2$ vs. D/ρ_o corresponding to Fig. 16a.

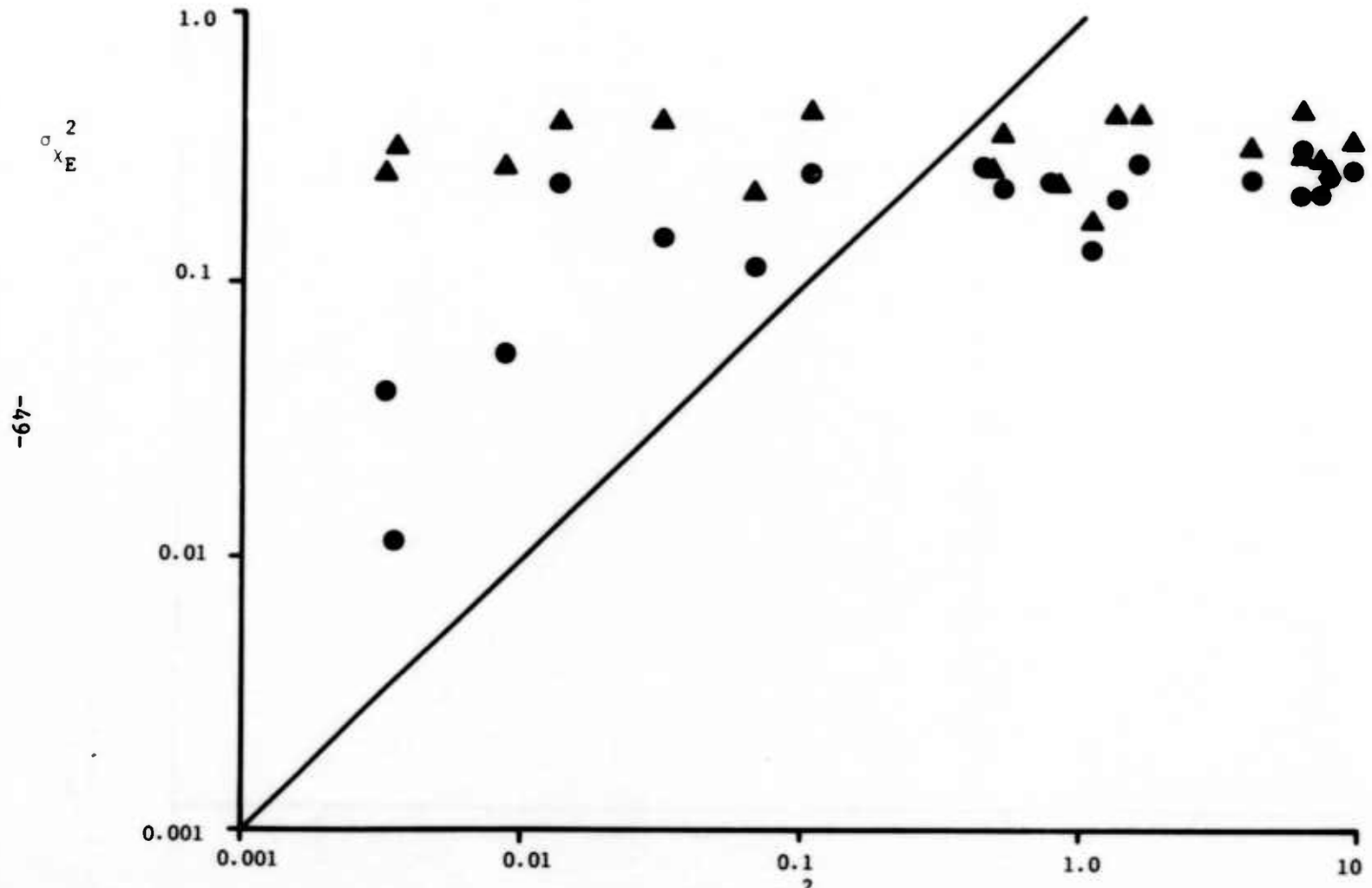

Figure 17. Experimental log amplitude variance ($\sigma^2_{\chi_E}$) vs. theoretical Rytov value for a point source ($\sigma^2_{\chi_T}$), with (●) and without (▲) wander-tracking. (———) indicates $\sigma^2_{\chi_E} = \sigma^2_{\chi_T}$ condition.

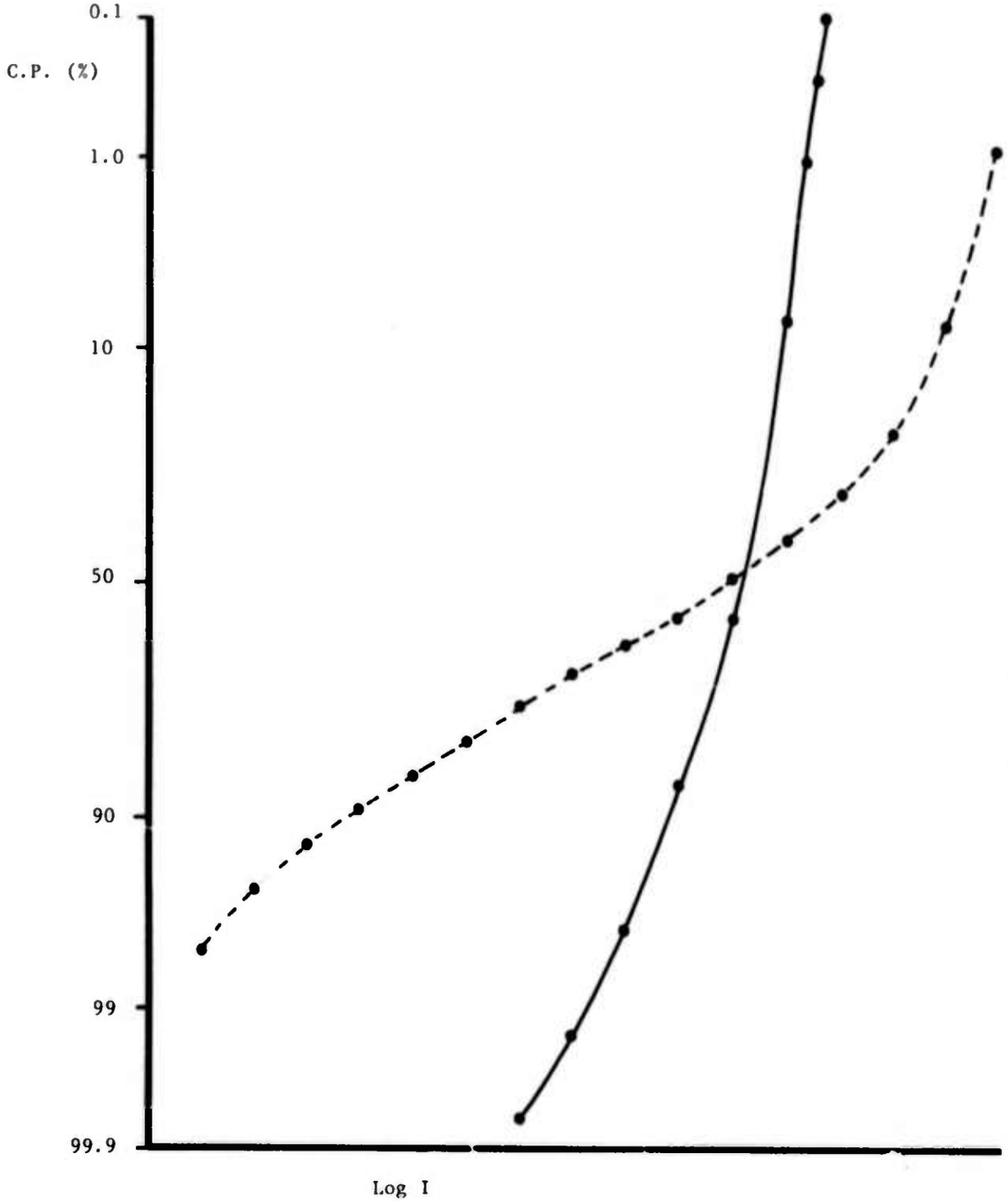

Figure 18. Cumulative probability (C.P.) for the log irradiance in weak turbulence, for the wander-tracked (———) and non-tracked (-----) cases.

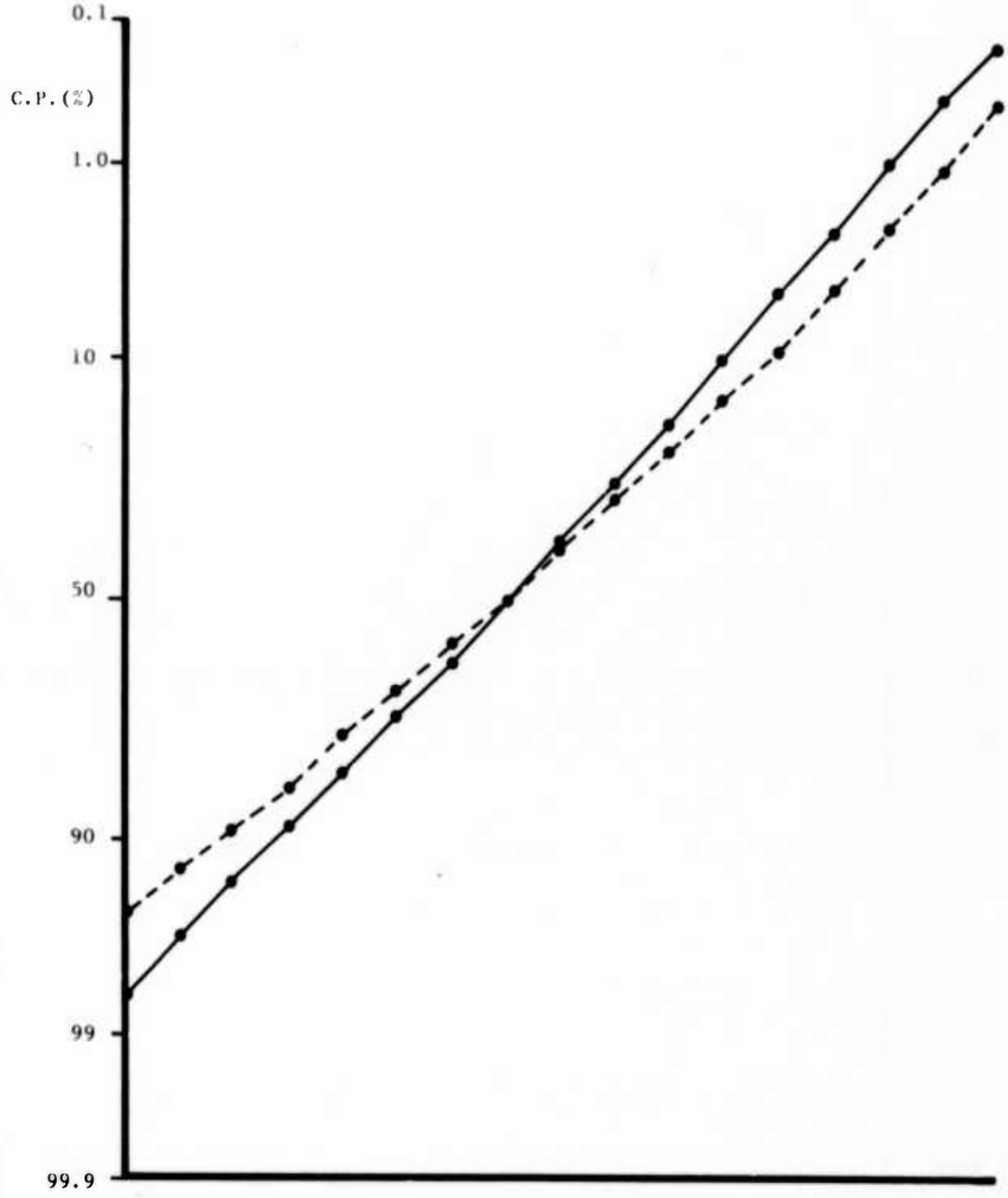

Figure 19. Cumulative probability (C.P.) for the log irradiance in strong turbulence, for the wander-tracked (———) and non-tracked (-----) cases.

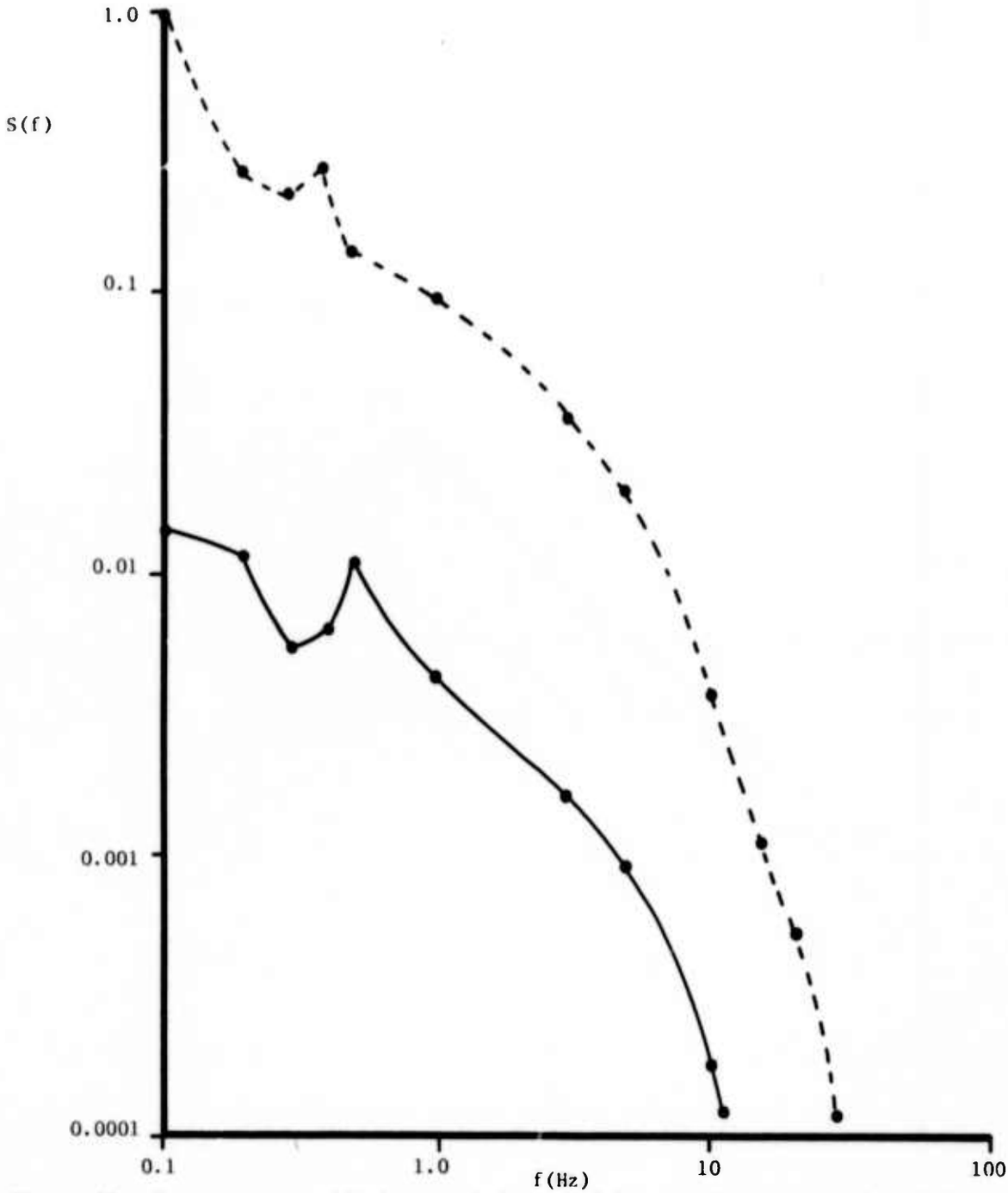

Figure 20. Power spectra S(f) for total fading of log irradiance in weak turbulence ($D/\rho_o = 0.97$), for the wander-tracked (———) and non-tracked (-----) cases.

note that at some (fractional-Hz) frequency, there is an apparent peak in the non-tracked spectrum, coincident with a dip in the tracked spectrum. This feature is noted in the other examples to follow, and is thus related to a peak in the spectrum relating to wander alone. The same curves, normalized by the log amplitude variance (σ_χ^2) for each case, are shown in Fig. 20a. For this low-turbulence case, the spectral-crossover between wander- and scintillation-predominance is evident but not dramatic. In Fig. 20b, we show the curves of Fig. 20 with the ordinate weighted by the frequency; the tendency toward separate peaks for wander and scintillation effects is apparent in the non-tracking curve.

In Figs. 21-23, we show the log fading spectra for progressively increasing turbulence (D/ρ_o = 5.7, 20, and 63 respectively). As beam break-up becomes more severe, so that scintillations predominate over wander, the spectral pairs tend to flatten out and come together, although the low-frequency advantage from wander-cancellation remains. In addition, as the turbulence grows, there is a tendency for the spectra of the tracked and non-tracked cases to cross-over at higher frequencies; this may be due to tracker response to beam-break-up scintillations and lack of total correspondence between the beacon image at the tracker and the actual distribution of energy at the target. This in turn corresponds to isoplanatism effects as they relate to the present application of reciprocity, and will be discussed further in a future report. The normalized and frequency-weighted spectra corresponding to Fig. 23 are given in Figs. 23a and 23b respectively (cf. Figs. 20a,b). With strong turbulence, the double peak is no longer evident.

4. Wander Characteristics

The control signal in the wander-tracking system is an analog of beam wander. An example of a real-time horizontal wander signal is shown in Fig. 24a. In some cases, the wander is strongly anisotropic, which can be a manifestation of both slow vertical refractive effects, and of large-scale ($> L_o$) turbulence anisotropies. An extreme example of the former is shown in Fig. 24b, which is from the same data run as Fig. 24a. This extreme is typical of night-time operation, but was observed to a much lesser extent in some of the daytime runs which comprise most of the data of this report. More typically, the rms vertical wander was less than the horizontal value, which is probably related to the anisotropy of turbulence at larger scales.

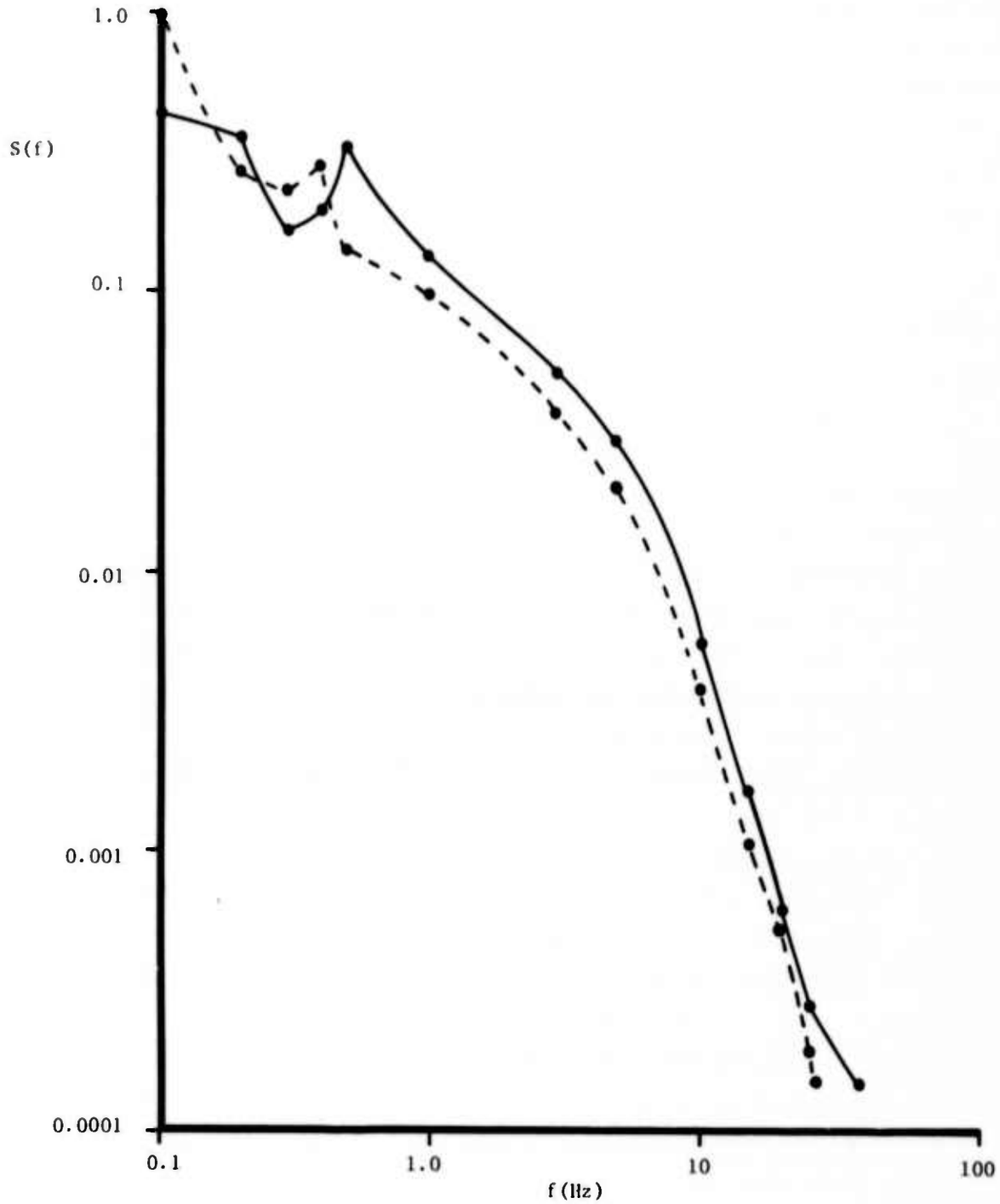

Figure 20a. Curves of Fig. 20, normalized by total log amplitude variance for each case.

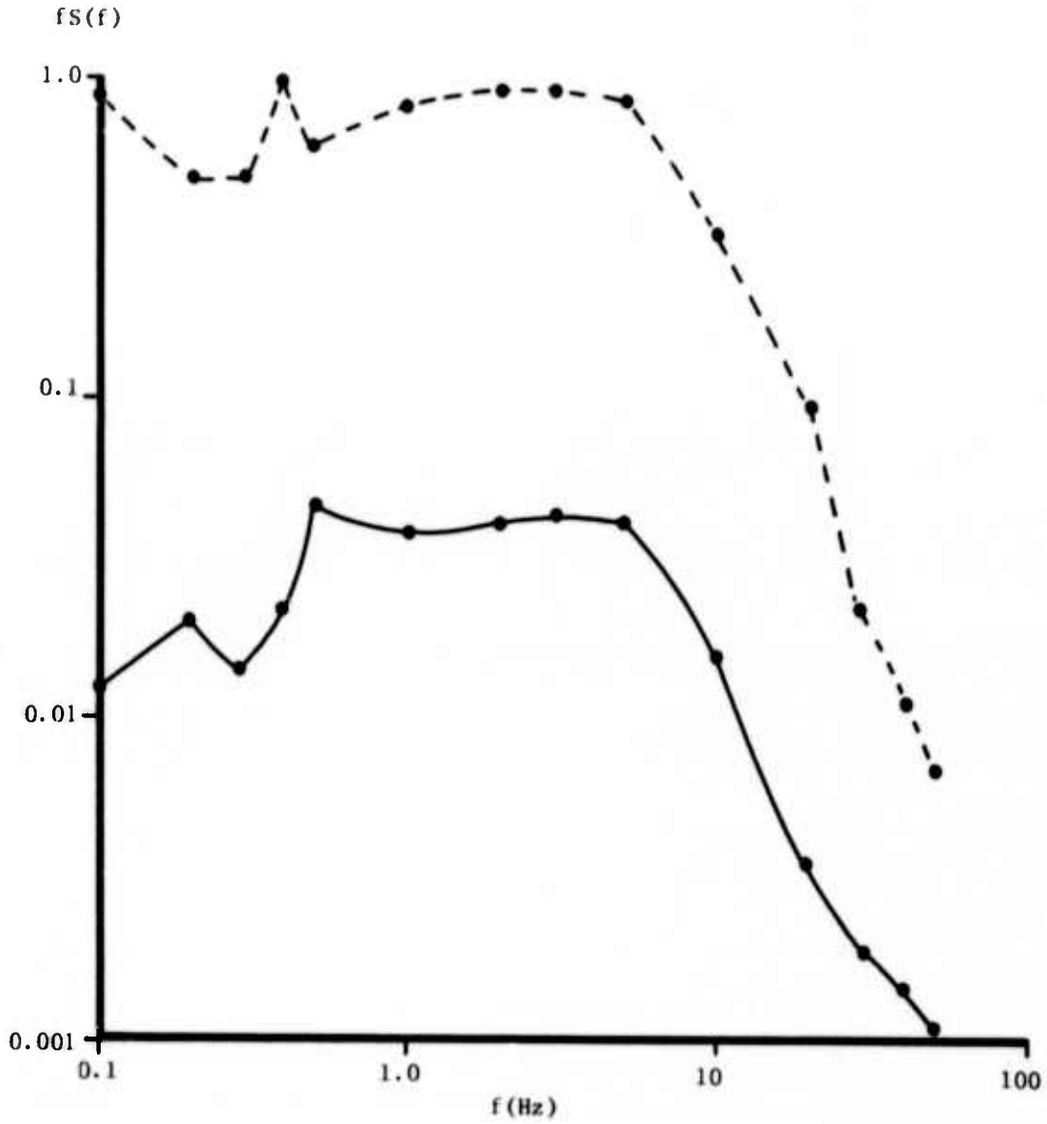

Figure 20b. Curves of Fig. 20, weighted by frequency.

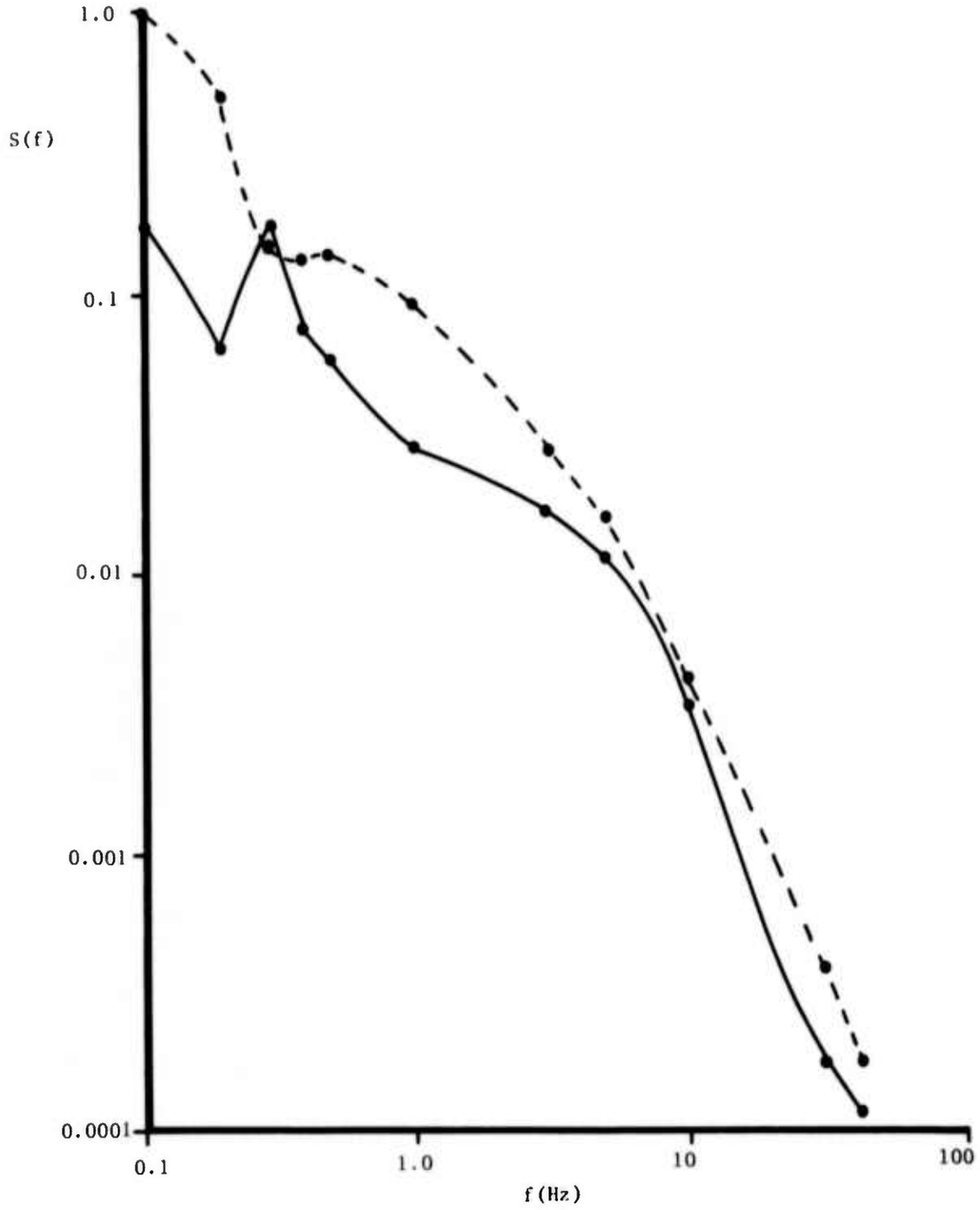

Figure 21. Power spectra as in Fig. 20, for $D/\rho_o = 5.7$.

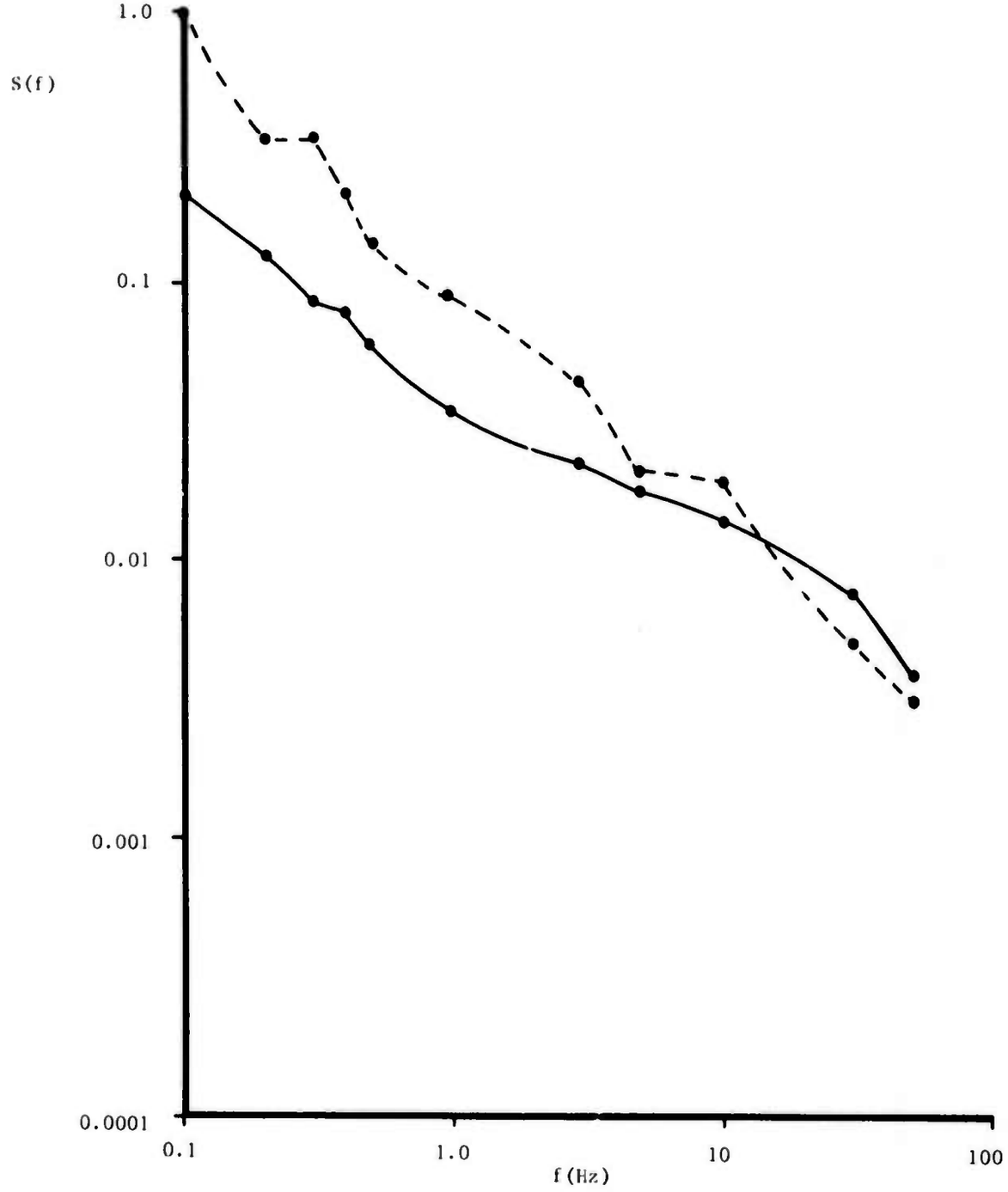

Figure 22. Power spectra as in Fig. 20, for $D/\rho_o = 20$.

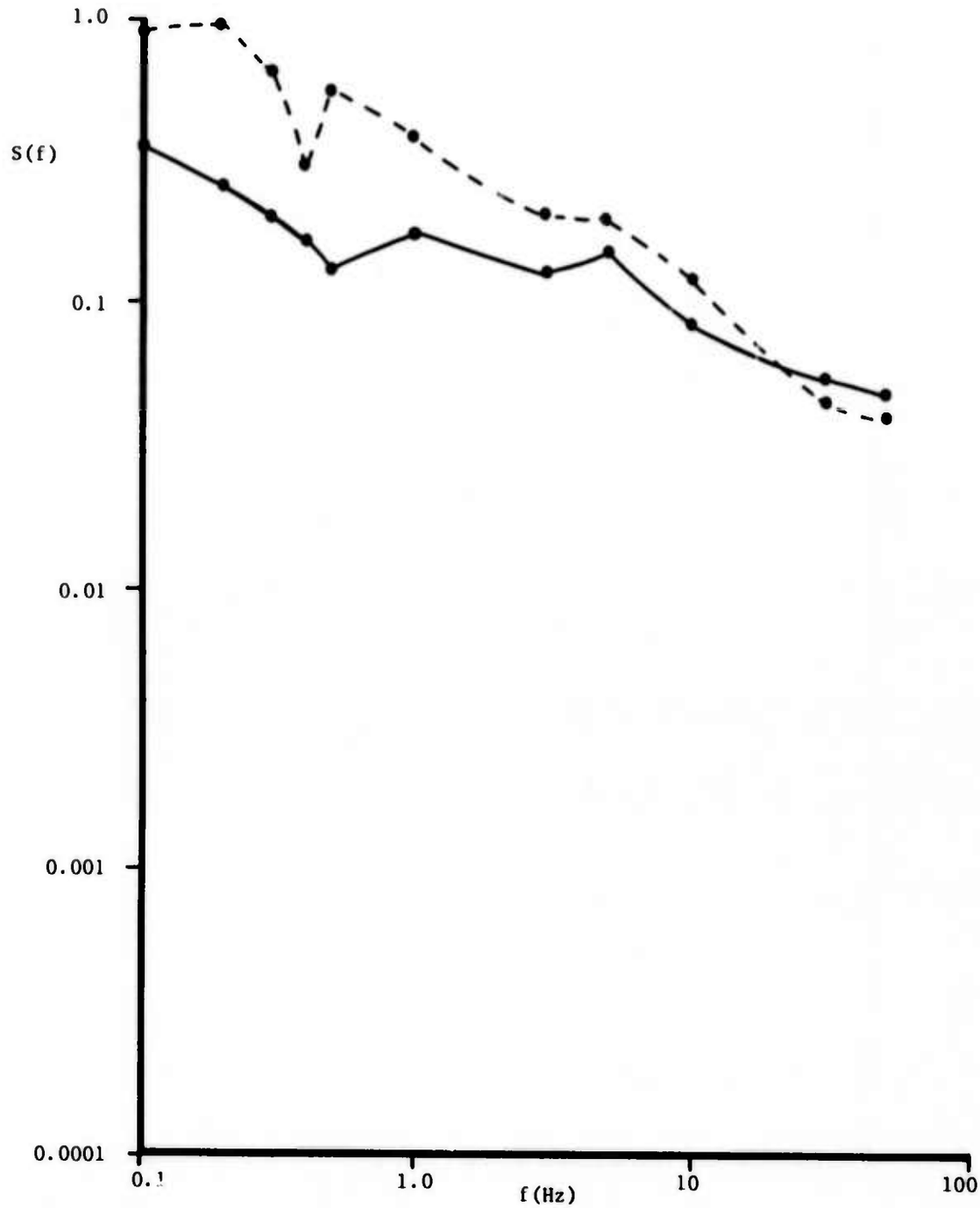

Figure 23. Power spectra as in Fig. 20, for $D/\rho_o = 63$.

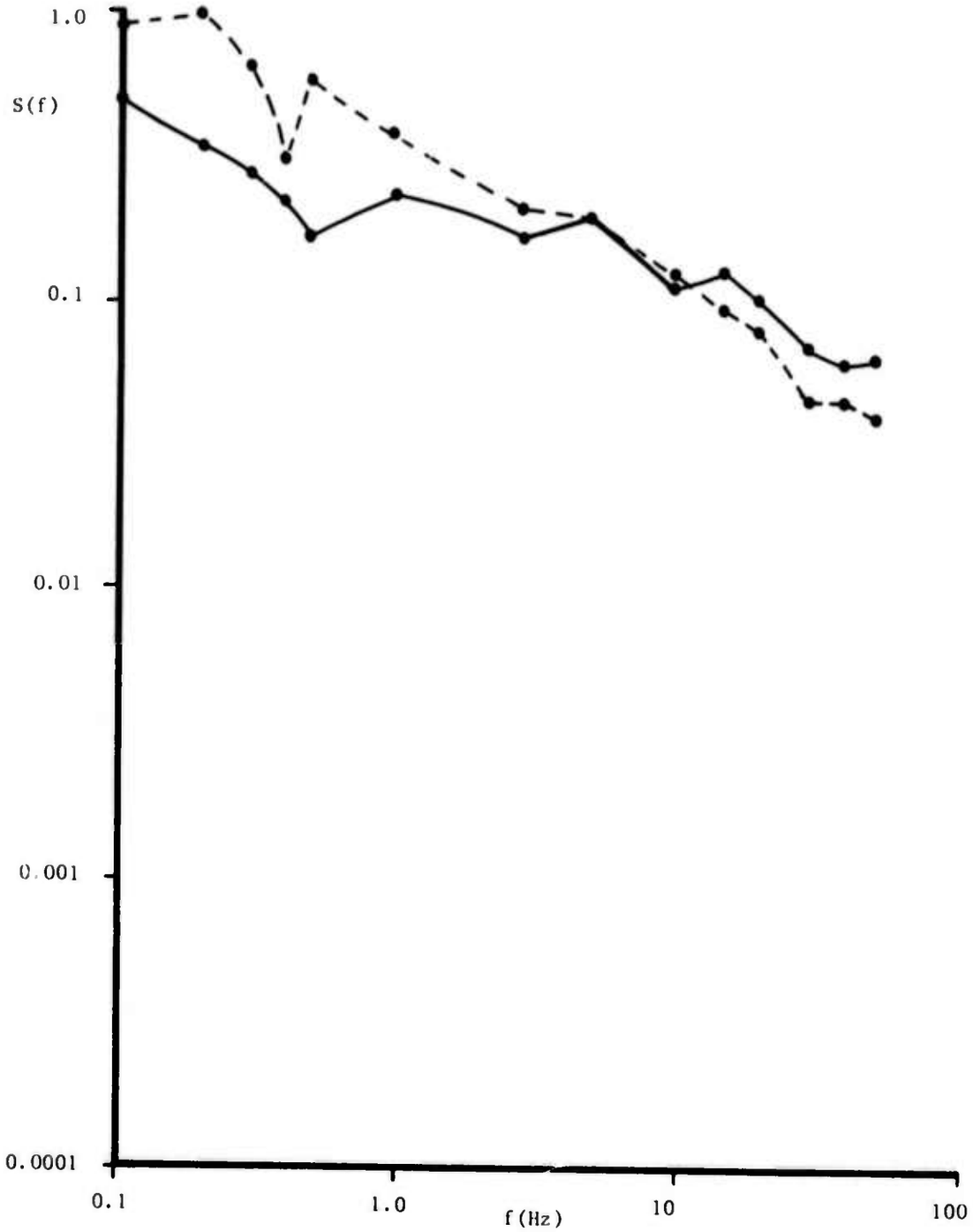

Figure 23a. Curves of Fig. 23, normalized by total log amplitude variance for each case.

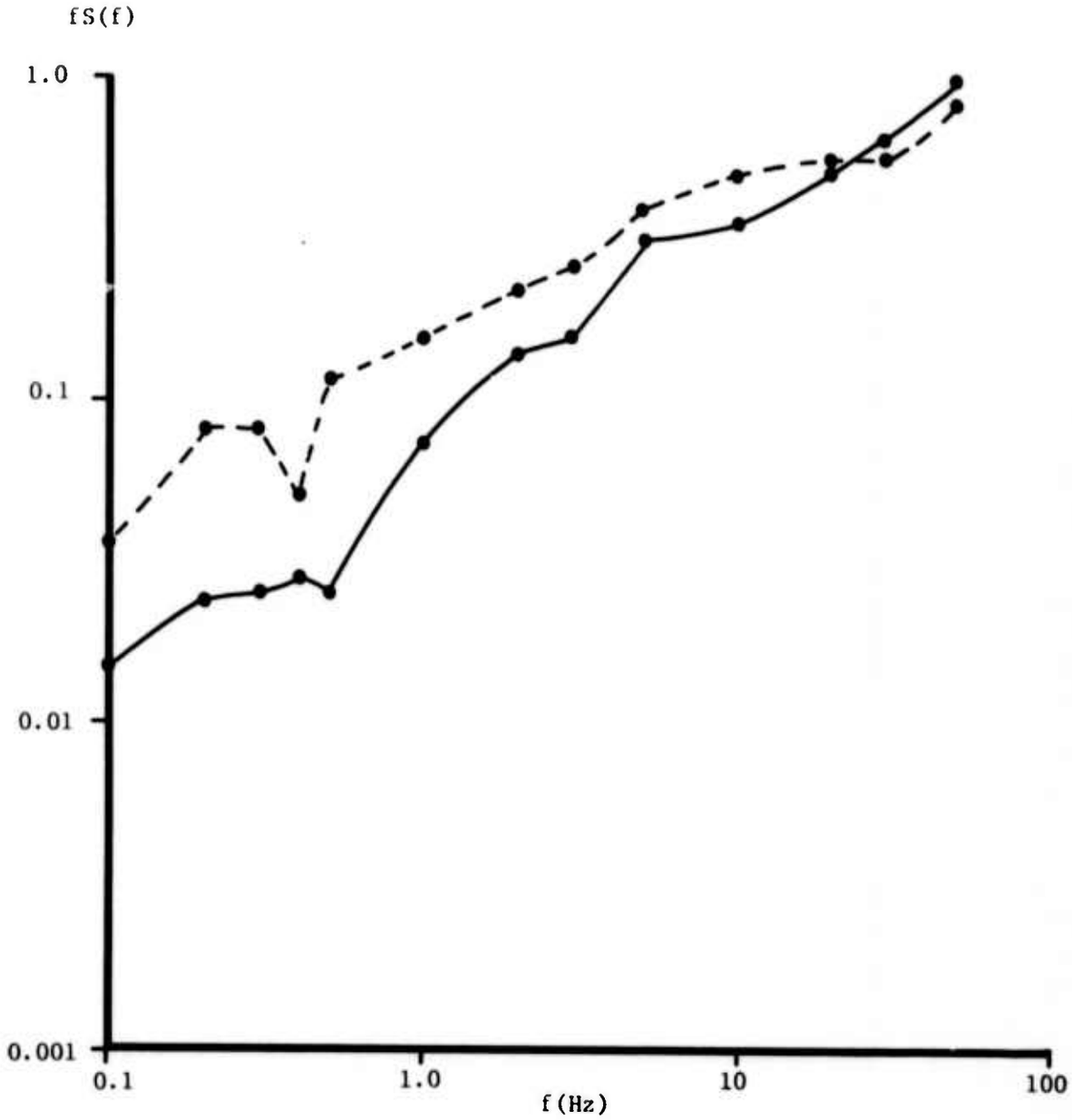

Figure 23b. Curves of Fig. 23, weighted by frequency.

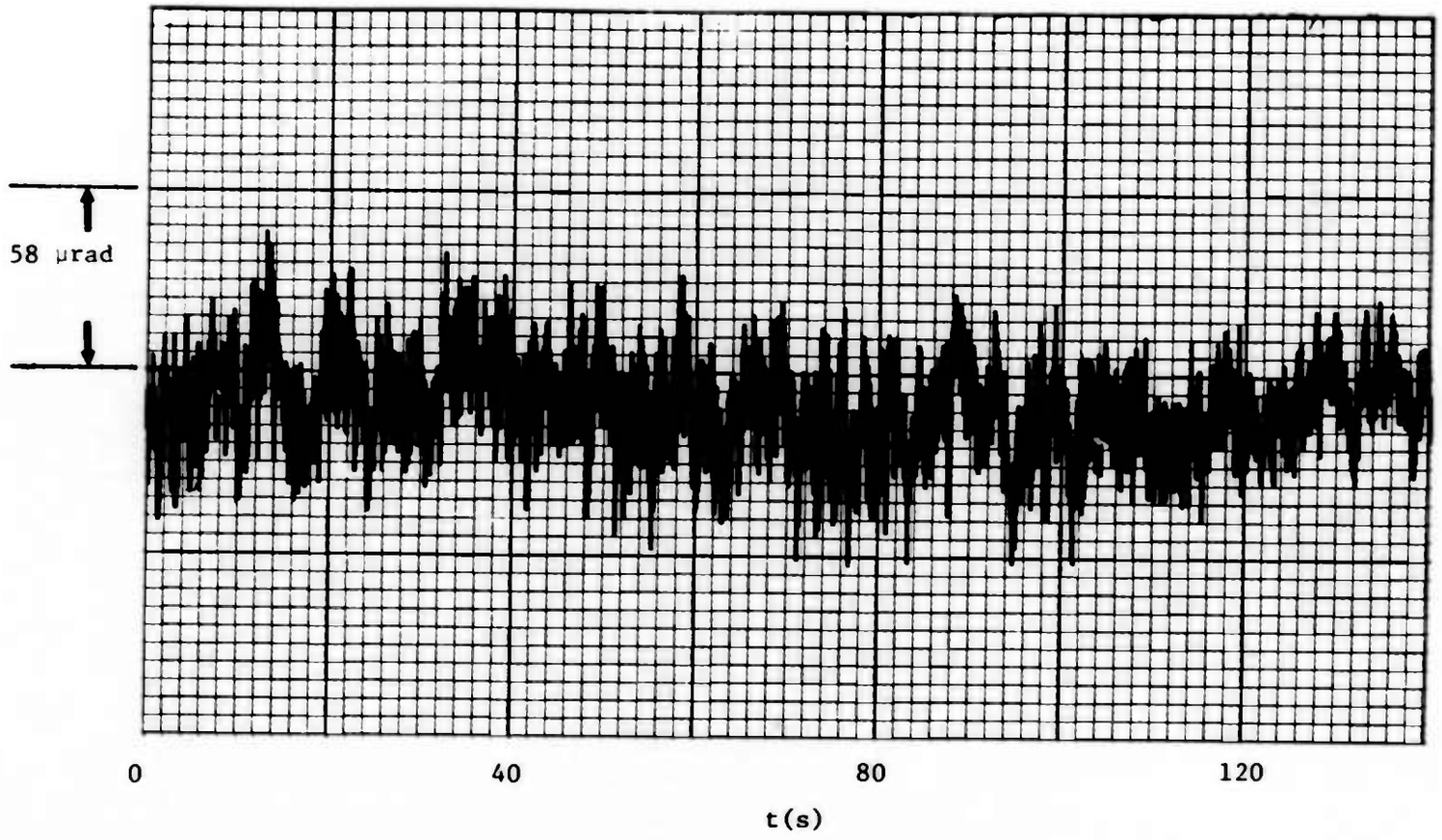

Figure 24a. Horizontal wander signal vs. time for a night-time run in low wind.

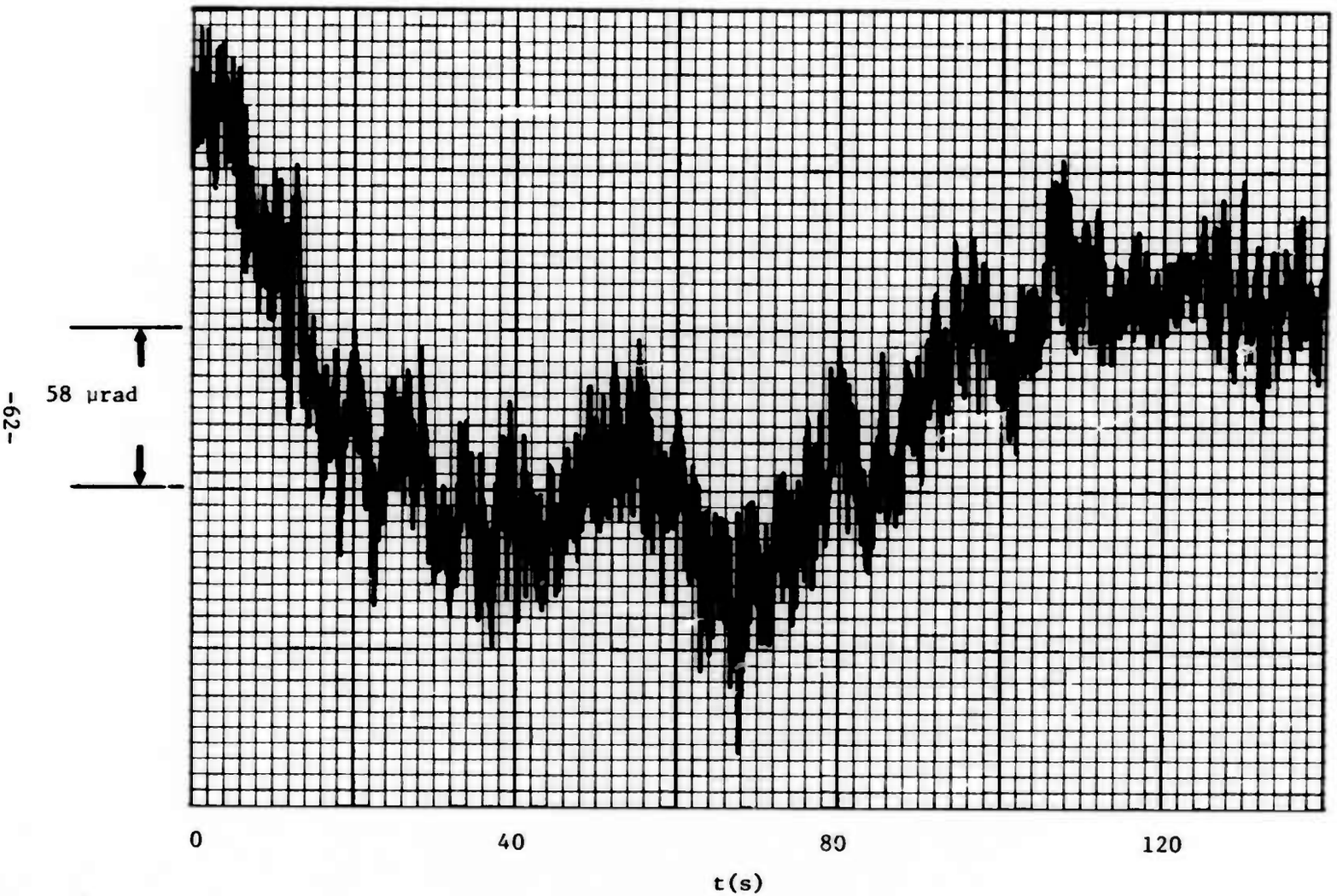

Figure 24b. Vertical wander signal vs. time for a night-time run in low wind.

The slow, refractive components, which have a period of half a minute or more, are difficult to characterize in terms of their relationship to turbulence effects vs. changing thermal stratifications. The effect does not appear in our fading data, in which 0.1 Hz high-pass filtering was effectively used. However, our measurements of $\bar{I}_{NT}$ were taken by centering the open-loop transmitter on the target axis and then averaging for 120 sec.; in this case, slow wander can reduce the apparent mean irradiance over that which would be obtained with shorter averaging times, and therefore enhance the ratio $\bar{I}_T/\bar{I}_{NT}$. Qualitative examination of real-time irradiance records does not indicate that this effect was large, for 120 sec averaging times, and shorter intervals results of course in greater data-spread. Ideally, each measurement of $\bar{I}_{NT}$ would be repeated a number of times, using shorter averaging times and re-centering each time.

A quantitative distinction between the two vertical beam-bending mechanisms can be made using the probability distributions of the wander signal. In Fig. 25a, we show the distribution for the horizontal signal of Fig. 24a, with equivalent high-pass filtering at four different cut-off frequencies. The distributions are gaussian, with coefficients of skewness and kurtosis for the 100 sec^{-1} case of 3.6×10^{-4} and 3.1, respectively. In Fig. 25b, we show the distributions for the vertical signal of Fig. 24b, where the non-gaussian nature is quite apparent. The best approximation to a gaussian distribution is seen to occur for an inverse cut-off frequency of 20 seconds.

A summary of the characteristics of the wander signals, averaged over a number of runs, is shown in Table I. The ratio of average horizontal/vertical (rms) wander angles is 1.6. The correlation coefficient refers to the basic theoretical prediction (wander term of Eq. 20), namely (mean-square wander angle) $\sim C_n^2$. In spite of the influence of slow refractive effects, the vertical wander exhibits much less bias than does the horizontal. This may be due to variable-wind effects, which influence the horizontal case only.

The average two-dimensional mean-square wander angle, for the runs included in Table I, implies a value of $|C_2|$ in Eq. (20) of 3.69, which is nearly equal to that deduced in the semiquantitative, phenomenological reasoning of a previous section.

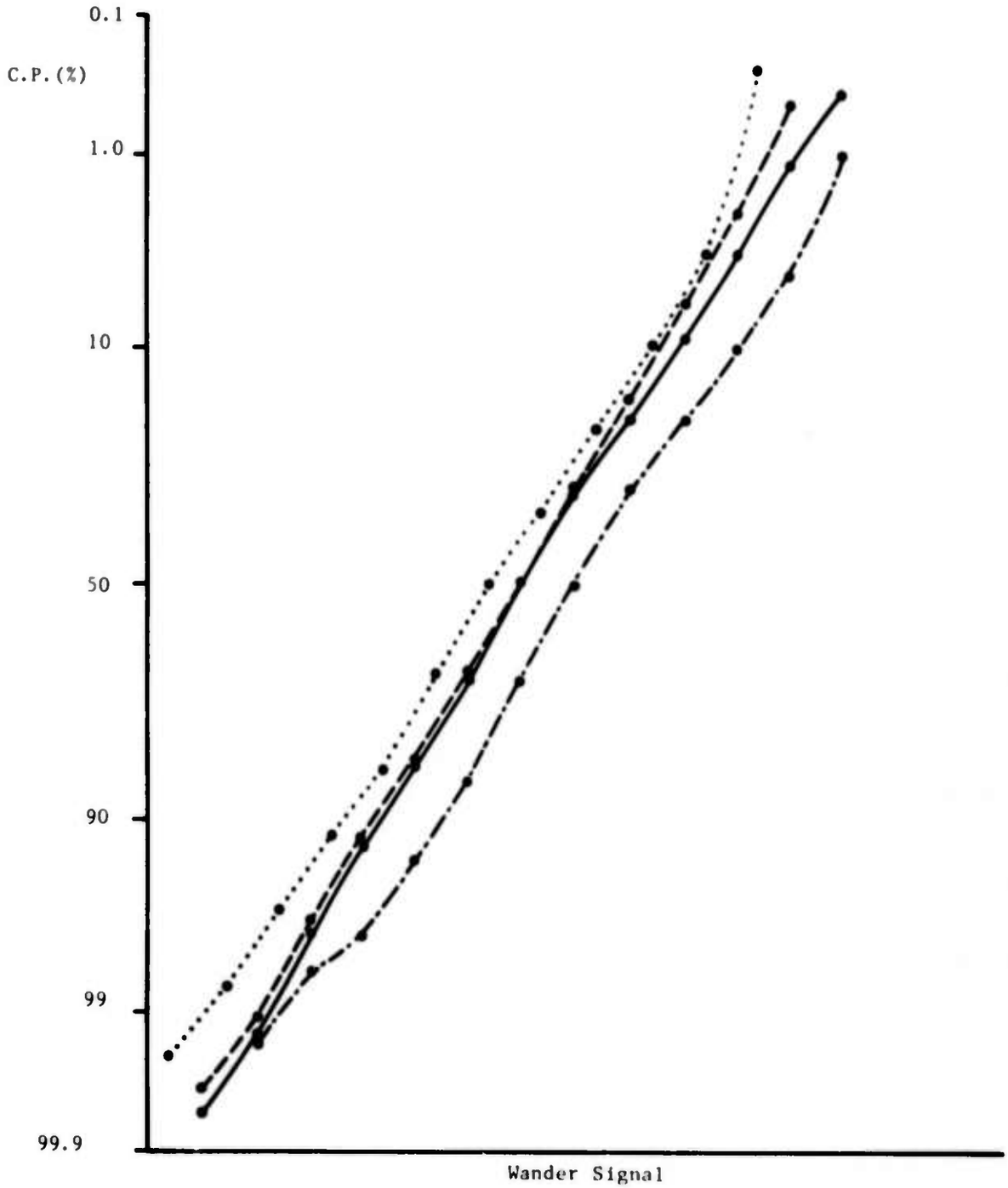

Figure 25a. Cumulative probability (C.P.) for wander signal of Fig. 24a, for various high-pass cutoff frequencies. The inverse cutoff frequency for (———) is 0.01; (-----), 0.017; (.....), 0.05; (-.-.-.-.-.), 0.1 sec.

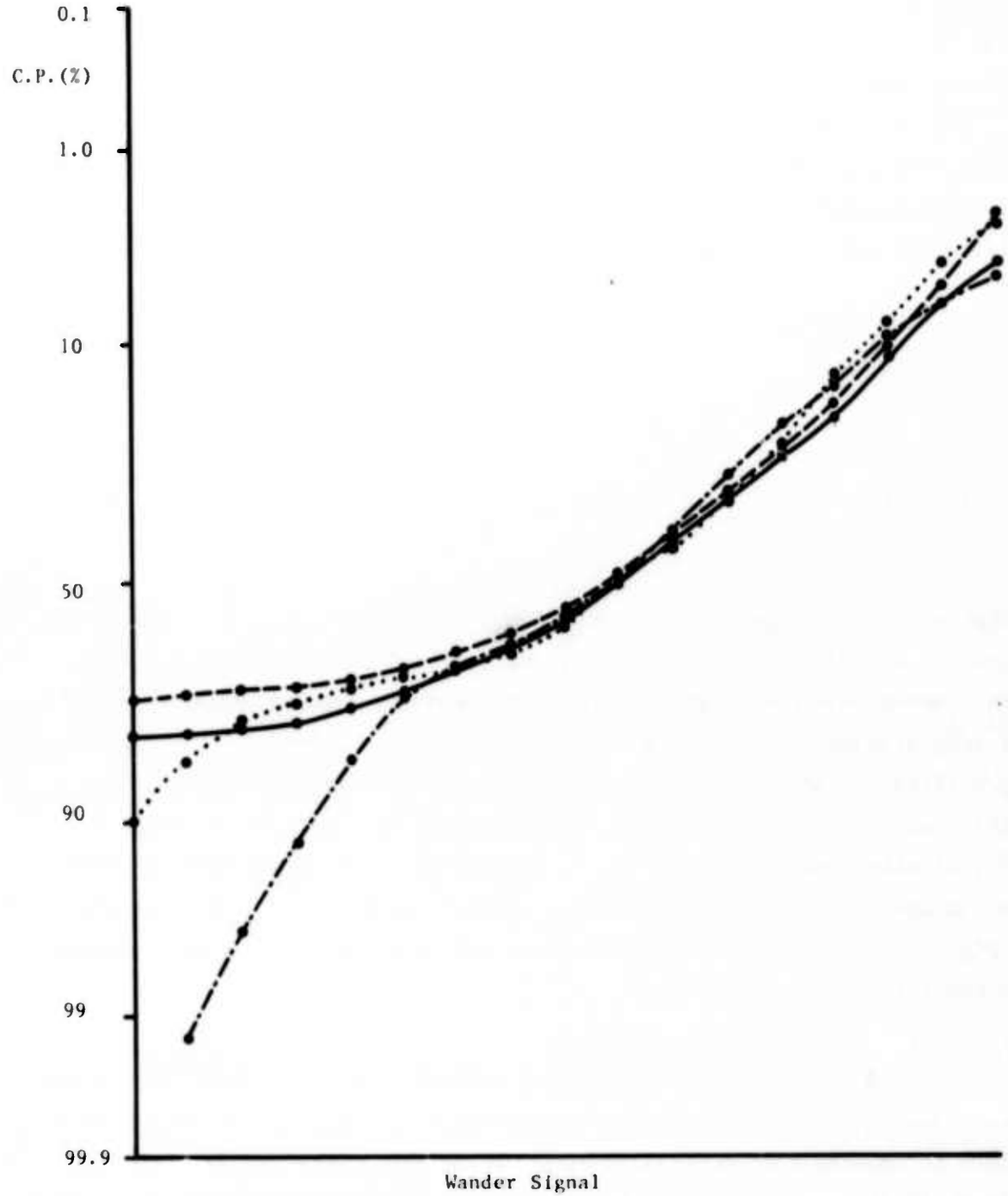

Figure 25b. Cumulative probability (C.P.) for wander signal of Fig. 24b, for various high-pass cutoff frequencies. The inverse cutoff frequency for (———) is 0.01; (-----), 0.017; (.....), 0.05; (-.-.-.-.-.), 0.1 sec.

TABLE 1. AVERAGE CHARACTERISTICS OF BEAM WANDER SIGNALS

	Skewness	Kurtosis	Correlation Coefficient (Exper. vs. Theory)
Vertical	2.0×10^{-2}	2.76	0.90
Horizontal	2.3×10^{-2}	2.89	0.36
Total			0.97

The power spectrum and frequency-weighted spectrum of the wander signal of Fig. 24a are shown in Fig. 26. The theoretical phase-difference spectrum, which is closely related, is predicted to fall off with an exponent of (-2/3,-8/3) for frequencies above breakpoints ($f_{1,2}$) respectively:[30]

$$f_1 \sim \frac{v_\perp}{L_o}$$

$$f_2 \sim \frac{v_\perp}{D} \quad , \qquad (41)$$

where $v_\perp$ is the perpendicular component of wind velocity. For frequencies below f_1, the behavior is very sensitive to the detailed behavior of the wind. Since this was a low-wind case, we expect a log-log slope of -8/3; the actual slope was -2.78 with a correlation coefficient of 0.98. In Fig. 27, horizontal and vertical spectra are shown for a higher wind ($f_{2_{\text{horizontal}}} \approx$ 4 Hz), and the -2/3 slope is well supported for the horizontal case. The vertical case shows a greater slope, and we note that f_2 for the vertical wind is approximately zero near the ground. In other cases, such as shown in Fig. 28 ($f_2 \stackrel{\sim}{} 0$), both the horizontal and vertical spectra fall between the two theoretical slopes.

5. Transmitter Focus Effects

As discussed in a preceding section, the first-order theory predicts that a focused, near-field transmitter with wander-cancellation will result in smoothing of scintillations. It is now understood that this effect, if it occurs, can only be realized for the condition $D/\rho_o < 1$. In

30. A. J. Huber, "Measurements of the Temporal Power Spectra of a Propagated 10.6 micron Wavefront", Technical Report, Rome Air Development Center, Spring 1973.

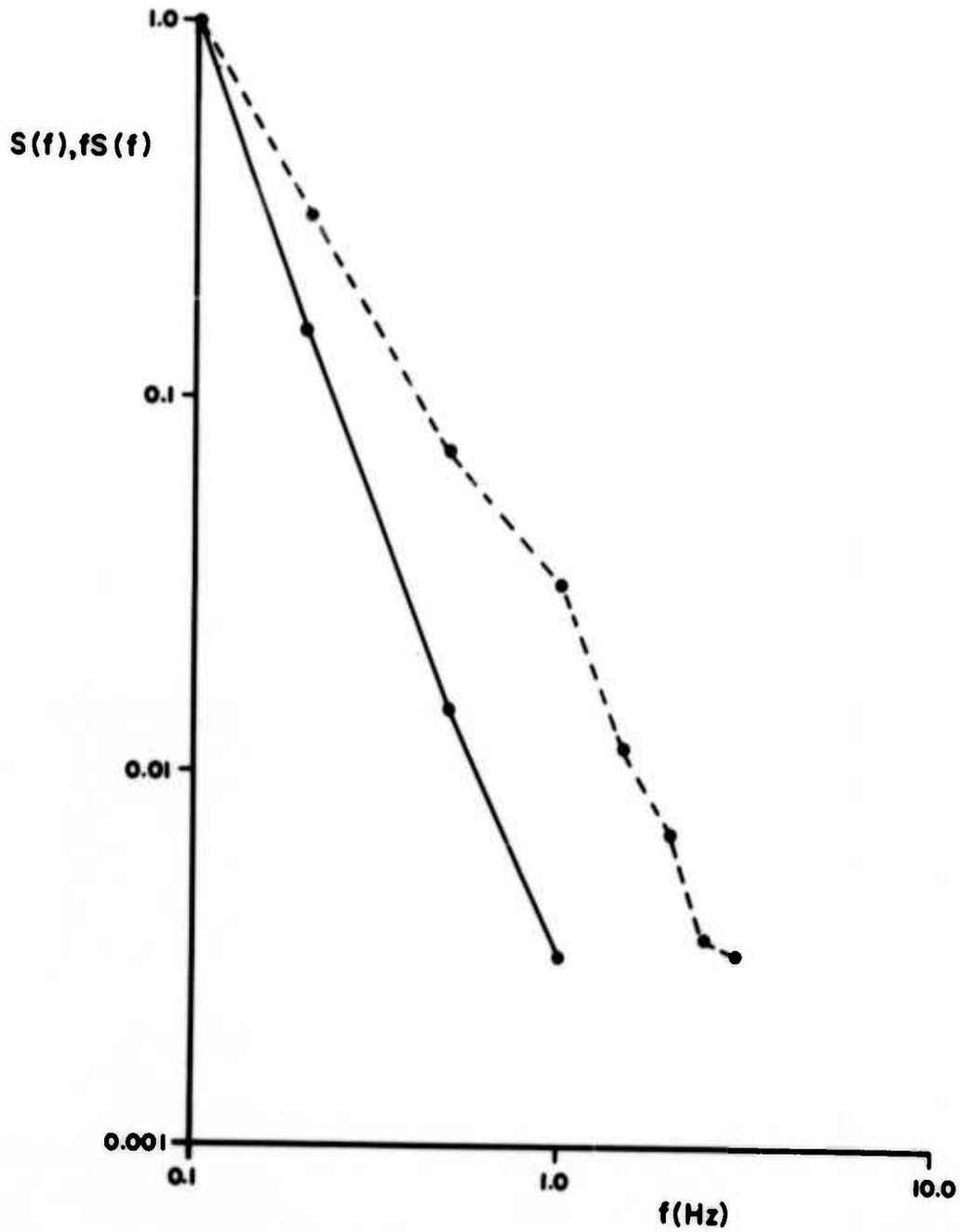

Figure 26. Power spectrum S(f) (———) and frequency-weighted spectrum fS(f) (-----) for wander signal of Fig. 24a.

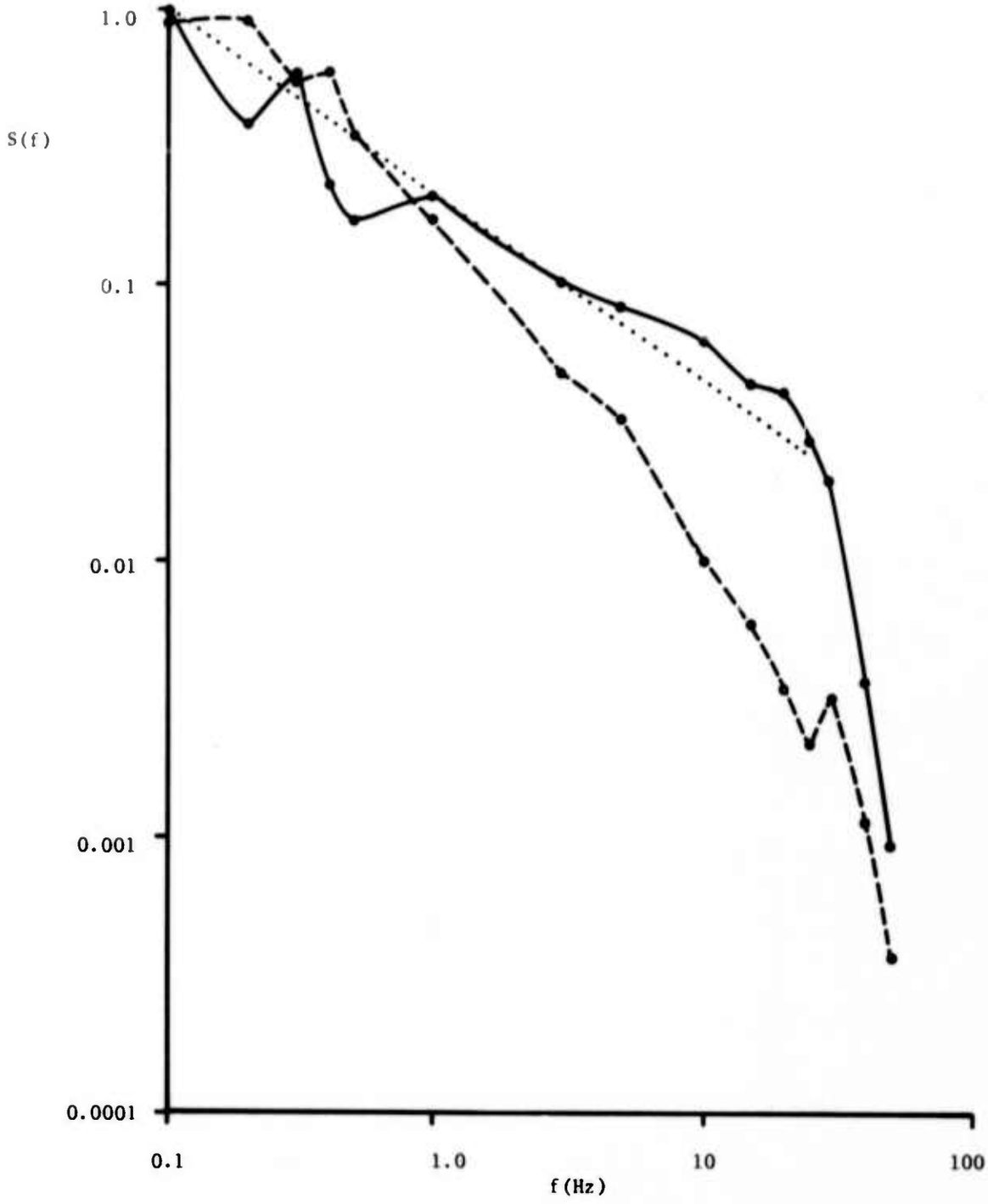

Figure 27. Power spectrum of horizontal (———) and vertical (-----) wander signals for significant horizontal wind. (.....) indicates $f^{-2/3}$ dependency.

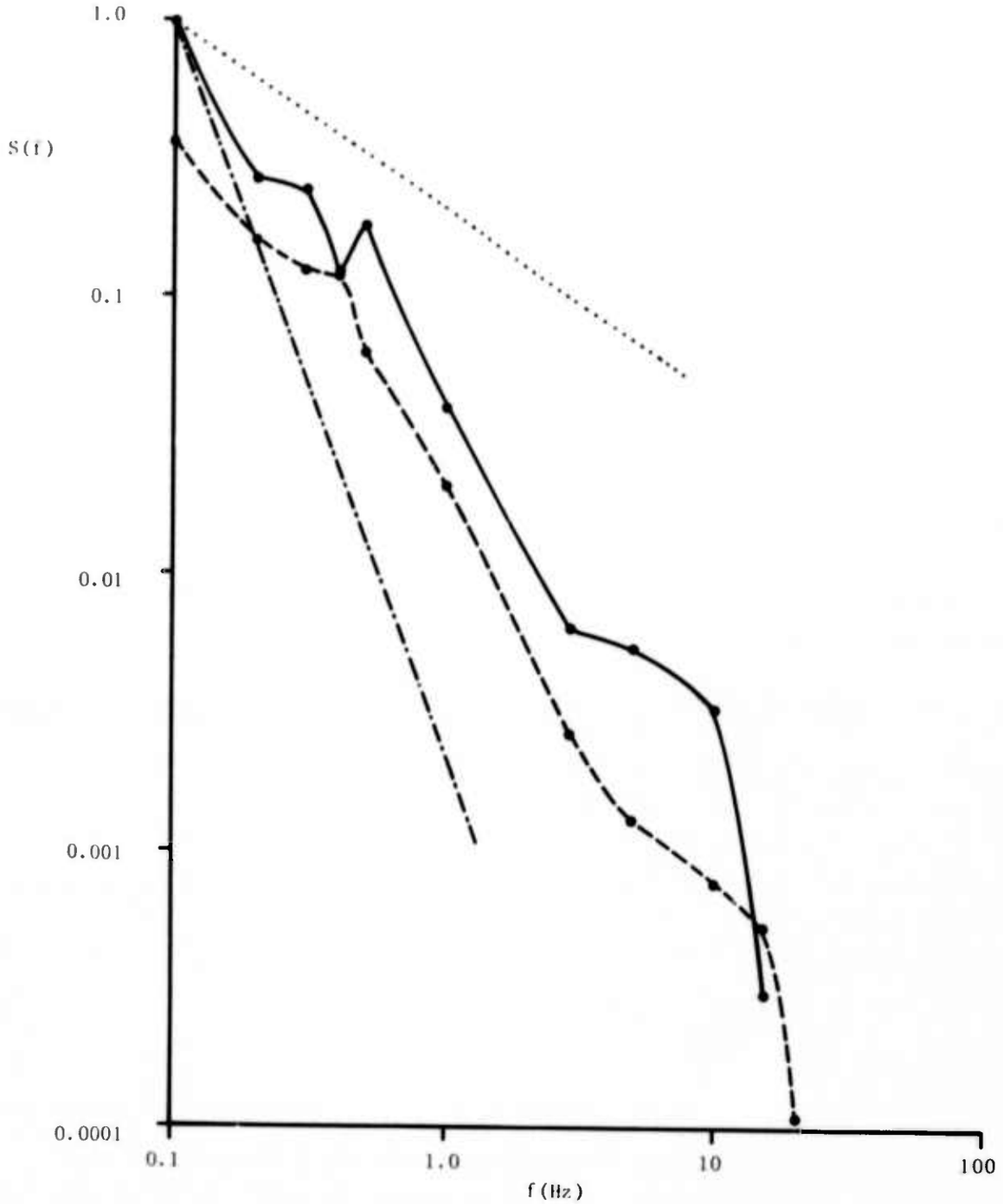

Figure 28. Power spectrum of horizontal (——) and vertical (-----) wander signals for low wind speed, exhibiting slopes intermediate to the theoretical values of -2/3 (.....) and -8/3 (-.-.-.-.-.).

fact, we expect that the actual requirement is $\frac{D}{\rho_o} << 1$, so that phase distortion is negligible. As a follow-up to our work as reported in Ref. 22, where qualitative evidence of such smoothing was seen, we are conducting experiments on the (wander-tracked) signal fading vs. transmitter focus adjustment. As discussed in that reference, the smoothing effect is expected to be very critically dependent upon focus adjustment.

Attempts to observe this effect are shown in Figs. 29a and b. The parameter $\alpha_2 z$ is simply z/R, where R is the radius of curvature of the transmitter wavefront. Since (D/ρ_o) was on the order of 3.5 for these runs, the effect was inconclusively observed.

As discussed below, we are now operating on a much shorter path. As seen in Fig. 30 a,b, the predicted effect is observed, including the large increase in scintillations with slight mis-adjustments. However, we have not yet operated with $\frac{D}{\rho_o} << 1$, and we have not observed a reduction to a value of $\sigma_{\chi_F}^2$ substantially below that for a point source on the same path. The point-source scintillations are necessarily quite low under these conditions, and any residual fading due to, e.g., tracker error or jitter will be quite important. However, the tracker resolution is 0.02 x the diffraction limit, and we still hope to see substantial smoothing. This effect has important practical implications for uplink beams,[17-19] especially at longer wavelengths.

6. Further Experiments and Parameter Variations

More data are obviously required, especially for $(D \lesssim \rho_o)$. However, the interesting case is that of large Fresnel number, $D >> (z/k)^{1/2}$. We thus require that the following ratio be large:

$$\frac{\rho_o}{\sqrt{z/k}} = \frac{0.411}{\left(\sigma_\chi^2 \text{ Point-Source Rytov}\right)^{3/5}} = 1.44\, k^{-\frac{7}{10}}\, z^{-\frac{11}{10}}\, C_n^{2\,-\frac{3}{5}} >> 1 \quad . \quad (42)$$

In order to achieve this at a reasonable C_n^2 (i.e., reasonably well-developed turbulence), we require long wavelengths and short pathlengths, with the stronger dependence on the latter. If we specify $\rho_o = D = 15$ cm, we can calculate the corresponding C_n^2 vs. pathlength and wavelength, and the resultant value of $(2\pi z/k)^{1/2}$ = $(\lambda z)^{1/2}$. This is shown in Table II.

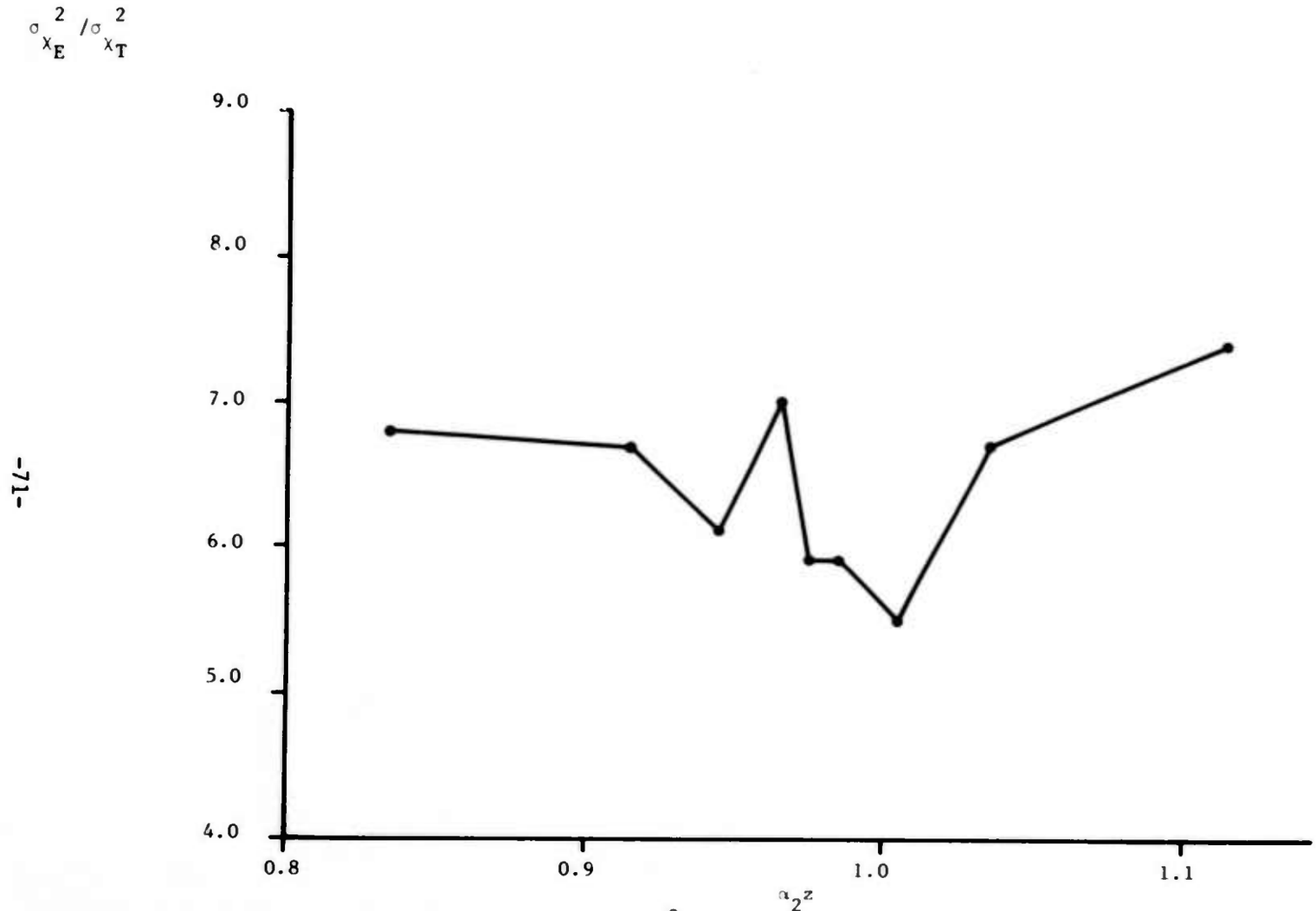

Figure 29a. Experimental log amplitude variances ($\sigma_{\chi_E}^2$) divided by the first-order theoretical values for a point source ($\sigma_{\chi_T}^2$), vs. focus condition $\alpha_2 z$ (Ref. 22). The value of D/ρ_o is 3.5.

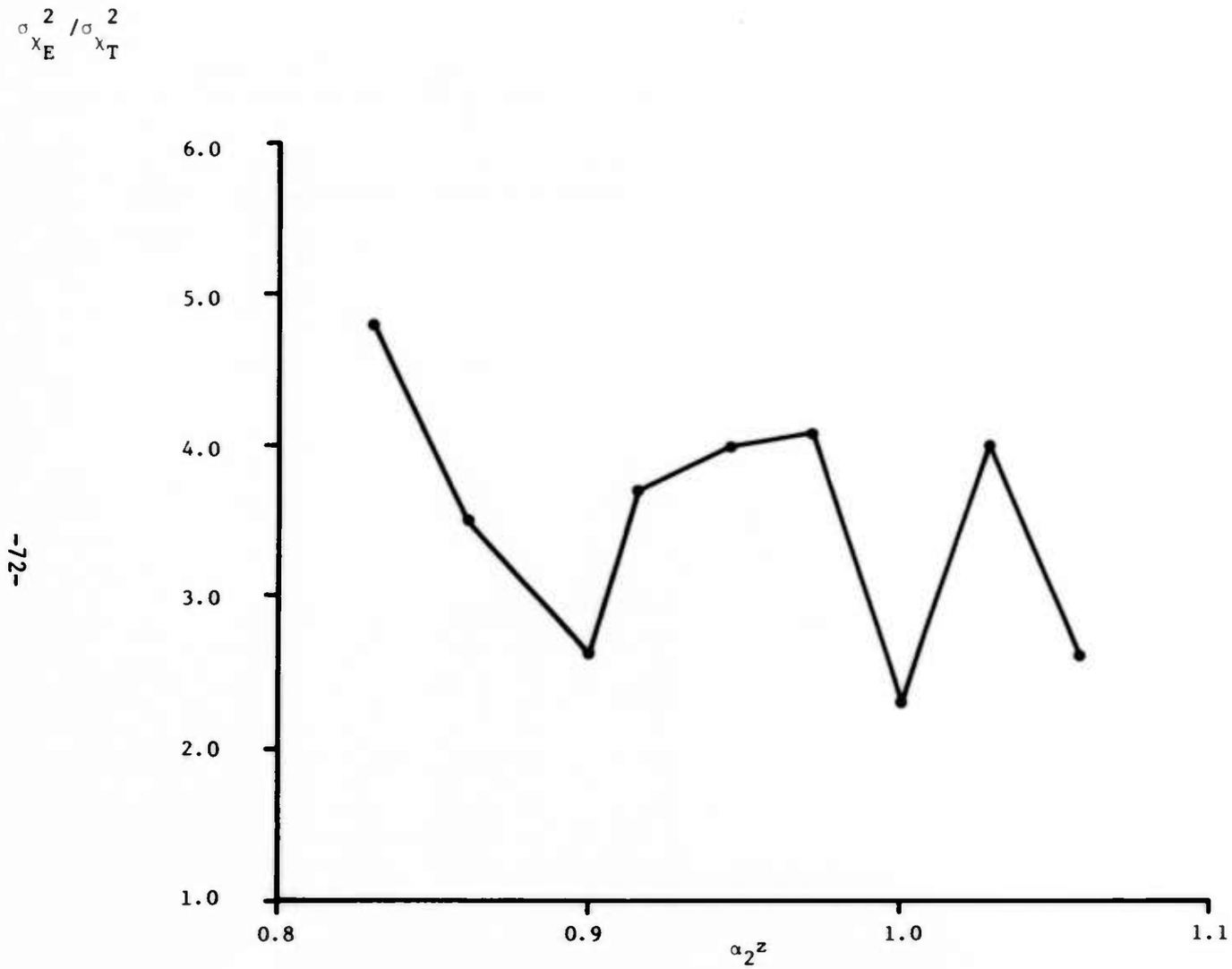

Figure 29b. Experimental log amplitude variances ($\sigma_{\chi_E}^2$) divided by the first-order theoretical values for a point source ($\sigma_{\chi_T}^2$), vs. focus condition $\alpha_2 z$ (Ref. 22). The value of D/ρ_o is 3.5.

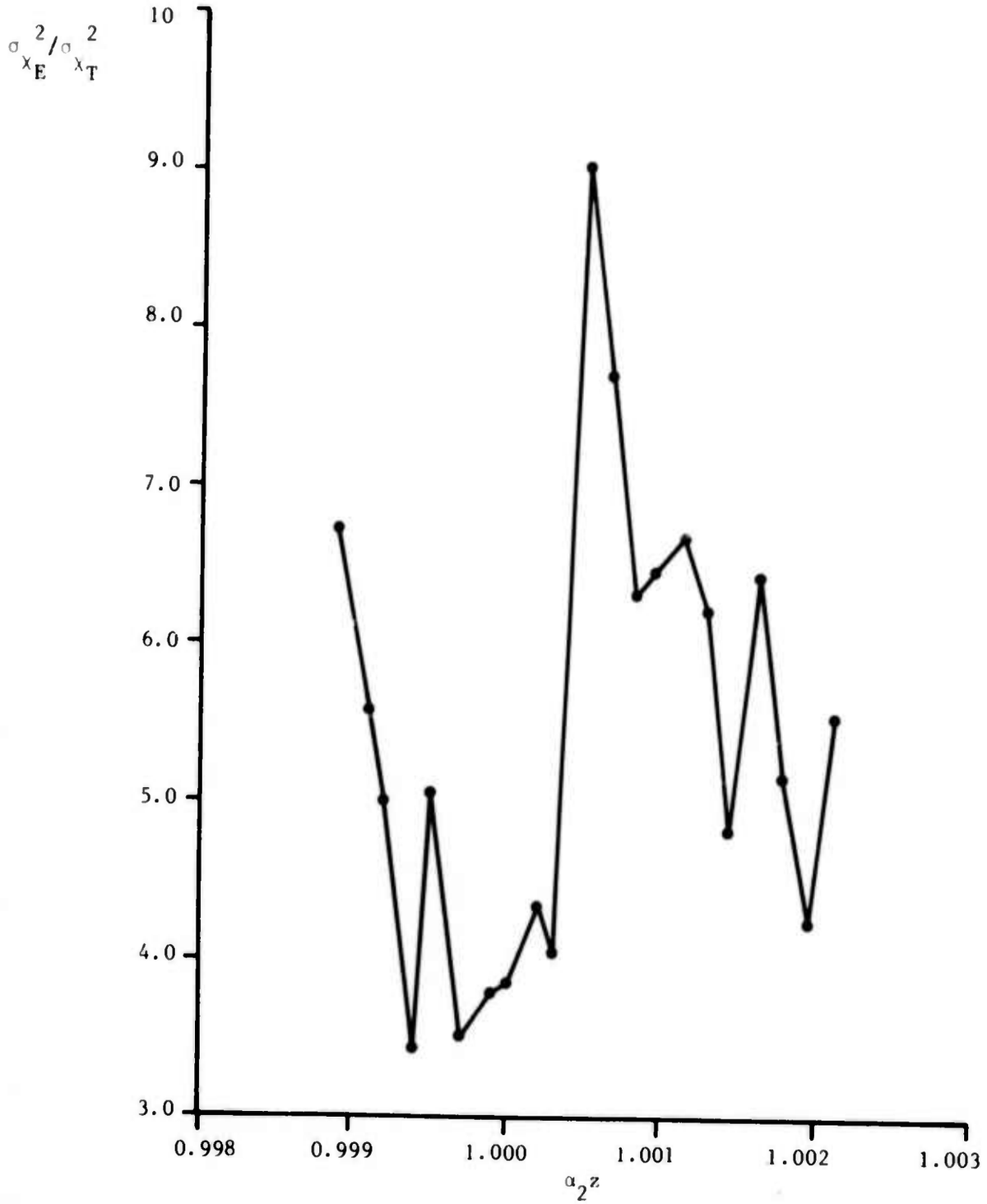

Figure 30a. Curves similar to those of Fig. 29. $D/\rho_o = 2.6$.

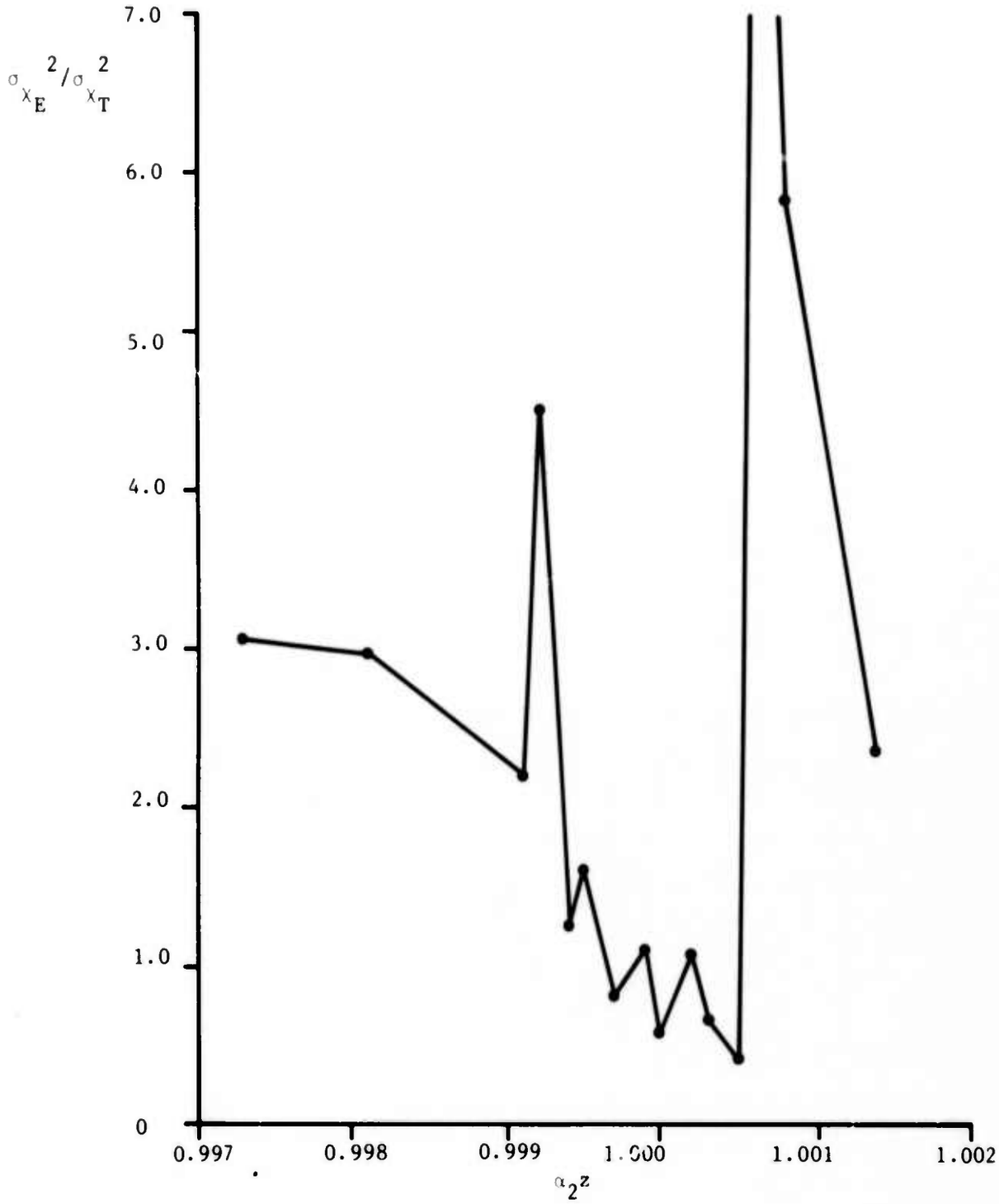

Figure 30b. Curves similar to those of Fig. 29. $D/\rho_o = 0.80$.

TABLE 2. REQUIRED C_n^2 VS. RANGE AND WAVELENGTH FOR COHERENCE SCALE = 15 CM, WITH RESULTANT FRESNEL NUMBER

z	λ	C_n^2	$(\lambda z)^{1/2}$
1.6 km	6328 A	2.7×10^{-16}	3.2 cm
1.6 km	3.8μ	9.9×10^{-15}	7.8 cm
1.6 km	10.6μ	7.7×10^{-14}	13 cm
100 m	6328 A	4.4×10^{-15}	8.0 mm
100 m	3.8μ	1.6×10^{-13}	1.9 cm
100 m	10.6μ	1.2×10^{-12}	3.2 cm

It is clear that, in order to achieve good ($\rho_o > D$) data with a 15 cm transmitter and suitable Fresnel number, the combination of a longer wavelength and short pathlength is desirable. We are currently utilizing a 91 m path at 6328 A, and we will subsequently modify the tracking transmitter to accommodate 10.6μ. These pathlength and wavelength variations will also serve to extend our comparisons with theory, which have previously been limited to variations in C_n^2.

In accordance with Eq. (40), since the cases of interest now involve $\rho_o \gtrsim 15$ cm, inner scale effects should be negligible. At 10.6μ for the short path, ρ_o may become substantially larger than 15 cm, permitting data for the $\rho_o >> D$ case; however, according to Eq. (38), outer scale effects may then become noticeable. This problem may be reduced by decreasing D and accepting a lower Fresnel number.

C. Future Work

In the above we have described future experimental work with a shorter pathlength and longer wavelength, and further theoretical efforts on the second moment of irradiance as well as the details of wander-tracking with a gaussian beam. In addition, we intend to determine the scintillation characteristics from generalized, extended sources such as laser-illuminated diffuse reflectors. This will include the strength and (transverse) structure of scintillations, which are important for remote-probing applications with non-cooperative targets.

As a related item, we plan to return to the problem of saturation

of scintillations over a long path,[1,31] using very small receivers and large (e.g., 10 kHz) bandwidths. We will compare the results, including covariances, with recent physically-based analyses by Yura[32] and Clifford,[33] and we expect to show that a new similarity theory appearing in the Russian literature[34] is incorrect. The results are again important for remote-probing applications.

Finally, we will return to such problems as outer scale effects, angular scintillation of retro reflectors, and isoplanatism as it relates to point-target reciprocity and wander-tracking.

---

31. J. R. Dunphy and J. R. Kerr, J. Opt. Soc. Am. 63, 981-986, August 1973.
32. H. T. Yura, J. Opt. Soc. Am. 64, 59-67, January 1974.
33. S. F. Clifford, G. R. Ochs, and R. S. Lawrence, J. Opt. Soc. Am. 64, 148-154, February 1974.
34. M. E. Gracheva, et al,"Similarity Correlations and Their Experimental Verification in the Case of Strong Intensity Fluctuations of the Laser Radiation",preprint, August 1973.

III. SHORT-TERM MICROTHERMAL AND SCINTILLATION STATISTICS

Since the preceding report on this program,[1] considerable progress has been made on the problem of short-term microthermal and scintillation statistics and their interrelationship. The analytical considerations and experimental data will appear in the next report, including data to be taken during the forthcoming summer. In this section, we will briefly review the progress which has been made.

Confidence Intervals

We can now analytically relate the data-spread or confidence intervals which are obtained from short-time-average measurements of strengths of turbulence and scintillation respectively. In particular, this involves the characterization of the spatial field of mean-square microthermal fluctuations. Significant experimental data have been obtained.

Averaging Time Effects

We have resolved the issue of the apparent inconsistencies in averaging-time theory as applied to measurements on intermittent turbulence and resulting scintillations. In addition, we can quantitatively specify the degree of "intermittency". Fourth moments of probability distributions are necessarily involved, as are the integral scales of squared and/or smoothed random processes.

Computer Simulation

We have formulated a means of computer simulating ensemble members of the instantaneous propagation path, within the short-path or geometrical-optics realm. These simulations will be performed, and related to the confidence-interval considerations mentioned above. In addition, attempts will be made to include the time-variation (over a fixed period) as part of the definition of each ensemble member, and finally, to extend the technique to the first-order physical-optics realm.

IV. PUBLICATIONS AND PRESENTATIONS

Forthcoming publications and presentations on work related to this program are as follows:

1. James R. Dunphy and J. R. Kerr, "Atmospheric Beam Wander Cancellation by a Fast Tracking Transmitter", to appear in Journal of the Optical Society of America, June, 1974.

2. J. R. Kerr, "Mean Irradiance and Fading for Near-Field Laser Transmitters with Beam Wander Cancellation: Unified Analytical Treatment", Paper TuA2, Topical Meeting on Optical Propagation Through Turbulence (sponsored by the Optical Society of America), July 9-11, 1974, Boulder, Colorado.

3. J. R. Dunphy and J. R. Kerr, "Mean Irradiance and Fading for a Focused, Near-Field Laser Transmitter with Beam Wander Cancellation: Experimental Results", Paper ThA3, above conference.

4. Philip Pincus, R. A. Elliott, and J. R. Kerr, "Short-Term Statistics of Turbulence and Optical Propagation", Paper WB8, above conference.

In addition to the above, written papers on each of these areas are contemplated in the fairly near future.

V. REFERENCES

1. J. R. Kerr, "Propagation of Multiwavelength Laser Radiation Through Atmospheric Turbulence", RADC-TR-73-122, August 1973.
2. J. R. Kerr, "Propagation of Multiwavelength Laser Radiation Through Atmospheric Turbulence", RADC-TR-73-54, January 1973.
3. R. F. Lutomirski and H. T. Yura, Appl. Opt. 10, 1652 (1971).
4. H. T. Yura, Appl. Opt. 10, 2771 (1971).
5. D. L. Fried and H. T. Yura, J. Opt. Soc. Am. 62, 600 (1972).
6. H. T. Yura, J. Opt. Soc. Am. 63, 567 (1973).
7. D. L. Fried, Proc. IEEE. 55, 57-67, January 1967.
8. D. L. Fried, "Effects of Atmospheric Turbulence on Static and Tracking Optical Heterodyne Receivers/Average Antenna Gain and Antenna Gain Variation", Technical Report No. TR-027, Optical Science Consultants, August 1971.
9. D. L. Fried, J. Opt. Soc. Am. 56, 1372 (1966).
10. R. Lutomirski, "The Tilt-Corrected MTF", Preliminary Report, Pacific-Sierra Research Corp., Santa Monica, California, March 1974.
11. D. L. Fried and R. Lutomirski, private communications.
12. A. I. Kon, Izv. VUZ Radiofizika 13, 61 (1970).
13. P. J. Titterton, Appl. Opt. 12, 423 (1973).
14. H. T. Yura, Applied Optics 11, 1399-1406, June 1972.
15. D. L. Fried, J. Quantum Electr. QE-3, 213 (1967).
16. V. A. Banakh, et al, J. Opt. Soc. Am. 64, 516-518, April 1974.
17. A. Ishimaru, Radio Science 4, 295 (1969).
18. D. L. Fried and R. A. Schmeltzer, Applied Optics 6, 1729-1737, Oct. 1967.
19. J. R. Kerr and R. Eiss, J. Opt. Soc. Am. 62, 682 (1972).
20. K. S. Gochelashvily, "Focused Irradiance Fluctuations in a Turbulent Medium", Optica Acta 20, 193 (1973).
21. W. P. Brown, Jr., "Research in Interaction of Coherent Light with Solids and with Turbulent Atmospheres", Research Report, Hughes Research Laboratories, Malibu, California, May 1972.
22. J. R. Kerr and J. R. Dunphy, J. Opt. Soc. Am. 63, 1 (1973).
23. R. F. Lutomirski and H. T. Yura, J. Opt. Soc. Am. 61, 482-487, April 1971.
24. H. T. Yura, J. Opt. Soc. Am. 63, 107-109, January 1973.
25. D. P. Greenwood and D. O. Tarazano, "A Proposed Form for the Atmospheric Microtemperature Spatial Spectrum in the Input Range", RADC-TR-74-19, February 1974.
26. J. P. Hansen and S. Madhu, Applied Optics 11, 233-238, February 1972.
27. R. Lutomirski, private communication.
28. T. J. Gilmartin and J. Z. Holtz, "Focused Beam and Atmospheric Coherence Measurements at 10.6μ and 0.63μ", preprint, Lincoln Laboratories, October 1973.
29. J. A. Dowling and P. M. Livingston, J. Opt. Soc. Am. 63, 846 (1973).
30. A. J. Huber, "Measurements of the Temporal Power Spectra of a Propagated 10.6 micron Wavefront", Technical Report, Rome Air Development Center, Spring 1973.
31. J. R. Dunphy and J. R. Kerr, J. Opt. Soc. Am. 63, 981-986, August 1973.
32. H. T. Yura, J. Opt. Soc. Am. 64, 59-67, January 1974.
33. S. F. Clifford, G. R. Ochs, and R. S. Lawrence, J. Opt. Soc. Am. 64, 148-154, February 1974.
34. M. E. Gracheva, et al, "Similarity Correlations and Their Experimental Verification in the Case of Strong Intensity Fluctuations of the Laser Radiation", preprint, August 1973.